

BOEING AEROSPACE SENIOR DESIGN

Final Report

April 17, 2020

Team SAILR - Team 4

EMBRY-RIDDLE
Aeronautical University
DAYTONA BEACH, FLORIDA

IOWA STATE
UNIVERSITY

P PURDUE
UNIVERSITY®

 BOEING®

Kayla Hollis
Josh Norris
Allen Perron

David Eddy
Jake Falck
Josh Neumann

Jaehyeok Kim
Evan Lee
Stanley Liu
Dylan Lurk
Coaches
Phil Baldwin
Dr. Greg Jensen

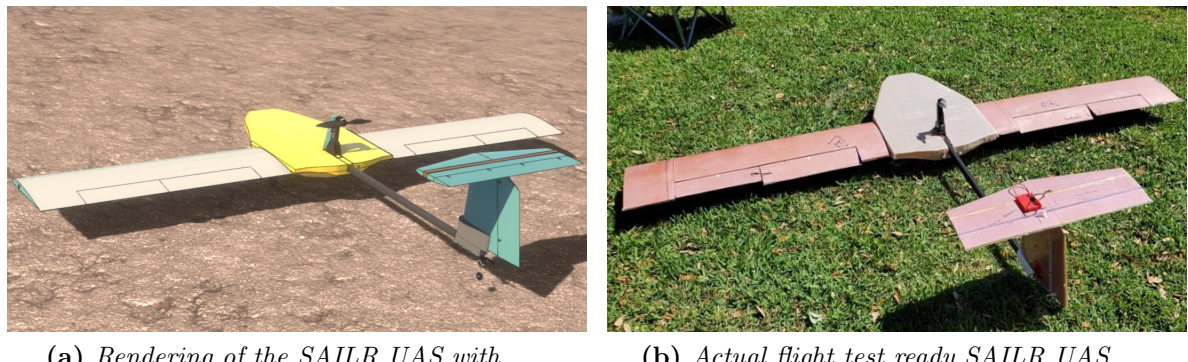
Boeing Mentors
Matt Gutzmer
Marilyn Jasmer

Executive Summary

Sea turtles are an endangered species, a problem exacerbated by nests formed in highly populated beaches. The current method to search for nests requires volunteers to patrol the beaches through daily morning walks. Considering nesting season begins in April and lasts the entire summer, this is a labor-intensive process. The mission of the team is to create a fixed-wing UAS that can autonomously survey the beaches and provide the location of possible nests to a ground operator. The product is called SAILR, which stands for Sea turtle Autonomous Identification and Locator Robot.

Concepts were generated at an airplane level by individuals on the team. Similar concepts were merged together, forming four primary concepts. Independent scoring with a weighted decision matrix was used to select the configuration; the selected design was a *pylon over wing* design.

With candidate wings identified from prior art, XFLR5 and Excel sheets were used iteratively in selecting a 7.5' wing span with chord of 1' and S9000 airfoil. The tail was sized with AVL and iteratively analyzed for stability. Raymer's Aircraft Design text was used to size the control surfaces. The design and prototype are presented in Figure 1. The stall speed is 16.68-mph, the takeoff speed is 20-mph, and the cruise speed is 40-mph (at 196').



(a) *Rendering of the SAILR UAS with expected weight of 11.64-lbs*
(b) *Actual flight test ready SAILR UAS weighing 10.5-lbs*

Figure 1: The SAILR UAS

The mission is an application of reconnaissance. Consequently, vision systems were considered for the payload. Infrared, LIDAR, and visual spectrum cameras were the modes examined to capture images. Due to balance among cost, range, weight, and volume, a visual spectrum camera will be used in the UAS with offboard image processing. The specific architecture will consist of a Sony IMX219 camera, Raspberry Pi with LTE hat, and Storm 32 3-axis gimbal.

Sea turtles average about 2.5'-3.5' across. At the cruise altitude of 196', the Sony IMX camera is expected to resolve 0.5" per pixel with a 93% frame overlap at 15-fps and 40-mph cruise. Images will be sent via LTE with GPS metadata to a remote processing server. The vision system utilizes a neural network based on Darknet, an open source neural network, and You Only Look Once algorithm. A positive sighting will be reported to the ground station.

The payload, controls, and electric propulsion will be powered by a single, shared battery. With a thrust requirement of 1.44-lbf at 40-mph, five candidate motors from KDE in the 515-kV to 965-kV class were examined before selecting the KDE2315XF 515-kV for its current draw, low cost, wide range of usable propellers, and low weight. To achieve the required takeoff performance of 3.59-lbf, an APC 11" x 8" propeller was used. The propeller diameter and pitch was determined in a trade study using MOTOCALC8 electric motor sizing software. The motor is driven by the recommended ESC, the KDEXF-UAS35. The flight controller utilized is the Pixhawk 2.1 Cube with an RFD-900 telemetry radio and Here2 GPS. Considering the power budget, the necessary battery capacity was determined to be 5865-mAh. The Lumenier 6S 8000-mAh LiPo battery selected will give an estimated 61 minutes of flight time in nominal weather conditions which can support flying in adverse wind conditions or future mission duration expansions.

Structural, material, and component interfacing decisions were made with decision matrices, and manufacturing of the UAS was shared among the three universities. Iowa State was responsible for the composite fuselage preparation, layup, and post processing. Purdue was responsible for the wing and tail sub-assemblies. Embry-Riddle was responsible for the payload board, pylon, motor mount, final assembly, and final system test.

Validation was conducted on a variety of levels. A scaled glider was developed in November 2019 that served as a platform for testing manufacturing processes. FEA was conducted to examine the wing bending, tail bending, and motor pylon stress & deflection. Static and dynamic propulsion testing was carried out to examine characteristics of the propulsion system. Limited testing was performed on the vision detection system as it was being developed. These tests helped to substantiate the design. Additional subsystem and system-level testing was planned; however, the COVID-19 shutdown inhibited further testing progress.

Risks have been identified at the mission and aircraft level, and failure modes have been identified at the component and subsystem level. The team experienced difficulty monitoring risks and failure modes as the project progressed. The impact of COVID-19 on the project served as an influential experience in recognizing risks.

The management of the 10-member, 3-university team was being led by a project manager and chief engineer with other members organized into 2 main structures over the duration of the project to best suit the nature of the work. The project manager oversaw the \$4,000 budget and subsequent subsystem limits which included margins. The total amount of funds spent was \$3,076. Traceability in purchases was tracked with a workflow. The workflow, along with the Gantt Chart, CAD, and FEA, was carried out using 3DEXPERIENCE.

At the conclusion of the project, the UAS sits as a fully assembled vehicle with complete controls integration. A pilot and controller are all that are needed to begin the ground test plan and flight test plan. Concurrently, the vision detection payload system needs to be finished and integrated into the airframe. Upon completion, final testing and refinements will be conducted before ultimately delivering the UAS to the customer.

Contents

Executive Summary	i
List of Figures	v
List of Tables	vii
Nomenclature List	viii
1 Management Summary	1
1.1 Team Organization	1
1.2 Schedule & Milestones	2
1.3 COVID-19 Impact	3
1.4 Expenses	4
2 Conceptual Design	5
2.1 Mission Definition	5
2.2 Stakeholders	6
2.3 Design Requirements & KPIs	7
2.4 Concept Generation	8
2.5 Concept Selection	10
2.6 Payload Definition	12
3 Detailed Design	13
3.1 Constraint Analysis & Sizing	13
3.2 Airfoil Selection	14
3.3 Stability	16
3.3.1 Definition and Assumptions	16
3.3.2 Tail Configuration	16
3.4 Control Surfaces	17
3.5 Propulsion	18
3.5.1 Motor & Propeller Sizing	18
3.5.2 Electronic Speed Controller Sizing	19
3.5.3 Battery Sizing	19
3.6 Structures	19
3.6.1 Design Considerations	20
3.6.2 Design Decisions	20
3.6.3 Design Outcomes	21
3.7 Payload	21
3.7.1 Architecture	22
3.7.2 Sensing	22
3.7.3 Processing	22
3.8 Controls & Electrical Design	23
3.8.1 Power Budget	23
3.8.2 Controllers	24
3.8.3 Radio Communications	24
3.9 Collection of Significant Preliminary Design to Detailed Design Changes	24

4 Components & Assemblies	26
4.1 UAS Assembly Drawing	26
4.2 Wiring Diagram	28
5 Production Plans & Manufacturing Process	28
5.1 Production Overview	28
5.2 Manufacturing	30
5.2.1 Embry-Riddle Aeronautical University	30
5.2.2 Iowa State University	31
5.2.3 Purdue University	31
6 Risks & FMEA	32
6.1 Risks	32
6.2 Failure Mode and Effects Analysis	34
7 Verification & Validation	35
7.1 Structural Testing	36
7.1.1 Wing Bending	36
7.1.2 Pylon Bending	37
7.1.3 Tail Boom Bending	39
7.2 Autonomous Flight Testing	41
7.3 Propulsion Testing	42
7.4 Payload Testing	45
7.5 Manual Flight Testing	45
7.6 Flight Checklists	46
7.7 Glider Prototype	46
7.7.1 Manufacturing	46
7.7.2 Test Results	48
7.7.3 Glider Use and Lessons Learned	49
8 Conclusion	49
References	51
Appendices	52
A Organization Structures	52
B Detailed Schedule	53
C Budget & Expense Breakdown	57
D Wing & Propulsion Sizing Sheets	58
E Stability Calculations	60
F Manufacturing Supplements	62
G Risks & FMEA Analysis	67
H Requirements Verification	77
I Wind Tunnel Testing	78
J Flight Checklists	83
K Drawing Package	86

The cross references are clickable

List of Figures

1	The SAILR UAS	i
2	Field of view diagram	viii
3	Organization of Team SAILR for manufacturing (MRR-end)	2
4	High level overview of project schedule	2
5	Team SAILR COVID-19 response plan	3
6	Budget breakdown by category with expenses	5
7	Purchase order workflow in 3DEXperience	5
8	Mission profile applied to section of Daytona Beach	6
9	General mission profile	6
10	4 Primary Concepts Generated	9
11	Electric hand-launch UAS constraint diagram	14
12	Coefficient plots	15
13	Raymer's tail efficiency graph	17
14	V-N diagram	20
15	Load path diagram	21
16	Payload wiring diagram	23
17	Control system components	24
18	An 8-lb glider made from scrap wood	25
19	SAILR 3-view Drawing	27
20	Pixhawk 2.1 wiring schematic	28
21	Day-by-day plan for manufacturing	29
22	Payload board versions	30
23	Fuselage versions	31
24	Curvature of the Wing-Aileron Joint	32
25	Wing foam sections	32
26	Completed wing showing control surfaces and servo installation	33
27	Risk matrix and major descriptions	33
28	FMEA matrix and major descriptions	34
29	Wing Bending FEA	37
30	Physical Wing Bending Setup	37
31	Motor Pylon FEA Setup	38
32	Motor Pylon FEA	38
33	Tail Boom FEA Setup	39
34	Tail Boom FEA: Von Mises Stress Distribution	40
35	Tail Boom FEA: Deformation	40
36	Modified Bixler Trainer Aircraft configured with SAILR avionics	41
37	Flight paths from trainer aircraft testing	42
39	Static condition ESC signal VS Thrust	42
38	Propulsion wind tunnel test setup	43
40	Static condition ESC signal VS Power	43
41	Dynamic condition ESC signal VS Thrust	44
42	Dynamic condition ESC signal VS Power	44
43	Payload testing	45
44	Prototype glider	47
45	Three-view drawing of 3D-printed bracket	47

46	Glider flight time lapse	48
47	Team photo	50
A.1	Organization of Team SAILR following the MCR/SRR to MRR	52
B.1	Preliminary Design Schedule.	53
B.2	Detailed design schedule	54
B.3	Manufacturing Schedule.	55
B.4	Test & Evaluation Schedule.	56
C.1	Budgeted vs actual expenses	57
D.1	Initial sizing constraint diagram inputs	58
D.2	Initial sizing weight analysis inputs and outputs	58
D.3	Motor & battery sizing sheet	59
F.1	Engineering bill of materials	62
F.2	Electronics bill of materials	63
F.3	Page 1 of a sample job instruction sheet for the fuselage manufacturing	64
F.4	Page 2 of a sample job instruction sheet for the fuselage manufacturing	65
F.5	Page 3 of a sample job instruction sheet for the fuselage manufacturing	66
G.1	Risks page 1 columns 1 through 10	67
G.2	Risks page 2 columns 1 through 10	68
G.3	Risks page 1 columns 11 through 14	69
G.4	Risks page 2 columns 11 through 14	70
G.5	Risks page 1 columns 15 through 19	71
G.6	Risks page 2 columns 15 through 19	72
G.7	Risks summary	72
G.8	FMEA page 1 columns 1 to 7	73
G.9	FMEA page 2 columns 1 to 7	74
G.10	FMEA page 1 columns 8 to 18	75
G.11	FMEA page 2 columns 8 to 18	76
H.1	Verification Status of System and Subsystem Requirements	77
I.1	C_L vs α	78
I.2	Drag polar	79
I.3	Lift-to-drag	79
I.4	C_L vs α with flap	80
I.5	Drag polar with flap	81
I.6	Wind tunnel testing	82
J.1	Day Before Flight Checklist	83
J.2	Pre-Flight Checklist	83
J.3	In-Flight Checklist	84
J.4	Post-Flight Checklist	85
J.5	Emergency Checklist	85

List of Tables

1	Design requirements and KPIs	8
2	Weighted decision matrix criteria and configuration scores	12
3	Aircraft sizing parameters	18
4	Design Decision Matrix Results	21
5	Estimated power & current Budget	23
6	Wooden Glider Speed Test	25
7	Wing Displacement Comparison	37
8	Tail Boom Displacement Comparison	40
A.1	Team organization prior to MCR/SRR	52

Nomenclature List

<i>AC or A.C.</i> - Aerodynamic Center of aircraft	<i>FPS</i> - Frames per second
<i>Aero team</i> - The aerodynamics team	<i>IMU</i> - Inertial measurement unit
<i>AOA</i> - Angle of attack	<i>It</i> - Placement of tail from tip of fuselage.
<i>AR</i> - Aspect Ratio	<i>ISU</i> - Iowa State University
<i>CDR</i> - Critical design review	<i>KPI</i> - Key performance indicator
<i>CFR</i> - Code of Federal Regulations	<i>kV</i> - The kV-rating is a motor performance parameter that when multiplied by the battery supply voltage yields the no load motor RPM.
<i>Clutches</i> - Groups of turtle eggs still buried	<i>LiPo</i> - Lithium polymer
<i>CG</i> - Center of Gravity	<i>MCR/SRR</i> - Mission concept review / System requirements review
<i>C.G.</i> - Center of gravity	<i>Mech team</i> - The mechanical team
<i>ERAU</i> - Embry-Riddle Aeronautical University	<i>NVH</i> - Noise, vibration, and harshness
<i>ESC</i> - Electronic Speed Controller	<i>PDR</i> - Preliminary design review
η - Effect of propeller down-wash	<i>SAILR</i> - Sea turtle Autonomous Identification and Locator Robot
<i>FAA</i> - Federal Aviation Administration	<i>Scrum team</i> - A managerial term from the agile methodology used to describe a type of team formed for a sprint
<i>FEA</i> - Finite element analysis	<i>Sprint</i> - A managerial term from the agile methodology used to describe a short, fixed period of time with defined objectives to accomplish by the end of the time period
<i>FMEA</i> - Failure modes and effects analysis	<i>UAS</i> - Unmanned aerial system
<i>FOV</i> - Field of view (see Figure 2). Field of view can be specified as an angle or length; when it is length, FOV is the same as “length of frame”.	<i>Wc</i> - Wing Chord
	<i>X_{CG}</i> - Location of CG from the head of the aircraft
	<i>X_{AC}</i> - Location of AC from the head of the aircraft
	<i>YOLO</i> - You Only Look Once, a vision detection algorithm

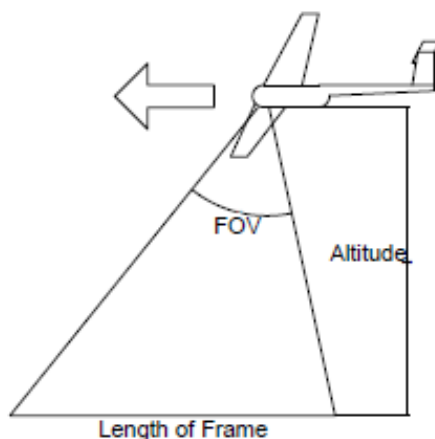


Figure 2: Field of view diagram

1 Management Summary

1.1 Team Organization

A project manager and chief engineer were determined from the outset; however, as the nature of the work evolved, the organizational structure of the 10 members has evolved through 3 organization structures.

The project manager, Dylan, and the chief engineer, Kayla, were constant for the duration of the project (despite providing an opportunity to change leadership in December). The project manager oversaw the schedule & deadlines, logistics, budget, and lead all team meetings. The chief engineer was responsible for technical decisions, ensuring designs met requirements, and reviewing engineering work. Organization of the team and task delegation were joint responsibilities.

The scrum formation, effective for the period of time prior to the MCR/SRR, is presented in Appendix A. This form was used to handle the substantial upfront work that was needed to define the mission and scope the project. Members were assigned to tasks that needed to be accomplished prior to the review.

A formal organization structure consisting of an aero and mechanical sub team was adopted for the period spanning from the MCR/SRR to the MRR to support the preliminary and detailed design work. This legacy structure is provided in Appendix A.

After the MRR, the nature of the work became focused on “making”. The team created 3 sub teams to best handle the new work. To support the controls development and vision development, a “Programming” sub team was created. To coordinate manufacturing among all schools, a “Manufacturing Programs” sub team was established. Finally, a “Test & Evaluation” sub team was established to coordinate analytical & experimental sub system & system tests. Responsibilities and member assignment are shown in Figure 3 with some members accruing secondary obligations to help with workloads as needed. A key lesson learned from first semester was applied in this new organization: responsibilities and areas of ownership were clearly defined at the outset.

Unchanged from the previous aero/mechanical organization structure is the presence and location of the stakeholders, coaches, and advisors. The entire team reports to the stakeholders since they are the end users of the product at hand. Additionally, the team has included the faculty coaches and Boeing mentors on the organization chart as parties interested in the design.

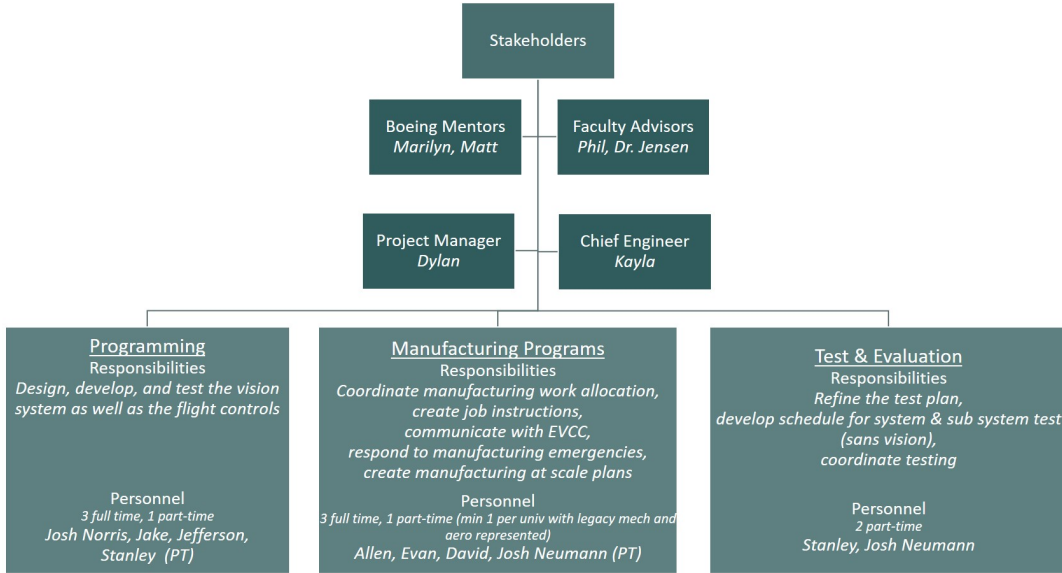


Figure 3: Organization of Team SAILR for manufacturing (MRR-end)

While this breakdown put a structure around much of the work, the team had a plan to handle unforeseen needs. People would be explicitly asked to work special tasks, and sprint teams with well defined objectives were to be formed on an ad hoc basis if needed.

1.2 Schedule & Milestones

The high level timeline for the project is shown in Figure 4 with a detailed breakout of the tasks within each phase provided in Appendix B. 3DEXperience was used to manage the work breakdown and schedule using the Gantt Chart capabilities. The tool reported tasks were 84% on-time. The team attributes this high performance to usage of the tool. Members received email notifications when tasks were assigned to them. On his/her 3DEXperience homepage, members had the ability to update the “percent complete” for each task and attach deliverables. All of this empowered the team to achieve progress incrementally rather than only during update meetings.

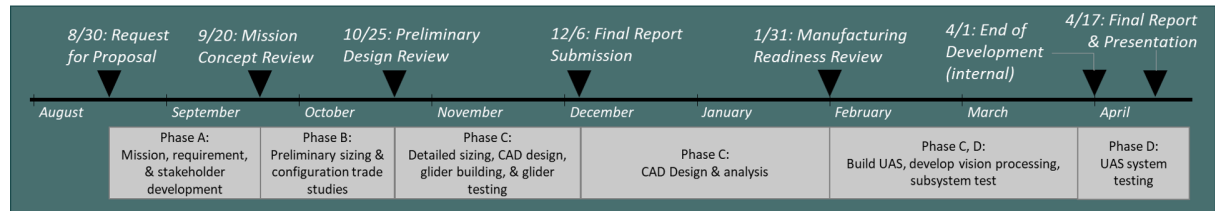


Figure 4: Project deadlines and high level overview of work in each phase. The 4/1 deadline was an internally agreed upon date to halt any manufacturing, assembly, or vision development work and transition the team’s resources to completing the end of project deliverables. (Testing continued as appropriate to complete the test matrix.)

The first of three major schedule problems that was encountered was in the late October to November time frame. CAD progress was delayed due to, in hindsight, an understaffed CAD team, significant upfront battles in learning the 3DEXPERIENCE rich apps, and

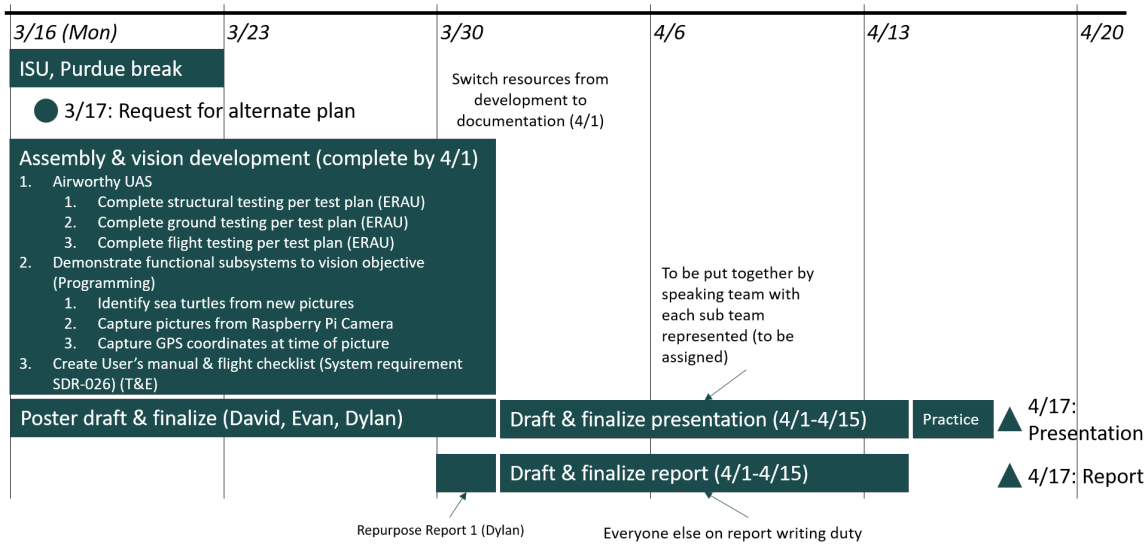


Figure 5: Team SAILR COVID-19 response plan

not recognizing the design would iterate as the detailed sizing work progressed. Consequently, the CAD work that was completed late November was rushed, so the team elected to improve the fidelity of the CAD model over the December/January holiday period. The trickle-down effect is that much of the FEA and subsystem testing was delayed into the manufacturing phase, where FEA and other tests occurred concurrently with manufacturing. The team realizes the structural analysis should have been completed before manufacturing; however, it was determined to work concurrently and resolve issues if they arise out of the FEA so that a plane would be available to fly before the fly-off.

No significant delays were encountered in receiving ordered materials or in the manufacturing of components besides a delay in shipping the wing set from Purdue to Embry-Riddle. The delay was due to underestimating the composite layup post processing and servo installation. This caused the wings to ship one day late outside of the 2/21-3/1 shipping window. This delay was absorbed in the final assembly time frame with increased man power.

A handful of tasks relating to physical testing were cancelled due to COVID-19 implications. These included wing bending, tail bending, ground testing, air testing, and noise testing.

1.3 COVID-19 Impact

Due to the COVID-19 guidelines set forth by health officials, universities gave abrupt notice of building closures. This impacted the planned activities of the team.

At the time of the news, sub-assemblies from ISU and Purdue had already been shipped to ERAU, so ERAU was the only school needing sustained lab access. Additionally, it was later discovered the Raspberry Pi and LTE hat were locked in the Purdue build lab after full closure. It was accepted the LTE functionality would not be able to be developed. Consequently, a plan was put into place, as shown in Figure 5.

Swift action by a team member at ERAU grabbed the team's supplies from the school's

lab before the full closure and took them to his house. With the help of a friend's 3D printer and the basic workshop the individual had, the team continued the final assembly as planned. It was thought that the team would have access to a controller and pilot; however, the shutdown orders became stricter before the team was ready to begin testing on 3/23. The COVID-19 impact also strained access to help resources that were going to be used to help with the vision development.

1.4 Expenses

A budget, which was updated twice, was first created using order of magnitude estimates for key systems of the UAS. Purchasing was processed using a 3DEXPERIENCE workflow, and expenses were logged against budget categories in accordance with predetermined rules.

The first of two budget updates occurred in January, prompted by the maximum budget reduction to \$4000. The original budget had buffer built into it associated with uncertainty in material and equipment needs early in the project. When the revised budget was requested, the design was well defined, so much of the margin was removed (while still keeping catch-all categories for miscellaneous hardware, wires, etc.).

The second budget revisit was in early March after needing to reallocate shipping funds to support manufacturing needs. Iowa State University requested that this project barter lab materials in exchange for the use of their facilities and lab tech assistance. Because inter-university shipping of the wings and fuselage was significantly cheaper than quoted, shipping funds were reallocated to purchase supplies for the ISU lab.

The most recent budget with expenses is provided in Figure 6, where the total project expenses were planned to be \$3582, \$418 less than the \$4000 provided. Shipping, propulsion, and controls came in “under budget” due to only needing limited buffer. Payload came in “under budget” due to not needing to purchase a data plan to support LTE development efforts. Build materials came in “at budget” due to needing all the buffer for miscellaneous hardware, and SAILR gear was “at budget” due to no margin built in. A detailed statement of the budget and actual costs associated with the items that comprise each category is provided in Appendix C.

The project manager provided guidelines to ensure consistent expense charging. More prominently, the shipping category was reserved for inter-university shipping. Shipping on purchases was tabulated under the same budget category as the item being shipped since it represented an additional cost to procure the item.

The SAILR procurement effort was organized using the 3DEXperience “Route” feature to ensure traceability in the team’s procurement. The route is detailed in Figure 7. Written instructions were provided to members detailing the order process. Upon creation, (in order) the chief engineer, project manager, and coach were required to review the purchasing documents for project need, budget tracking, and information completeness, respectively, before the documents were sent to the Purdue Engineering Procurement Center.

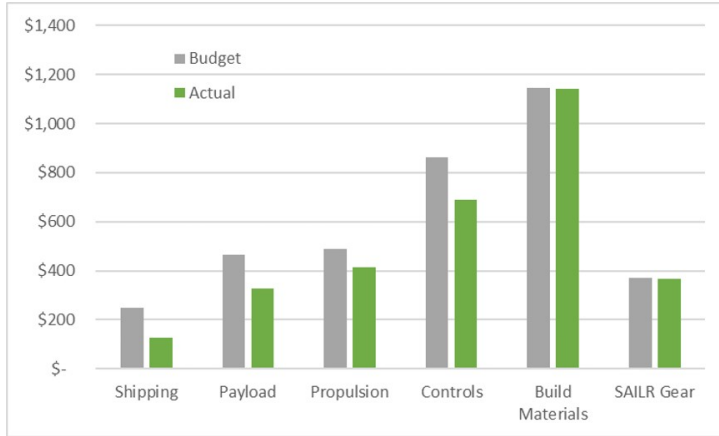


Figure 6: Budget breakdown by category with expenses

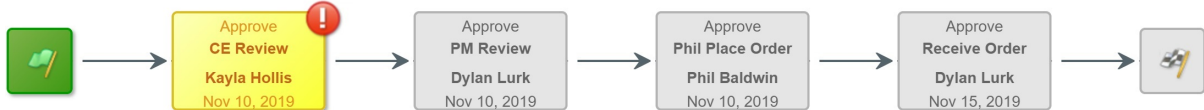


Figure 7: Purchase order workflow in 3DEXperience

2 Conceptual Design

2.1 Mission Definition

To combat decreasing sea turtle populations, additional protection to their fragile nests is needed. However, the length of Florida coastlines makes it difficult to manually locate turtle nests inhibiting the ability to provide protection. Therefore, a UAS capable of flying along the coast to detect turtle nests from the air is needed.

The intended mission, presented in Figure 8, is applied specifically to the section of Daytona Beach stretching from International Speedway Blvd. to the city limit covered by the Volusia County Sea Turtle Conservancy. The time of day will be early morning (after the sun comes up), before the beaches become crowded. Setup of the aircraft and ground station shall take no more than 30-minutes, including reviewing the pre-flight checklist and inputting the mission waypoints. Autonomous, wheeled takeoff will occur on a beach access driveway; the UAS will begin ascending to the cruise altitude of 196-ft and heading towards the surveillance path. It begins capturing images of the beach as it flies through the established waypoints for a maximum distance of 15-mi (approximately 30-min, plus an additional 15-min reserve capacity). The images will be sent via LTE to a remote server for processing. If the server vision program determines a positive sighting of any sea turtle nests or tracks, the ground station (being manned in a follower vehicle) will be alerted with the corresponding GPS coordinates. Once the UAS reaches the final waypoint, it will begin descending to a predetermined safe landing area. Following landing, post-flight checks are carried out and the aircraft is disassembled & stowed in under 30-minutes. The UAS will be transported in a hard-shell case to prevent damage. A general mission profile is provided in Figure 9.

In this concept of operations, a minimum of a two-person crew is required. A pilot with Part 107 drone license, who is capable of taking over the aircraft in the event



Figure 8: Mission profile applied to the section of Daytona Beach stretching from International Speedway Blvd. to the city limit covered by the Volusia County Sea Turtle Conservancy. Yellow- takeoff & ascend, blue- cruise, orange- descend & land.

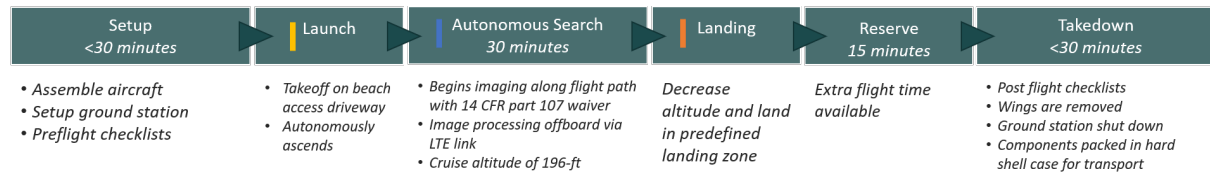


Figure 9: General mission profile

of an emergency, performs pre/post-flight checks, as well as monitors the data being transmitted. The second person is a driver of the follower vehicle who assists with marking the nests as well as assembly and disassembly.

This concept of operations requires a 14 CFR Part 107 waiver. The waiver would explicitly be sought for exemption of operating from a moving vehicle and operating beyond line of sight. The team believes a waiver could be obtained because the entire mission profile is autonomous from takeoff to landing, and crowds will be minimal in the early morning when the mission is conducted.

2.2 Stakeholders

Various stakeholders and customers for the team's proposed solution were consulted in order to determine the mission requirements, a baseline mission profile, and a general guide regarding the required payload for the UAS.

Boeing, as a major stakeholder, provided high-level requirements that must be met by the UAS. These requirements are reproduced below:

- The aircraft shall be a fixed-wing design.
- The UAS shall have an electric propulsion system.

- The UAS shall weigh less than 12.5-lb with payload.
- The UAS shall be able to fly with autopilot to established mission profiles.
- The total program cost shall not exceed \$4,000 (after a \$1,000 budget reduction in early January 2020).
- The UAS shall either be hand launched or takeoff from 200-ft of unimproved runway.
- The UAS shall be able to fly with autopilot to established mission profiles.
- The UAS shall be easily transportable.
- The UAS shall operate within the chosen mission requirements.

In addition to Boeing, major stakeholders in this project include staff & faculty members of Embry-Riddle Aeronautical University, Iowa State University, and Purdue University, as well as two Boeing engineers (Matt Gutzmer and Marilyn Jasmer). These individuals have served as advisors and mentors for the team by providing timely, significant feedback on the team's direction and by guiding decisions as development of the UAS progressed.

Several additional stakeholders of the UAS were identified and consulted in order to understand the use case for the intended product. Insight was gleaned on critical mission requirements that the system must accomplish as well as on improvements that could be made to current solutions. Among these individuals are Sami McCorkle and Jennifer Winters, both of the Volusia County Sea Turtle Habitat Conservation Plan program in Florida. They provided guidance that helped the team establish mission requirements for flight range, GPS tracking capabilities, real-time on-board data processing needs, and the necessity for compact stowage for ease of transport. These individuals were again consulted in early January with a project status update. Additionally, Robbin Trindell, a biological administrator with the Florida Fish and Wildlife Conservation Commission, noted the risk of UASs when dealing with critically endangered species, as they run the risk of interfering with wildlife. Therefore, a mission requirement was also created to minimize interference with any marine life present in the area.

Overall, these stakeholders showed significant interest in this UAS-based solution to the problem. They provided guidance and feedback throughout the mission development process.

2.3 Design Requirements & KPIs

Stakeholder needs were translated into technical needs which were then translated into design requirements and/or relevant Key Performance Indicators (KPIs) to serve as quantitative design points for the UAS. These quantitative metrics have enabled the team to utilize quantifiable data to determine whether requirements were met instead of relying on qualitative observations. The measurable values set by KPIs demonstrate how well the UAS is able to perform to specifications set by the team and by the stakeholders.

The most critical design requirements and their associated KPI(s) are shown in Table 1.

Table 1: *Design requirements and KPIs*

Design Requirement	KPI
The UAS shall weigh less than 12-lbs with payload	Total weight \leq 12-lbs
The UAS shall be able to fly with autopilot to established mission profiles	Autonomous operation \geq 90% of flight duration
The UAS shall be launched on an unimproved runway shorter than 200-ft.	The vehicle performs a wheeled takeoff
The UAS shall have a range of at least 15-mi	One-way ground distance range \geq 15-mi radius
The UAS shall be easily transportable	UAS must fit within 10-in x 24-in x 100-in box
The UAS shall locate its GPS coordinates within a User Range Error (URE) of 16.4-ft when requested with a 95% probability.	GPS accuracy radius of 16.4-ft
The UAS shall produce no more than 50-dB of noise at a distance of 196-ft altitude	Noise produced by plane flying at 196-ft \leq 50-dB

2.4 Concept Generation

With a mission identified and requirements defined, concepts were generated for the UAS. Members worked independently utilizing intuition, existing designs, & experience to create mock-ups. These were visualized by either sketching them by hand and converting into OpenVSP designs, or designing directly in OpenVSP. Through this independent concept brainstorming, 15 separate designs were generated. Upon review, some designs were determined to be similar with small differences. These were merged into single designs. After taking into account limitations invoked by the mission requirements and recommendations based on member intuition & experience, the aero team compiled the concepts into the four configurations shown in Figure 10. These concepts are discussed in the ensuing paragraphs.

The *pylon over wing* design, shown in Figure 10a, uniquely features a motor mounted over the main airfoil. By mounting the motor over the wing, the propeller is positioned away from operators which was important when the launch was originally anticipated to be by hand. Additionally, the wing provides a surface to inhibit the propagation of sound which was a concern from the stakeholders. Lastly, it reduces kicking up sand during takeoff and landing.

The tail of this design is a high T-tail mounted via a boom to the fuselage. The high mounted wing provides additional unobstructed viewing range for a camera payload.

However, there were concerns with this design. Due to the over wing motor mount, a large pitching moment will be created by the motor. To increase the effectiveness of the tail it was decided to use a T-tail configuration positioned in the propeller air stream. The increase in velocity of the propeller air stream over the horizontal tail provides more lift counteracting the pitch down moment created by the propeller mounted on the pylon.

The *conventional tractor* configuration, shown in Figure 10b, is a mid wing design with

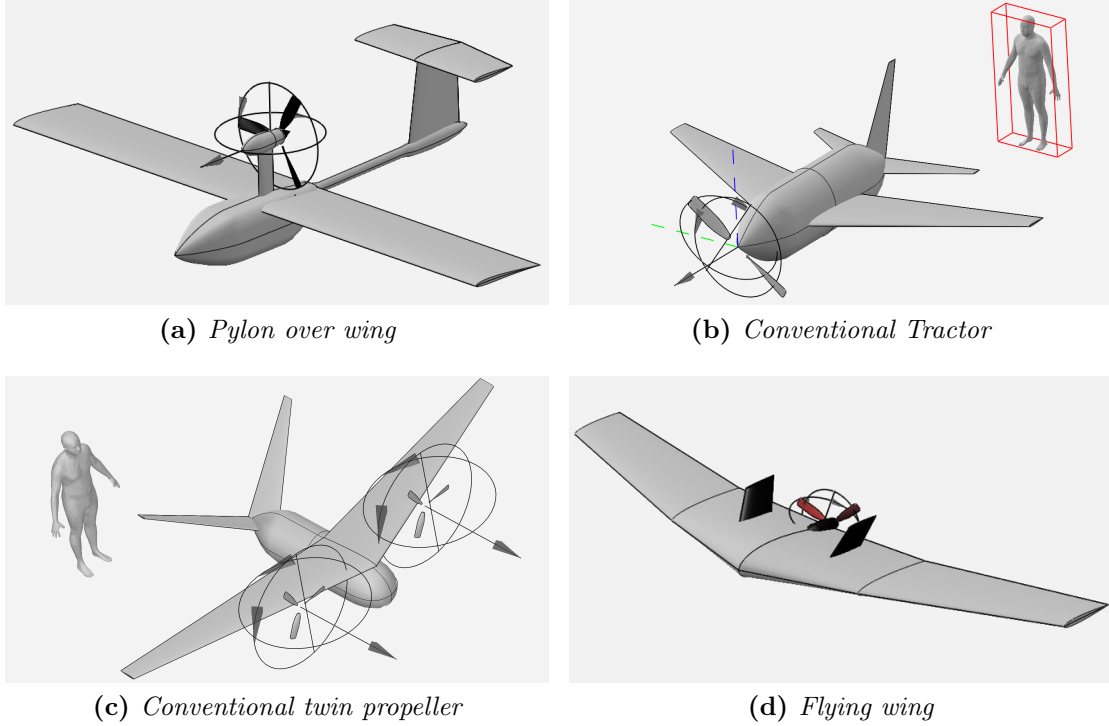


Figure 10: 4 Primary Concepts Generated

the motor installed in the nose of the fuselage. This is to move the propeller far from an operator during a hand launch. Since this is a conventional, proven design, a benefit is ease in aerodynamic and structural analysis as well as manufacturing.

Despite being a conventional design, it still has drawbacks. The field of view for a camera would be restricted with the front mounted propeller and mid wings. A camera would need to be positioned in a sub-optimal position for viewing. The positioning of the propeller would also predispose it to propeller strikes.

In the *conventional twin propeller* configuration, viewed in Figure 10c, the wing is mounted high with two motors positioned on the leading edge of the wing. A benefit to this configuration is that each motor can be smaller for the same current draw. Additionally, the two propellers can each be smaller in diameter than a single motor system, reducing the noise created.

Drawbacks to this design are tied to increased weight. The presence of the second motor requires an additional speed controller, motor mount, and wiring. These items scale minimally (if at all) with the decreased size of each motor.

The *flying wing* configuration is a completely different design compared to the designs discussed thus far. Shown in Figure 10d, the configuration is comprised of a wing body with a rear mounted propeller and a vertical stabilizer mounted directly onto the wing. It is easy to launch and is very agile when in flight.

This design carries with it operational challenges. The placement of the propeller creates a hazard for the hand launch condition. Moreover, the propeller placement positions the

propeller close to the ground, presenting a unique challenge to land without damaging the propeller. From an aerodynamics perspective, the flying wing has a tendency to stall while being challenging to recover.

All mock-ups were paired with a brief list of strengths and weaknesses for each configuration. Upon sharing this briefing with the entire team, the team was reminded the OpenVSP mock-ups do not represent a final model, as multiple variations of the theme were presented so as to minimize an individual identifying with an exact design.

2.5 Concept Selection

Each team member scored the 4 designs against criteria pertinent to the mission using a weighted decision matrix. By summing the scores for each design from each member, the selected configuration was the highest scoring concept, the *pylon over wing*.

To create a well-balanced design that would successfully achieve the mission objectives as prescribed by the stakeholders, a weighted decision matrix was created to identify airplane level details that configurations should be scored against. Mechanical and aerodynamic related criteria were considered as recommended from the mechanical and aero teams.

For aerodynamics, five criteria were considered:

- *Acoustic mitigation*: The stakeholders emphasized that noise is a known factor that affects wildlife. They expressed concern that the drone flying at a low altitude over the beach would create a negative effect on not only the turtles but other marine and avian life. Thus, an acoustic mitigation criterion was considered.
- *Propeller airflow*: The efficiency of the propeller was considered by adding a criterion to assess quality of the airflow experienced by the propeller. The guiding question for this criteria was “Does the propeller experience clean, undisturbed airflow?”
- *Adverse aerodynamic interactions* This refers to whether interactions among the propeller, wing, and tail have the potential to negatively impact the stability of the aircraft.
- *Ease of C.G. placement*: This refers to the ability to place the C.G. at a desired location to provide enough static margin.
- *Aerodynamic modeling complexity*: This was to ensure that the design could be analyzed in a reasonable amount of time with tools available to the team. This was assessed on intuition.

Five additional criteria were investigated from a mechanical standpoint:

- *Flight controller configuration complexity* With limited team resources to achieve the system requirement of full autonomy, this was an important internal metric. The guiding question was “Does the configuration have any special channel mixing that would need to take place or parameters that would need special tuning?”
- *Hand & propeller clearance* Considering that the original mission profile stated the takeoff would be a hand launch, this was an assessment of the inherent danger of the design to the person that launches the aircraft.

- *Propeller ground clearance* The plane will likely be landing in unimproved terrain, such as sand or grass strips, so the propeller ground clearance was considered in weighing designs to ensure that the propeller would be clear of damaging itself by striking the ground. A lesson learned in hindsight is that this should have been weighted much higher than the “1” weight it received due to a requirement guiding component failure.
- *Structural design complexity* This assessed the complexity of the structure of the aircraft to model. This is an indirect assessment of how robust the structure is. If it is complex to model, the loading may not be fully understood; however, if it can be modeled easily, the loads will be well known which will influence the structure.
- *Manufacturability* This measures the complexity to manufacture the aircraft. It incorporates consideration for tool availability within each university to manufacture the aircraft.

These criteria are summarized in Table 2 which also shows the weights assigned to each criterion as well as the weighted score in each criterion for each configuration. Weights were defined to be between 1 and 5 where higher values indicate more significant criteria. The values for the weights were determined by taking an average of the weights suggested by aero team members for the aero criteria and an average of the weights suggested by the mechanical team members for the mechanical criteria.

All 10 team members were asked to score each configuration against all 10 criteria on a scale of 1 to 5. Members were provided with mock-ups, strengths, and weaknesses for each design. They then completed a Google Form independently so as to not influence other members’ scores. The criteria scores for each configuration were determined by summing the scores given by each member of the team and multiplying that by the weight. The total weighted score is the summation of the 10 weighted scores for each category.

As shown in Table 2, the highest scoring configuration was the *pylon over wing*. This was the selected configuration.

Table 2: Weighted decision matrix criteria and configuration scores

Criterion	Weight	Pylon over wing	Conventional tractor	Conventional twin engine	Flying wing
Acoustic mitigation	3.6	154.8	64.8	82.8	79.2
Propeller airflow	3.2	140.8	108.8	124.8	86.4
Adverse aerodynamic interactions	4.2	117.6	134.4	147	96.6
Ease of C.G. placement	4.8	163.2	192	177.6	72
Aerodynamic modelling complexity	2.8	81.2	103.6	86.8	70
Flight controller configuration complexity	3	75	111	96	69
Hand & propeller clearance	4	196	140	140	68
Propeller ground clearance	1	50	25	36	16
Structural design complexity	5	160	190	170	180
Manufacturability	3	99	117	90	114
Total Weighted Score		1237.6	1186.6	1151.0	851.2

2.6 Payload Definition

To define the payload, the relevant constraints first needed to be defined in order to complete trade studies. As a team, the rating criteria decided upon to evaluate the search method were as follows: cost, detection range, weight and volume, complexity, and robustness. A thermal imaging system, LIDAR system, and visual spectrum system were the candidate payloads considered.

Preliminary research showed that thermal imaging for detecting clutches was possible with the correct equipment. Research by a Duke University student of ecosystem science and conservation in an article for Wildlabs.net showed that a FLIR Duo Pro R was sensitive enough to detect the 1- to 2-°F difference in surface temperature of clutches near hatching (Ossmann, 2018). The major drawback to thermal imaging, however, is the cost. Weighted highest on the trade study, cost has the largest impact on the project. When a single sensor can cost as much as \$5,000, a significant burden is placed on the project budget and overall product affordability. A slightly more cost-effective solution was to utilize several cheaper, lower resolution sensors and stitch the images together in post-processing. This still had a significant cost associated with it.

With a LIDAR solution, locating tracks leading to nests were of interest, rather than directly locating nesting sights. However, there is little or no research to support that this was a viable solution. Furthermore, it shares many of the same shortcomings as thermal imaging, namely cost. Even hobby level LIDARs are on the order of several hundred dollars, and even though this is not budget destroying, it is still not ideal. Another drawback is the significantly reduced sensing range with a maximum distance in ideal conditions being 60-80-ft. Flying this low is more dangerous than at high altitudes and increases the chance of wildlife interaction, a potential requirement violation. It also requires a higher frequency of scanning and image processing.

The final, most cost-effective solution utilized commercial-off-the-shelf single board visual spectrum cameras to gather video. As far as processing goes, this is quite similar to the LIDAR solution; however, instead of searching for tracks through changes in elevation of the surface, this system identifies contrast in light in the beach terrain. This solution requires pairing with significant software and hardware to process the images. Despite the software and hardware needs, the visual spectrum solution was the option the team deemed to have the best balance among cost, range, weight, and volume attributes.

3 Detailed Design

3.1 Constraint Analysis & Sizing

Sizing of the UAS's aerodynamic surfaces began with calculations for wing loading and power loading. Initially, the mission would be hand launched, so the "Constraint Sizing Electric Hand Launch" sizing sheet provided by the course mentors was used to determine both of these values. When the mission was switched to a wheeled takeoff, the takeoff performance was well within our 200ft takeoff distance requirement at 35ft. A screenshot of the Excel sheet showing the inputs to the constraint diagram can be seen in Appendix D. Many of the default inputs given in the sheet remained constant, as they were deemed sufficient and were less influential to the design. The critical inputs changed were *aspect ratio* = 7, *CL_{max}* = 1.5, and *throw velocity* = 22.15-ft/s. From this point, the team selected a power and wing loading combination that placed the UAS in the feasible region, seen by the green circle in Figure 11. A power loading of 45-W/lbs (10-W/N) and a wing loading of 1.3-lb/ft² (60-N/m²) was selected, as they represent the most optimal design parameters with respect to the aforementioned constraint. To determine the actual sizing and weight of the aircraft, the "Electric Aircraft Weight Analysis" sheet provided by the course mentors was used. The weight analysis sheet shares many of the same parameters of the constraint hand launch sheet, with the addition of the power loading, wing loading, and other parameters used to specify the mission profile. The electric aircraft sizing sheet outputs the weight, wing area, and wing span. From this point, the airfoils for each of the lifting surfaces could be determined, along with tail sizing.

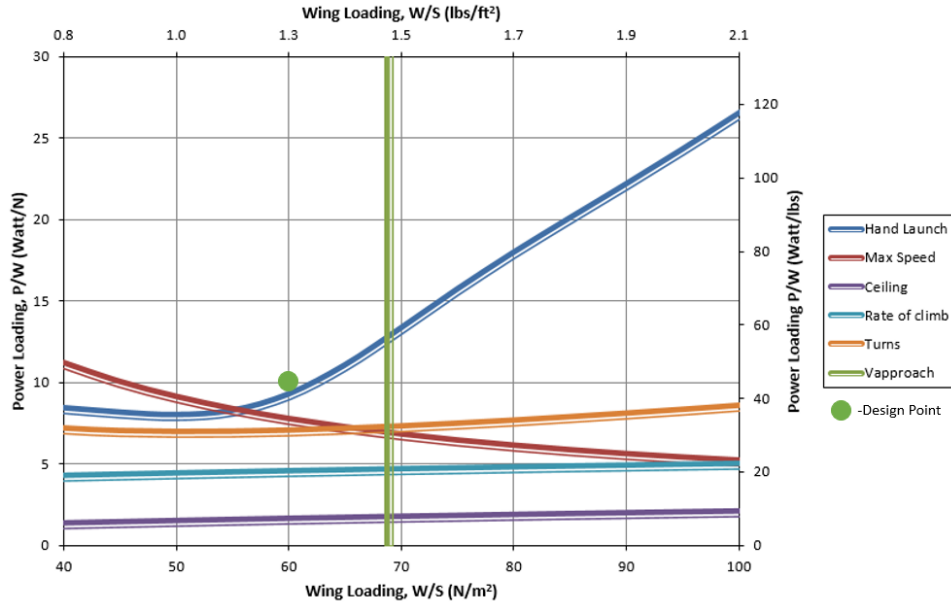


Figure 11: Electric hand-launch UAS constraint diagram

3.2 Airfoil Selection

The initial process for selecting the airfoil for the wing was evaluating the airfoil selection for similarly sized UASs currently on the market using publicly available data. Doing this, 9 airfoils were selected from current market designs similar to the performance needs of SAILR. These included the AG12, AG35, CLARK Y, HOBIESM, ISA571, ISA960, NACA 6412, S9000, and S9037. XFLR5 was used to determine flight characteristics of each airfoil. These characteristics included coefficient of lift, coefficient of drag, coefficient of moment, and lift over drag ratio. All of these characteristics were set as functions of the angle of attack so that the characteristics could be seen as alpha changes.

Determining which airfoil to use from the data was based on the lift over drag ratio for the airfoils. By calculating what the cruise coefficient of lift would be for the aircraft, which was calculated to be 0.6, the angle of attack was found from the XFLR5 plot of coefficient of lift versus angle of attack shown in Figure 12. Then, from that angle of attack and the lift over drag versus alpha plot, the lift over drag ratio was identified for the needed angle of attack. The deciding factor for the airfoil was how close the lift over drag ratio for the needed lift was to the maximum lift over drag ratio of the airfoil and if the airfoil can cruise at a small AOA.

This process was repeated for each of the possible airfoils to identify the best fit for the mission needs. After analyzing each airfoil at the low Reynolds Number of 256,538, determined for the cruise velocity of 33-mi/hr with chord length 10", air density of 0.002377-slugs/ft³, and dynamic viscosity of 3.737×10^{-7} -slugs/ft-s, the S9000 airfoil was selected as the best choice of airfoil for the wing. Note that later in detailed design, the chord length was increased to 12" to achieve more lift. A study was not completed if the increased chord length would change the optimal airfoil selection because the Reynolds Number only slightly increases to 307,858, so the effect was assumed to be minimal.

The airfoil choices for the vertical and horizontal tail surfaces were also based on current

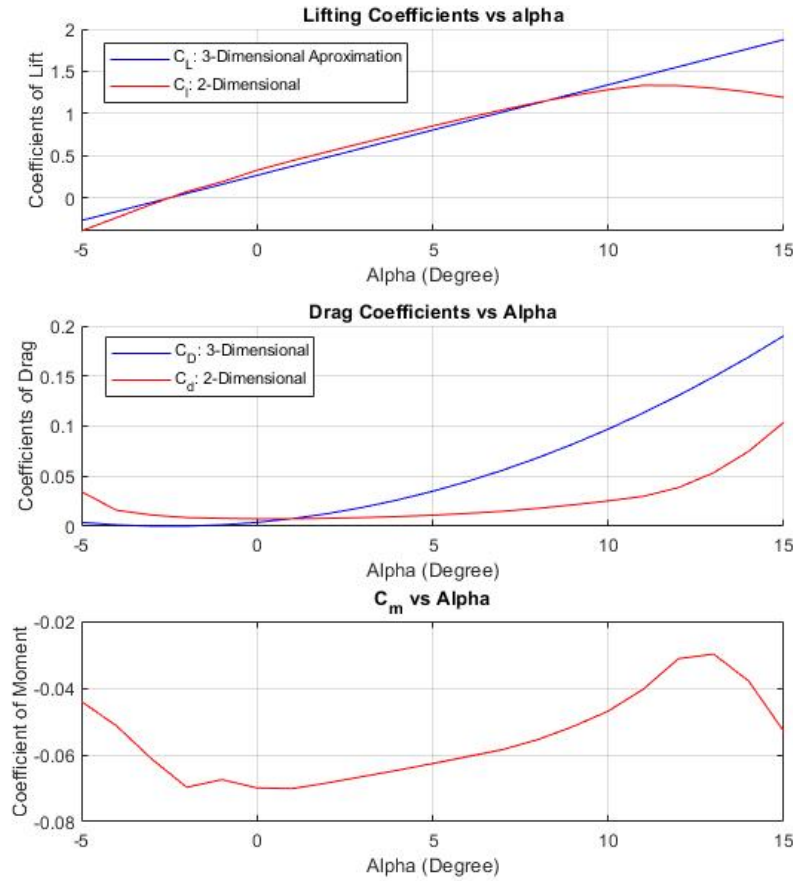


Figure 12: Coefficient plots

market designs as well as other research on building tail surfaces. For the vertical tail, the NACA 0010 airfoil was chosen since the only restriction was that it needed to be a symmetric airfoil. For the horizontal tail surfaces, the NACA 2210 was chosen based on it being an asymmetric and thin airfoil. Asymmetric airfoils produce lift at zero angle of attack allowing the airfoil to be carefully selected to give the right amount of tail force at cruise, resulting in zero elevator deflection. Because of mounting schedule pressures that resulted from a detailed study on candidate airfoils, a horizontal airfoil tail was selected that would achieve the job without deeply studying a swath of candidate orientations and airfoils.

3.3 Stability

The stability of an aircraft is directly affected by the tail sizing, wing sizing, and placement of both. The stability of the aircraft is also a mission-critical component that significantly affects aircraft performance. With a good tail trim position, the aircraft will be able to cruise efficiently. On the contrary, the aircraft would have to use more power in cruise, resulting in reduced endurance and range, for poor trim positioning. With the selected configuration of a pylon motor mount, the thrust vector is above the centerline of the aircraft. This displaced thrust vector creates an induced downward pitching moment. The AVL stability analysis software was used to estimate the aerodynamic stability parameters. The AVL simulation accounted for the additional pitching moment to confirm the appropriate tail size and placement. Special consideration will be given to $C_{M\alpha}$, $C_{L\beta}$, and $C_{N\beta}$ stability derivatives as they heavily influence the aircraft's overall stability.

3.3.1 Definition and Assumptions

The stability analysis was started by reviewing the mission type. As defined by the mission type, the aircraft needs to be stable for long cruise flights. This mission type means that the static stability margin should be defined so that the aircraft is stable while still having suitable maneuverability. Due to the mission type, a static margin of 15% was chosen as that will give the right amount of maneuverability and stability in cruise.

The aerodynamic stability is tightly coupled with the weight and balance of the aircraft. The two main factors are the A.C. of the airfoil and the C.G. of the entire aircraft. For static stability in forward speed, the C.G. must be placed in front of the aircraft's A.C. This C.G. placement allows the moment force from the wing and the tail to be appropriately balanced. The x displacement of C.G per chord length is 0.25 (X_{CG}/C).

3.3.2 Tail Configuration

The pylon mounted propulsion system brings about many unique design challenges. The displaced thrust vector from the center-axis causes an induced pitching moment. This causes the tail to need much more control effectiveness, especially at take-off and lower speeds. To this end, it was hypothesized that a T-tail configuration will allow the propeller wash to generate the extra effectiveness required for the aircraft to be controllable in those flight conditions.

Some preliminary analysis was performed using AVL to determine the tail geometry that will give the desired handling qualities. Using AVL allowed the team to quickly observe the impact to the overall flight dynamics of the aircraft by changing geometric properties of the model. The initial size of the tail was estimated based on other RC aircraft and what looked proportionately correct. With AVL, parameters including the tail boom length, horizontal stabilizer span and chord, and horizontal stabilizer incidence angle were varied in the AVL geometry file to achieve the desired stability derivatives. In the analysis, $C_{M\alpha}$ was the primary stability derivative that was tuned. The tail has been sized and can be seen in the drawings in Appendix K.

Using data from the AVL analysis, the C.G. location is at 15.58" measured from the nose of the aircraft (the calculations are provided in Appendix E). This is positioned in front of the A.C. which means the aircraft is stable for this tail. Current CG location based

off 3DEXPERIENCE shows $G_x = -13.25"$, $G_y = 2.75"$, $G_z = 0.26"$ and the measured CG of the manufactured aircraft was $G_x = -14.5"$, $G_y = 0.00"$, $G_z = -3.00"$ (both as measured from the nose of the aircraft). Due to the COVID-19 pandemic, the physical CG was not measured with varying the battery location (which was a feature of the slots cut in the payload board). This placed the CG before the AC, and with the weight of the aircraft being lower than anticipated, the stability of the aircraft was maintained with tail placement and sizing.

3.4 Control Surfaces

With a given aircraft sizing, control surfaces of the aircraft were estimated with the method adopted from *Aircraft Design: A Conceptual Approach* by Daniel P. Raymer (Raymer, 2004).

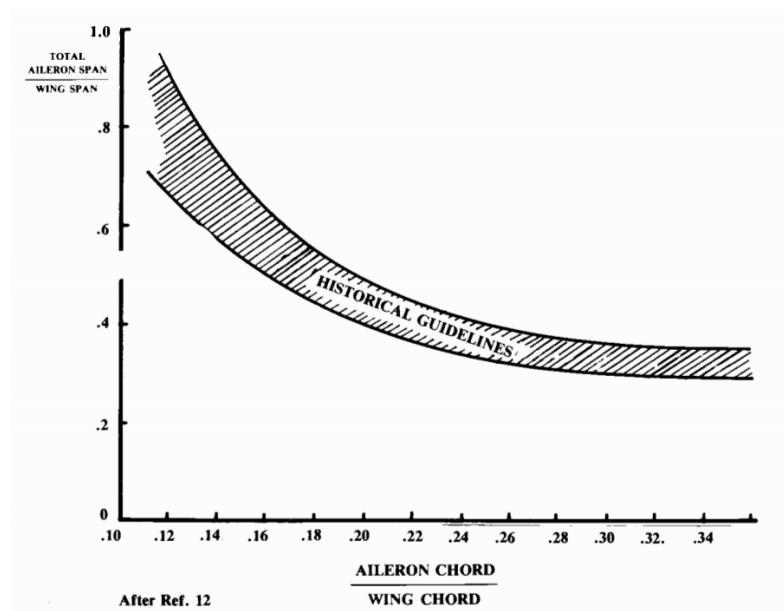


Figure 13: Raymer's tail efficiency graph

Using Raymer's tail efficiency curve, reproduced in Figure 13, control surface sizes were estimated. Figure 13 presents a range of ratios to size the aileron and wing span for a given chord ratio. Raymer claims that the elevator, rudder, and aileron for trainer aircraft should be 15 - 20%, 10 – 15% and 15 - 20% of the chord, respectively. After the chord ratio for the control surfaces was selected, the team referenced Figure 13 to determine span ratios. For instance, the aileron chord to wing chord ratio is 0.15 or 15%, and based on the historical guidelines, a range for the span ratio for aileron to wing could be between 0.55 to 0.75. A span ratio of 0.55 was selected for the initial control surface estimation. With it, the the control surfaces could be designed while maintaining the aspect ratio at full span of the wing. Since the UAS must be highly stable with no need to be agile and acrobatic, a trainer aircraft was selected as the base line for estimation.

Table 3: Aircraft sizing parameters

	Wing (in)	Horizontal Tail (in)	Vertical Tail (in)
Span	102.5	24	8.5
Root Chord	9	15	7
Tip Chord	6.5	46	5

With the final aircraft configuration, an identical standard of 15% control surface estimation was applied to design three different control surfaces: aileron, elevator, and rudder. Each of these control surface areas were calculated to be (aileron area), 27.9 in^2 , and 7.65in^2 . It was assumed that aspect ratio of control surfaces were identical to their parent surfaces to ensure easier manufacturing and control axis alignment. This design also allows the aerodynamic center for all control surfaces to be easily estimated since their relative location to chord would be the same as their parent surface. To maximize moment, the axis of all control surfaces were placed close to their leading edge.

3.5 Propulsion

The propulsion system was defined based on its relevant requirements. A Boeing requirement stipulated the propulsion mode must be electric, which is common for UASs of this size. Another driving factor in the propulsion design was the requirement for the acoustic noise to be below 50-dB to minimize disturbances to area wildlife. From the mission profile and constraint sizing, the standard mission time was expected to be 30-minutes. To account for varying weather, modeling inaccuracies, and other outside factors, a 15-minute reserve requirement was appended to the power system requirements; thus, the flight time requirement totaled to 45-minutes. Next, the propeller diameter must be minimized due to structural considerations with the pylon mounting method (smaller propeller diameter equates to a smaller pylon so the moment arm is smaller). To minimize weight, a LiPo battery pack requirement was defined since they have high energy density and are common in small UASs. LiPo battery cells are typically wired in series to increase the total battery pack voltage. This gives flexibility in selecting motor voltage. The nominal cell voltage of a LiPo system is 3.7-V, so a 4S battery pack is rated at 14.8-V (“xS” multiples the standard voltage (3.7-V) by a factor of “x” in a series arrangement). From these initial requirements and constraints, the propulsion system could be defined.

The propulsion system is made up of many components that each have their own performance characteristics that must be individually analyzed for the full system to be designed properly. These components include the propeller, brush-less DC motor, electronic speed control, and battery pack.

3.5.1 Motor & Propeller Sizing

The first step for motor and propeller sizing was to determine the cruise thrust required for the intended mission. The thrust required was calculated to be 1.44-lbf at 40-mph, which was acquired by using the non-linear drag model. Motor and propeller combinations could then be analyzed.

Five candidate motors from KDE were identified with kV ratings varying from 515-kV to 965-kV. By reviewing the performance charts for those motors, the cruise thrust was identified and current draw was interpolated. These values were entered into a mentor-provided Excel propulsion sizing sheet which defined the required battery size (more

information on battery sizing can be found in Section 3.5.3). The KDE2814XF-515 515-kV motor met all the requirements set forth for the propulsion system; it offered a low required battery capacity, low cost, light weight, and a wide range of usable propellers.

Based on the minimum take-off power loading requirement of 10-W/N (44.5-W/lbs), which was determined in the hand-launch electrical constraint sizing sheet, the required power for take-off is 378.3-W. Based on this analysis and data available from trusted vendors, an APC 11”x8” propeller was selected for the propulsion system which was later subjected to propulsion tests (see Section 7.3).

3.5.2 Electronic Speed Controller Sizing

For the KDE2315XF 515-kV motor and 6S battery selection, it was found that on takeoff, the UAS would be drawing at least 22.4-A of continuous current. A factor of 1.25 was tacked on upping the requirement to 28-A draw capability. The KDEXF-UAS35 (35A+) ESC is the recommended ESC for KDE2315XF motor and fits all the requirements which is why it was selected as the ideal choice.

3.5.3 Battery Sizing

From the power budget conducted of non-propulsion components in Section 3.8.1, the total estimated current draw in cruise was 1.32-A (1320-mA). Adding the required current draw from the propulsion system (6500 mA at cruise) resulted in a total system current draw of 7820-mA. To determine the required battery capacity $C_{Battery}$ in mAh, equation 1 was used.

$$C_{Battery} = I_{Battery} * t_{mission} \quad (1)$$

In the equation, $I_{Battery}$ is the total system current draw in mA (7820-mA) and $t_{mission}$ is the mission time in hours (0.75-hours). Equation 1 yielded a required mission battery capacity of 5865-mAh. Surveying online retailers, several 6S batteries were identified with varying capacities, C-ratings, and form factors. The C-rating was used to remove two GensAce branded battery packs from consideration; their cost was high likely due to the higher C-ratings, which were much higher than the mission requires. The Lumenier 6S 8000-mAh LiPo battery was selected primarily for the excess capacity that allows for margin in the flight time calculations, as well as increased current draw capacity if a larger propeller than initially considered is needed to meet the mission requirements. The 8000-mAh Lumenier pack has a higher capacity to cost ratio and capacity to weight ratio than its 6600-mAh counterpart. The form factor of the 8000-mAh battery pack is also better suited for integrating into the air-frame as the pack is long and slender, versus the cube shape form factor of the 6600-mAh pack. Therefore, the battery pack selected for use in SAILR is the Lumenier 6S 8000-mAh LiPo battery pack. The selected battery pack will be able to keep the aircraft aloft for an estimated 61 minutes of flight time.

3.6 Structures

The structure of the aircraft was very important to the durability and longevity of the aircraft. As a team, a large amount of time was spent determining how the structures of the aircraft were going to be manufactured. An equally significant amount of time was put into material selection. This section will review the process behind structural design decision making and structural design outcomes.

3.6.1 Design Considerations

Prior to starting the structural design stage, there were important considerations that were made. The most important design consideration that was made was the structural integrity in flight which came from the aerodynamic loads as shown in the V-N diagram in Figure 14.

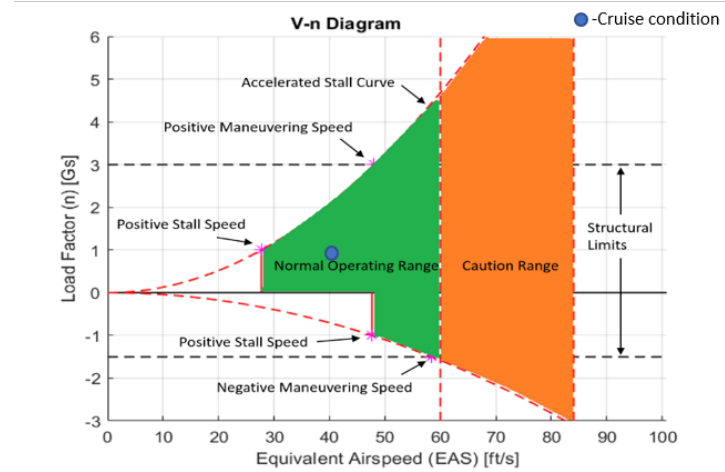


Figure 14: V-N diagram

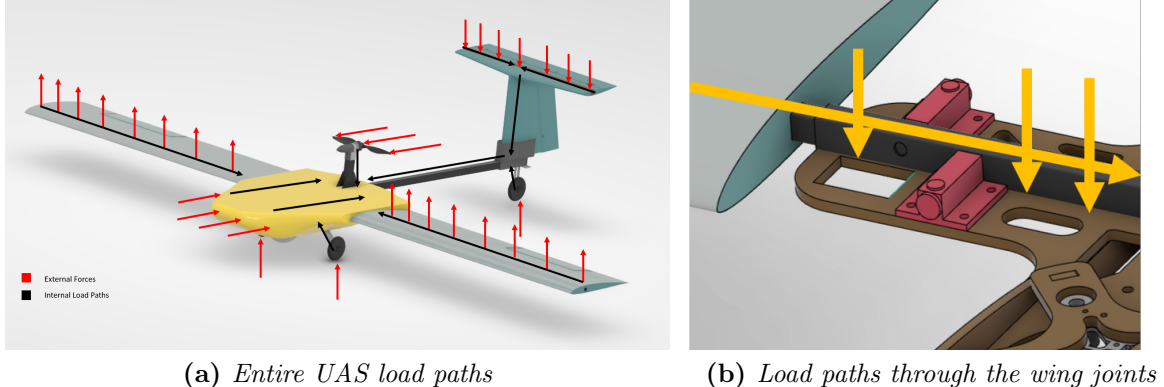
The V-N diagram shown in Figure 14 shows the flight regime for which the structure was designed to handle. An object under no load would have a load factor “N” of 1, representing the acceleration of gravity. The allowable structural range extended from +3 to -1.5 g. The curved red lines were the stall limits where flight is possible. Finally, operation between the maximum structural cruise speed V_{no} and velocity never exceed V_{ne} was structurally possible, but came with additional caution. For simplicity, gust conditions were ignored in this diagram.

This diagram dictates the structural strength required from each component. For this analysis to be satisfied, the wing, tail, motor, payload, etc. must withstand a force equivalent to +3 and -1.5 g.

Once the overall airframe loads were established, a load path diagram was made to show which structural members carried which loads. Figure 15 shows this diagram for the final design iteration. Note that loads due to lift were directly transferred to the fuselage insert tube. The latches just provided a left-to-right lock.

3.6.2 Design Decisions

The mission profile, payload, and concept of operation dictated the general shape and layout of the air-frame. More specific design decisions were handled by decision matrices which combined the importance and severity of many outcomes to yield a mathematical winner. There were two main aspects of the design that were considered when using the decision matrix, the materials and the method used to make the structure. For example, a decision matrix was made for the manufacturing method of the fuselage, as well as for the materials best suited for the fuselage.

**Figure 15:** Load path diagram

3.6.3 Design Outcomes

The outcomes from the decision matrices created can be seen below in Table 4. It consists of the major structural components that were decided on. The manufacturing method as well as the material for each component is shown. Some of the results from the decision matrices were changed over time due to different circumstances, for example the first choice for the tail construction was originally 3D printing, then the cost and weight penalty associated came to be an issue, so the decision matrix was reevaluated to yield the results of a glass slipper construction method.

Table 4: Design Decision Matrix Results

Decision	Winner	Runner-up	Leading Factor
Fuselage	Composite Shell	Wooden Box	Weight
Fuselage Materials	Honeycomb/fiberglass	Carbon fiber	Cost
Wing Construction	Glass slipper	Rig and spar	Manufacturability
Wing Materials	Foam/fiberglass	Honeycomb/fiberglass	Manufacturability
Tail Construction	Glass slipper	1-piece 3D-print	Cost
Tail Materials	Foam/fiberglass	PLA plastic	Cost
Spars	Carbon fiber	Fiberglass	Strength
Motor Pylon	Composite rod	Wooden rod	Weight
Wing attachment	Ball detents	Locking lever	Simplicity
Tail attachment	3D-print	Bolts	Rigidity

3.7 Payload

The purpose of the payload is to successfully and repeatably detect sea turtles. Numerous methods of identifying the presence of turtles were considered including looking for the animal itself, looking for their tracks from the ocean to the dry sand, and looking for their nests. While a robust model deployed in the field would likely make use of many detection scenarios, the team elected to detect the animal as a proof of concept to use in custom training the vision data set. This was based on the ease of creating a test object to create the training image set. The known mission constraints limit the time of flight to early morning before traffic on the drive-able sections of Daytona Beach. This is advantageous,

as it creates lighting conditions that elongate the shadows and increase contrast. Other flight characteristics, such as ground speed, altitude, and available power, outline major constraints for the design of the payload.

3.7.1 Architecture

The architecture is sub-categorized into three major sections: sensing, processing, and communication. Onboard sensor data is collected and processed on either the Raspberry Pi 4 or the Pixhawk 2.1. The Pixhawk communicates directly to the ground control station and is controlled either by the ground operator or autonomously via the QGroundControl software. The Raspberry Pi 4 communicates the partially processed images, position data, and camera orientation to the computer vision server via an LTE hat. The server collects and processes the images & data and passes the necessary information to the image with GPS coordinates of a positive sighting. The connections are shown in Figure 16.

3.7.2 Sensing

The aircraft has onboard sensors for GPS, airspeed, camera orientation, ground imaging, and battery management. Images are taken on the IMX219 at 1080x1920 resolution. The camera communicates to the Raspberry Pi 4 over camera serial interface. The Raspberry Pi also gets camera orientation information over I2C from the Storm32 brushless control board. The Storm32 utilizes a 9-axis IMU for its position information. It was determined that a minimum requirement for the camera would be 15 frames per second at 1080p resolution. The resolution allows for a ground size of 0.5" per pixel, giving more than enough resolution to correctly identify tracks (usually 2.5'-3.5' across (*Information About Sea Turtles: Loggerhead Sea Turtle*, n.d.)). GPS position is retrieved from the Here2 GPS module from the Pixhawk 2.1 and communicated to the Raspberry Pi via UART. Airspeed and battery management directly communicate to the Pixhawk 2.1.

To combat NVH, which can severely damage certain electronics and have major negative impacts on others, all the electronics were secured inside the fuselage with vibration-isolating mounts. Furthermore, to improve sensor data integrity, all data lines are twisted pairs, and run separately from power connections, with as few connectors as possible.

3.7.3 Processing

Two key types of data are necessary to successfully accomplish the mission, image data and position data. Images need be analyzed to identify evidence of sea turtles, and the position of that evidence needs to be marked. To process the images and identify tracks, computer vision was utilized. Specifically, a neural network based on Darknet, an open source neural network, and YOLO algorithm. This neural network was trained using a mock test model due to the limited number of aerial images of actual turtles that were available. This architecture and a MongoDB database was ran on a remote server that communicated to the plane, in theory, through a LTE cellular network. The server utilized port forwarding and SFTP to send files securely between the two devices. This is the limit of where the prototype stage stopped due to COVID-19 induced complications. It was planned to process the images, GPS, and gimbal orientation data to determine the exact ground position of the suspected evidence of turtle activity. This was to be accomplished using simple trigonometry and the elevation of the aircraft (data received from the Pixhawk 2.1). The image with a bounding box and certainty, along with the GPS position would then be sent to the end user.

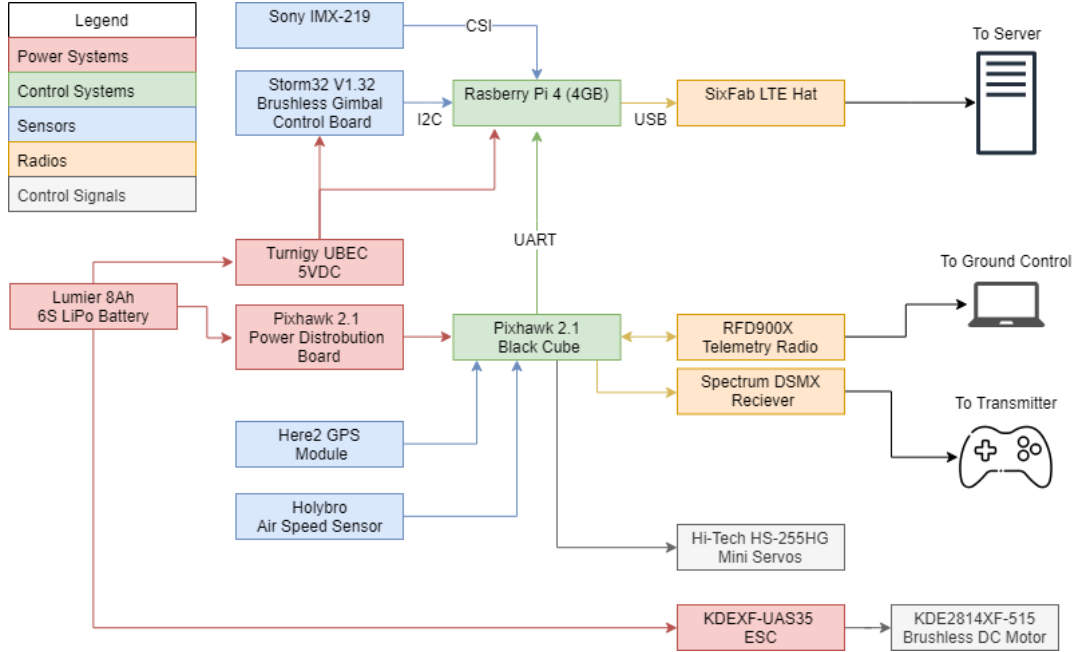


Figure 16: Payload wiring diagram

3.8 Controls & Electrical Design

3.8.1 Power Budget

Table 5 provides a breakdown of the estimated power consumption and required current draw of the electrical components on-board the UAS.

Table 5: Estimated power & current Budget

Component(s)	Power (W)	Voltage (V)	Current (A)
Raspberry Pi 4 Model B	6.4	14.8	0.432
STorm32 Gimbal	2.1	6	0.35
Sony IMX219 Camera	0.3	3	0.1
Servos (6)	14.4	6	2.4
RFD-900 Telemetry Radio	4	5	0.8
Pixhawk + add'l components*	2.5	5	0.5
Total	29.7	—	—

* Additional components included the digital airspeed sensor, Here2 GPS Module, the LTE hat, and the RC receiver, all of which were considered to be low-power devices.

Data regarding current draw, operating voltages, and power consumption for each non-propulsion component was collected using their respective data sheets. Current draw and power consumption for the Pixhawk and additional components were estimated, as these values were not available in their data sheets; they were assumed to be low-power devices that did not draw a significant amount of current. For components where power consumption was not given, power (P) was calculated with Ohm's Law with respect to voltage (V) and current (I), given by equation 2.

$$P = I * V \quad (2)$$

The power consumption of each component was summed to calculate an estimated total power consumption of 29.7-W. To calculate the total current draw, equation 2 was rearranged to solve for current. Using a battery voltage of a 6S battery (22.5-V), Equation 2 yields an estimated total current draw for non-propulsion components of 1.32-A, or 1320-mA.

3.8.2 Controllers

The Pixhawk 2.1 with a Black Cube (Figure 17a) was chosen as the flight controller for the UAS. The Pixhawk 2.1 was chosen over the Pixhawk 4, the alternative option, due to its IMU redundancies, simplified power distribution, and its flexibility with using legacy flight controller software (ArduPilot). Another benefit of the Pixhawk 2.1 is its use of the Cube to house all the flight controller hardware. The Cube opens the possibility of condensing hardware into a smaller form factor (i.e. a PCB) when scaling up manufacturing; the Pixhawk 4 flight controller hardware is fully integrated within the Pixhawk itself and cannot be modified.

3.8.3 Radio Communications

An RFD-900 (Figure 17b) was chosen for telemetry radio communication with the ground station due to its long-range communication capabilities. Long-range communication was critical due to the design requirement for flight range (at least 24.9-MI from launch site). Alternative solutions for telemetry communication (such as the Transceiver Telemetry Radio V3) did not provide evidence to support the long ranges necessary for the mission. RC communication capabilities is to be implemented via a Spektrum SPM4648 RC receiver to provide users with the ability to manually control the UAS if autonomous operation behaved unexpectedly or was deemed unnecessary for a specific flight.



Figure 17: Control system components

A detailed wiring schematic depicting the layout and connections between the Pixhawk 2.1 and the described sensors and components, control surface servos, and the on-board microprocessor is shown in Figure 20.

3.9 Collection of Significant Preliminary Design to Detailed Design Changes

The team faced cyclical trade off challenges in the detailed design phase. The tail increased in size to counteract the motor pitching, but this increase in size added more weight, so the wings also increased in size to provide more lift. Calculations were showing the takeoff speed needed to be 31.8-ft/s. The team became concerned that as the

weight increased and the wing span increased, it would become difficult to throw the UAS and achieve that takeoff speed. A test was conducted that heavily informed the decision to switch the mission to a wheeled takeoff.

Shown in Figure 18 is a glider made of scrap wood that weighed 8-lbs. This was thrown 5 times into the wind and 5 time with the wind. The wind velocity was unknown. The throws were recorded with speeds shown in Table 6. By averaging all the throws, a net no-wind velocity was determined to be 16.6-ft/s. This was significantly less than the required 31.8-ft/s needed, so the team elected to switch to a wheeled takeoff. Resizing the entire plane was considered; however, this was deemed a lesser option considering the time constraint the decision was made under ahead of the MRR.

Moving away from a hand launch was helped by considering that the stakeholder will ultimately be the one to throw the plane in the field. To ensure a high successful launch rate, the plane would need to be easy enough to throw for an average adult. The individual throwing the wooden glider stated it was uncomfortable to throw which helped steer the team completely from hand launching a plane of this magnitude.



Figure 18: An 8-lb glider made from scrap wood

Table 6: Wooden Glider Speed Test

Throw Number	Speed with wind (ft/s)	Speed into wind(ft/s)
1	16.1	13.3
2	19.8	12.8
3	17.7	14.4
4	21.4	10.9
5	21.4	18.6

This change was reevaluated against the concept of operations. The wheeled takeoff was deemed acceptable due to the prevalence of beach access driveways and compacted sand that could be used to takeoff. It was checked that the UAS would meet the minimum takeoff distance requirement of less than 200-ft. The calculated distance for the final plane, weighing 10.5-lbs, was 33.6-ft.

When reviewing the concept of operations, the team identified a change that would help the team reduce weight in the form of less battery capacity. Previously, the concept of operations called for an out-and-back style mission. Recognizing the identified nests would need to be marked, the team engaged with the stakeholders and proposed the UAS land at the end of its surveillance path. The autonomous operation would be monitored by a passenger in a follower vehicle which requires a 14 CFR part 107 waiver. This saved the return journey, permitting a one-way flight of 15-mi taking about 30-min (with reserves).

Despite this, an effort was still being made to reduce weight. One such effort was switching the image processing from a slightly heavier but computationally superior NVIDIA Jetson TX2 to a Raspberry Pi. This required the vision processing to be conducted off board using a Raspberry Pi LTE hat instead of on-board with the TX2. This saved 0.12-lbs, which was negligible in hindsight, but in the moment, the team was looking to cut any weight possible.

4 Components & Assemblies

This section details the final structural design and electrical design of the UAS.

4.1 UAS Assembly Drawing

A full assembly drawing of the SAILR UAS is shown in Figure 19. Exploded views of the full assembly, as well as additional drawings for major sub-assemblies, are provided in a drawing package located in Appendix K. An engineering bill of materials is provided in Figure F.1.

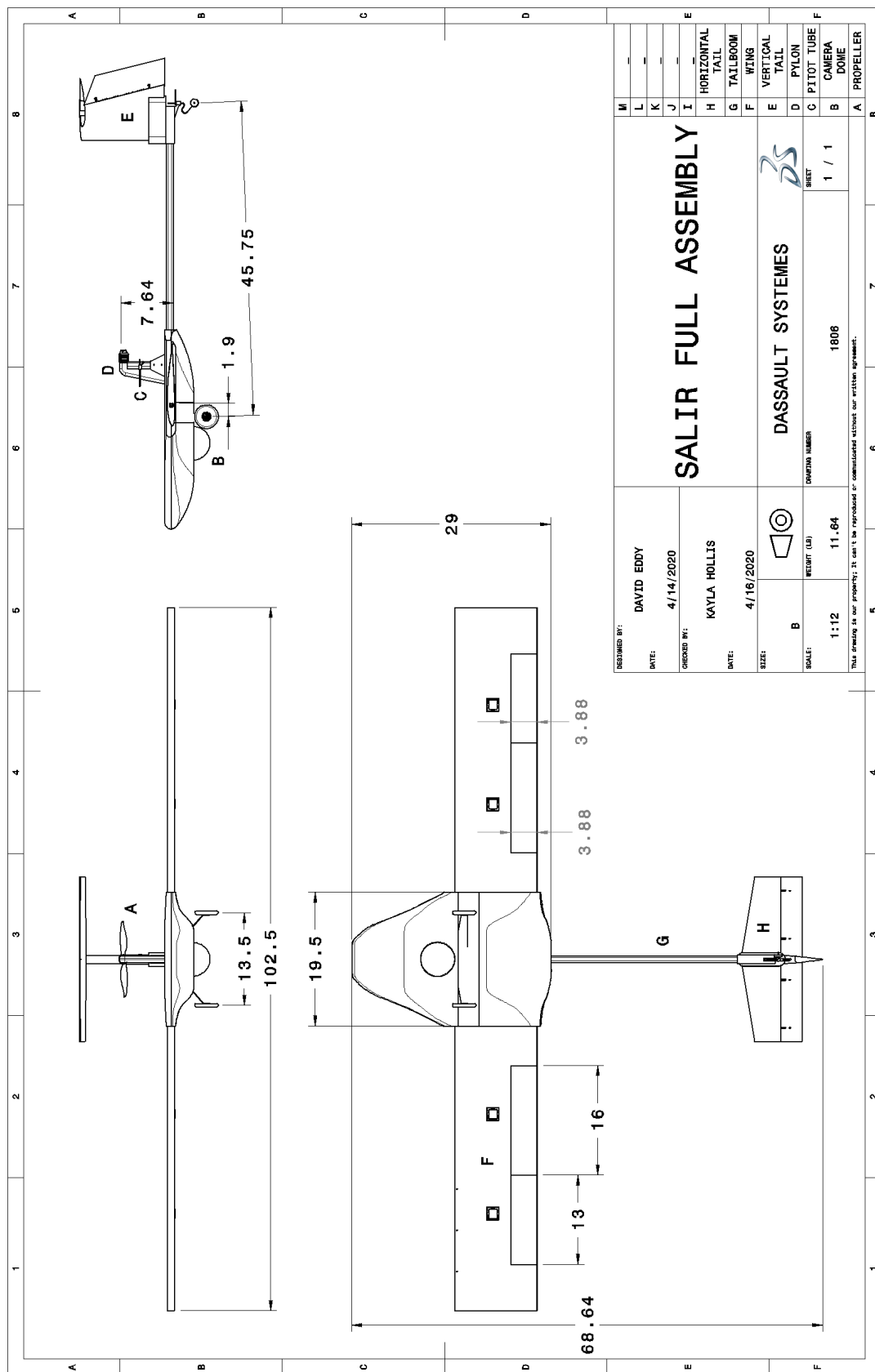


Figure 19: SAILR 3-view Drawing

4.2 Wiring Diagram

A full wiring diagram detailing the required electrical connections from the battery to the payload, sensors, control systems, actuators (motor and servos), and avionics systems is shown in Figure 16. Note that an electronics bill of materials is provided in Figure F.2.

Additional sensors connected to the flight controller for retrieving state parameters include a Here2 GPS module (Figure 17c) for GPS tracking of the UAS and a digital air speed sensor with a pitot-static tube to monitor air speed during operation.

A wiring diagram of just the controls components and their interfacing path with the Pixhawk is shown in Figure 20.

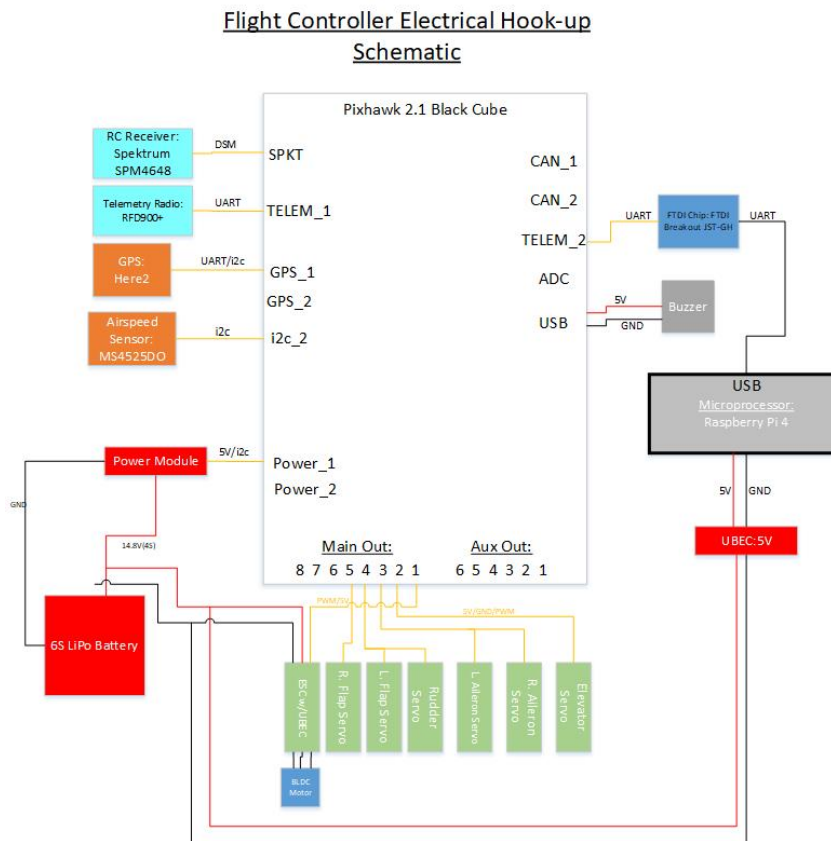


Figure 20: Pixhawk 2.1 wiring schematic

5 Production Plans & Manufacturing Process

5.1 Production Overview

In order to move through the manufacturing process smoothly, three tools were used: a detailed build schedule, a bill of materials, and job instruction sheets.

The build schedule outlined when each school should complete each build task, and how long it should take. This is provided in Figure 21. By planning the work that should occur each day, incremental progress was able to be tracked so an idea of the target ship date was always known. Weekends were not planned to have work done, so they served as catch up days. Additionally, the manufacturing programs team reviewed the plan at their weekly subteam meeting and made updates as necessary.

Date	ERAU	ISU	Purdue	Other events
1/26/2020				
1/27/2020	Talk to shop people	Talk to JoBo about CNC molds	Talk with foam cutter people	
1/28/2020		Talk to Matt about		
1/29/2020	Source Materials - Electronics	Source Materials - tailboom	Source Materials	
1/30/2020	Source Materials - Plate, fasteners	Source Materials - Composites	Source Materials	
1/31/2020	Source Materials - Wiring, etc.	Source Materials - Foam	Source Materials	MRR / CAD done
2/1/2020				
2/2/2020				
2/3/2020	Machine Payload board			
2/4/2020				
2/5/2020	Cut motor mount plates	Submit CNC mold work		
2/6/2020	Cut motor mount rod	Score honeycomb	source materials	
2/7/2020		Prep for composites	Cut Main Airfoil	
2/8/2020				
2/9/2020				
2/10/2020	Start motor mount drawing Mount gimbal to board	Composite layups	Order main wing spar	
2/11/2020	Order remaining parts discussed at 2/10 meeting)	Source landing gear tailwheel structure	Cut tail airfoil	
2/12/2020		Sanding/finishing fuselage shell	Cut tail airfoil	
2/13/2020		Double check all landing gear components	Cut tail airfoil	
2/14/2020		Cut fuselage into sections. Pre-drill mounting holes, landing gear slots.	Cut tail airfoil	
2/15/2020				
2/16/2020				
2/17/2020		Assemble fuselage parts	Insert Main spar and epoxy together	
2/18/2020	Motor mount part		fiber glass overlay of main wings	
2/19/2020	Start receiving orders		Fiber glass overlay of tail HT and VT	
2/20/2020			Put tail together.	
2/21/2020		Ship all parts		Flight Readiness Review
2/22/2020				
2/23/2020				
2/24/2020	Put fuselage fasteners into CAD			
2/25/2020				
2/26/2020			Ship all parts	

Figure 21: Day-by-day plan for manufacturing

The engineering bill of materials provided a single document reference for every part, quantity needed, CAD file name, link to the part, price, and more. This is provided in Appendix F. This helped the team see at a glance all the parts that were needed. Because the BOM also included the school that would need it for their respective subassembly, it was clear which manufacturing programs school representative was responsible for ordering it.

Finally, the job instruction sheets allowed team members to plan ahead to avoid in-work delays. These sheets provided information on the manufacturing process, tools and PPE needed, and step-by-step instructions. By thinking through the processes ahead of time, mistakes and time delays were likely reduced. A sample is provided in Appendix F. Job instruction sheets were created for the payload board, fuselage layup (a first version and second version incorporating learnings from the first version), wing construction, and tail construction.

5.2 Manufacturing

In order to evenly divide the manufacturing responsibilities, each university's students were assigned a part or parts of the UAS to build. This workload delegation was based on each university's capabilities and the members' availability. Each university was allotted two weeks to source materials, reserve lab space and equipment, and prepare for manufacturing. A further two weeks were allotted for manufacturing. Finally, a one week window was provided for ISU and Purdue to ship their completed parts to ERAU.

5.2.1 Embry-Riddle Aeronautical University

ERAU's main responsibilities were final assembly of the UAS and manufacturing of the payload board. This included integration of structural and electronic components. Team members laser cut a payload plate from 1/4" plywood. This plate served as the mounting platform for the electronics and an attachment point for the various UAS sub-assemblies. A nationwide COVID-19 shutdown prevented the team from continuing manufacturing on campus, so final assembly took place in team members' houses.

Analysis of FEA results on the loads carried through the payload board required a slight redesign. Due to the shut down, the redesigned board was not able to be created. However, an older version was repurposed to suit the needs where the increase in material was considered negligible added weight. The changes are better summarized with figures, as shown in Figure 22.

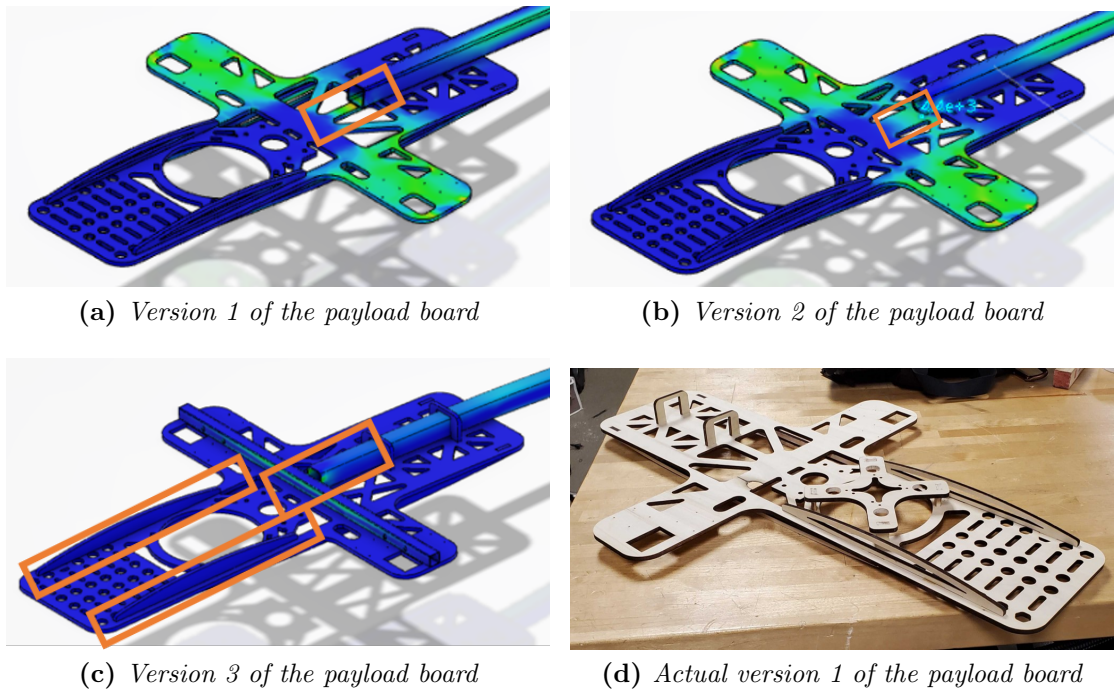


Figure 22: Payload board versions. Figure (a) was the original version. At a high level, FEA showed the area in orange should be stiffer, so the board was redesigned to Figure (b). COVID-19 restricted this board from being produced so the existing board in the team's possession, of Figure (a) was repurposed by manually cutting solid struts (previously, a section was removed from them) and lengthening the tail boom to meet with the spar.

5.2.2 Iowa State University

ISU was responsible for the fuselage shell. The shell design allowed a strong, aerodynamic shape to be used with lower weight and more internal space compared to other fuselage options. 3-oz fiberglass was used instead of carbon fiber to allow radio communication through the shell. To increase the stiffness of the shell, a 1/4" Nomex honeycomb core was sandwiched between the fiberglass layers. The honeycomb core weighed about the same as one layer of dry fiberglass, but greatly increased the shell's rigidity. The fiberglass, honeycomb, and epoxy were wrapped around the upper and lower positive molds and put under vacuum. The first attempt at the fuselage shell successfully matched the multi-directional curves and produced a stiff structure, but the 2.4-lb weight was well over the target of 1.5-lb.

To cut weight, a second shell was made with thinner honeycomb (1/8" thickness) and carefully weighed epoxy. Instead of brushing the epoxy onto the fiberglass while on the mold, the epoxy was spread evenly through the fiberglass cloth to form a "pseudo-prepreg" fiberglass layup. This ensured any excess epoxy was removed before going under vacuum and not filling in the honeycomb air pockets. While noticeably more flexible than the first fuselage shell, the second shell weighed only 10.5-oz, or 0.66-lb; half the 1.5-lb target weight. Both versions are shown in Figure 23.



(a) Version 1 of the fuselage with 1/4" Nomex and pour-as-you-go epoxy
 (b) Version 2 of the fuselage with 1/8" Nomex and premeasured epoxy

Figure 23: Fuselage versions

5.2.3 Purdue University

Purdue University was responsible for manufacturing the wings, horizontal stabilizer, and vertical stabilizer, all of which shared the same materials and construction method; Foamular XPS 250, from Menards, served as the core by using a CNC hot wire to cut the airfoil. Control surfaces were manually cut from the parent wing using the hot wire following a semi-circular path that matched the wing as shown in Figure 24. This was done to reduce airflow separation over the section. A design for manufacturability decision was made to move the flaps and ailerons adjacent to each other (the control surfaces were resized as necessary) so the root and tip portions could be kept as a continuous airfoil

with the middle section being reworked to have both control surfaces removed at once, as shown in Figure 25. The carbon fiber spar was epoxied into the wings before the wings and control surfaces were separately covered with a single layer of 3-oz fiberglass, followed by the necessary post-processing. A complete wing is shown in Figure 26.

The length of square carbon fiber wing spar the design called for was not available in the size needed, so a wooden ferrule, measuring 2" in length was machined to a tight tolerance fit on one end and interference fit on the other. This was epoxied into place to ensure as homogeneous of a connection as possible.

The process was nearly identical for the tail airfoil surfaces. The only difference was that the control surfaces were not “nested” due to the swept nature of the surfaces. The joint was cut straight with the elevator tail being attached by tape and the rudder attached with elbow hinges.

Purdue’s responsibility also included installing the servos. Servo trays were used so that servos could be interchanged if needed. The pockets the trays sat in were cut using an end mill for a Dremel and ruler as a guide which ensured a clean fit. A pocket and control horn is shown in Figure 24.



Figure 24: Curvature of the Wing-Aileron Joint



Figure 25: One wing is shown separated into the root and tip sections with the third section, the center, having the control surfaces cut out.

6 Risks & FMEA

6.1 Risks

A tracking system was developed within 3DEXPERIENCE for risk management. The tool tracks the description of the risk, the impact number, the probability number, the risk

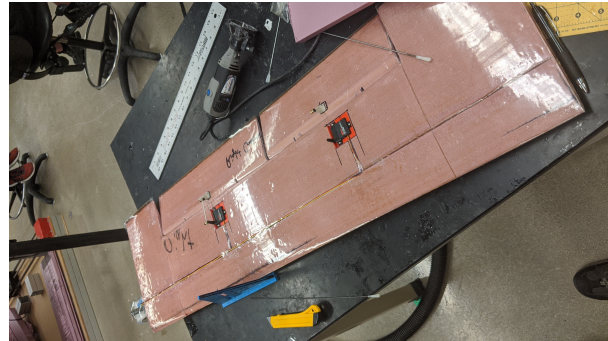


Figure 26: Completed wing showing control surfaces and servo installation

probability number, the abatement plan, and the measure of success. The risk probability number is the impact number multiplied by the probability number. This number is used to sort the risks from highest to lowest. The risks associated with this system have been properly documented to bring these issues to light and to aid in mitigation techniques.

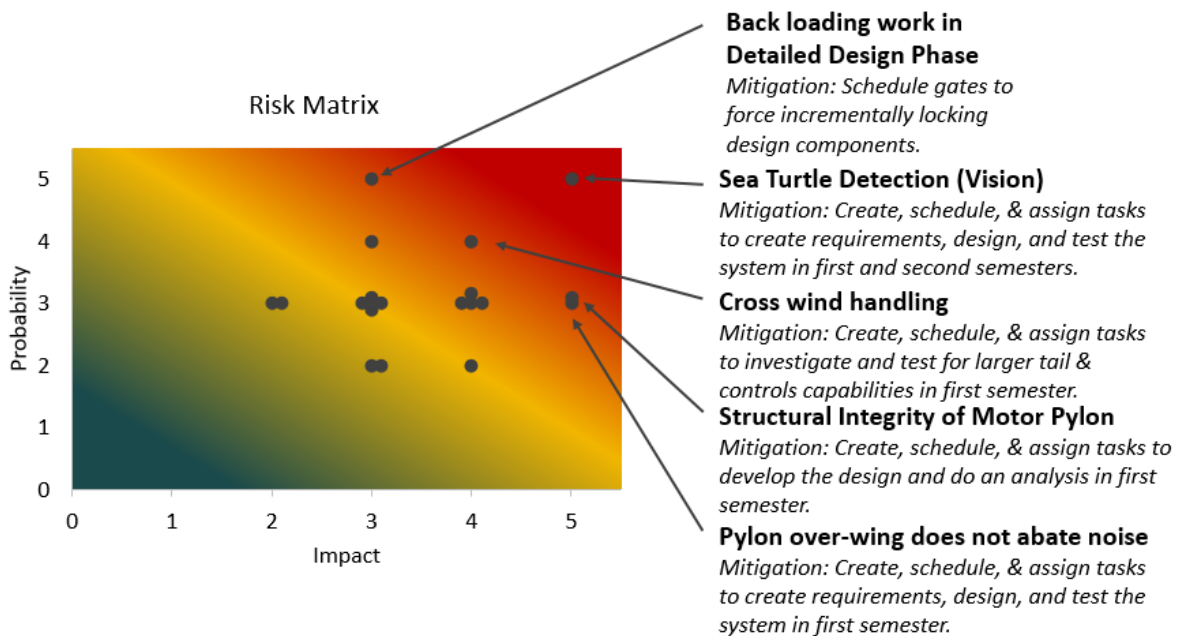


Figure 27: Risk matrix and major descriptions

The risk matrix can be seen in Figure 27, this shows the impact versus the probability and the colors indicate the severity. In Figure 27, the grey dots indicate risks, with major risks being described in the figure. A large number of these risks are medium to high in their exposure to the team; the abatement plan seeks to move the high- to medium-range risks to a lower-risk region. The complete risks analysis can be seen in the Appendix G.

It was intended to review and update the risks periodically; however, the time was never set aside to do that beyond the initial risk review. Updating it at the conclusion of the project has little value since everything already played out. The irony is that had time been set aside to periodically review the risks and create mitigation plans, the team likely

would not have had to treat many situations that emerged as high priority. This is a major lesson learned. To identify risks is next to worthless without creating mitigation plans (and reviewing their accuracy as they age) and periodically reviewing the risk exposure. To be clear, some risks were examined when making decisions; however, they were not logged and monitored. Tangentially, the COVID-19 impact to the project is a lesson in risk recognition. While it is impossible to identify every possible situation that could occur, it is reasonable to define “catch-all” scenarios and mitigate those. For instance, a risk could have been defined as “an external act mandating work stoppage”. In which case, the team would have been better equipped to handle the situation. This comes from the perspective that projects in the workplace generally must carry on even in times of crisis because they cannot afford work stoppages. Effective workplace leadership comes from properly preparing employees for even the most unlikely situations.

6.2 Failure Mode and Effects Analysis

Anticipating, identifying, and prioritizing failure in a system is a great way to limit failure modes that can occur. To limit the failures associated with the UAS, the FMEA methodology was used. The main difference between risk analysis and FMEA is that risks isolate an event while FMEA associates a system or device with an event. By using FMEA and risk analysis, the whole system and the components will be assessed for failures. To document this, an Excel sheet was created. This documents the component, the failure modes associated with that component, the effects of failure, severity, occurrence, detection, risk probability number, and lastly recommended actions. Members were solicited to complete this document.

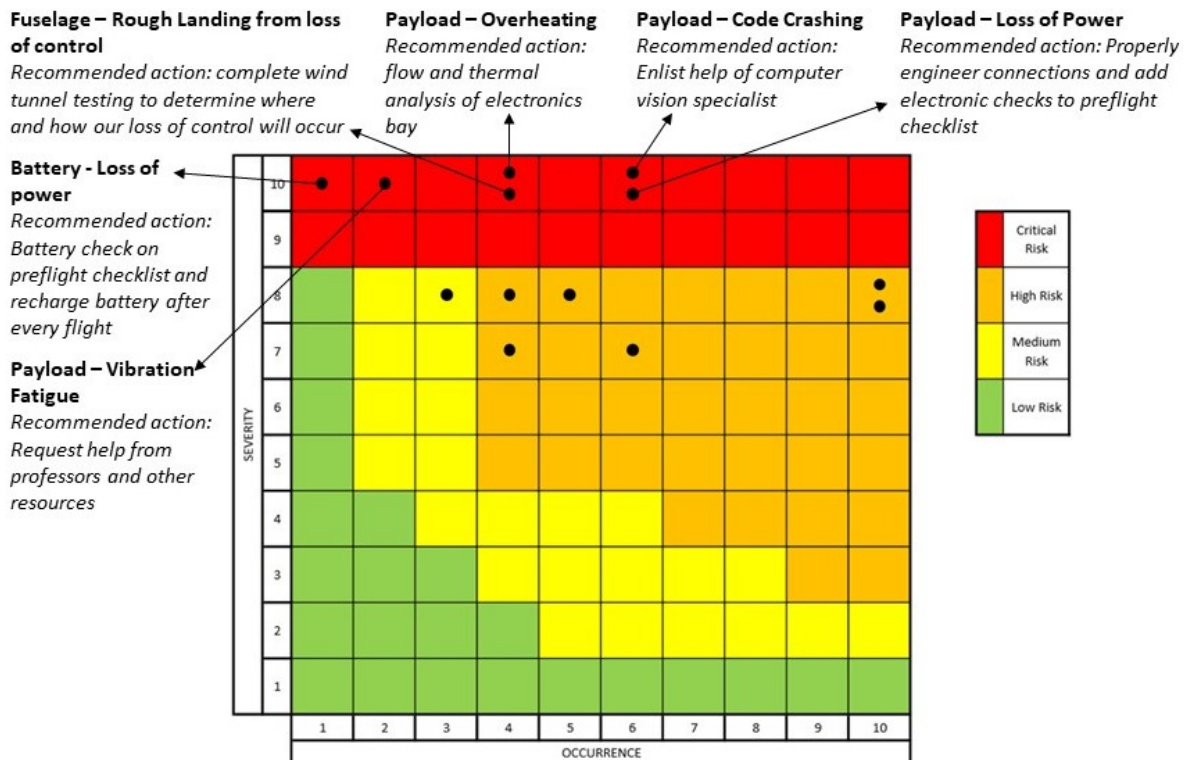


Figure 28: FMEA matrix and major descriptions

In Figure 28, the critical risks are pointed out with the recommended actions for each

risk. Each risk is associated with a component of the UAS. For example, a high risk concern is that the battery would cause loss of power; a way to combat that is to ensure it is charged after every flight and to check the voltage on the battery before flight. Such an action would transition this high risk to a low risk. Therefore, by doing this analysis, components that pose a high risk can be mitigated and moved from a high risk to a lower level of risk. Through this analysis, the correct actions and precautions will be taken to ensure the safest and most successful flight possible. The entire FMEA analysis can be seen in Appendix G.

Despite initial efforts to update the FMEA matrix, the effort fell to a lower priority to outright doing the work. Failure modes were being mitigated through FEA and subsystem tests and through discussions in making decisions. These were treated as necessary to substantiate a design in comparison to recognizing it as a failure mode mitigation step. Of course, FEA and testing is not the only way to mitigate failure modes, so this is another lesson learned in hindsight. Failure modes should be tracked throughout the design and development process with the FMEA matrix. The matrix, specifically the mitigation tasks, should be used to influence upcoming tasks. Much in the same way the team pursued traceability in purchasing with the workflow, traceability is desired in responding to recognized failure modes from an accountability perspective.

7 Verification & Validation

Every requirement was paired with a test procedure to ensure that requirement will be satisfied. Most system-level requirements were planned to be tested with a visual test on the ground or with data collected from a flight test. The verification status of each requirement can be found in Appendix H. Assembly of specific test plans and their execution fell to the responsibility of the Test and Evaluation team. This team was also responsible for determining any additional sub-system checks that may have been advantageous to complete before system-level tests.

Structural testing of the full-scale UAS was conducted theoretically using FEA in SIMULIA, and then paired with physical tests at Embry-Riddle. Unfortunately, the COVID-19 pandemic prevented the team from conducting all the physical tests planned for the UAS. Regardless, various elements of the structure were analyzed for structural integrity via tail boom bending, wing bending, and pylon bending.

In the fall, the team built a scaled glider prototype, with the intention of using the glider as a test bed for the full-scale UAS. However, due to poor glider quality and significant aircraft sizing and configuration changes, the glider was abandoned, and an off-the-shelf UAS with an over-wing motor (HobbyKing Bixler) was sourced and utilized as a test bed, instead. Power and controls components were installed on the aircraft to test the validity of the planned configuration. Autonomous flight testing conducted on the Bixler was of significant assistance to the team's efforts in developing autonomous operation of the full-scale UAS. However, the effects to the COVID-19 pandemic hindered the team's efforts to prove autonomous operation of the full-scale UAS, as well as to conduct system flights as a whole.

Static and dynamic testing of the propulsion system was conducted at Purdue University to ensure that measured thrust values from the propulsion system matched theoretical

values gathered from MotoCalc. Test procedures were written for noise mitigation testing to prove the effectiveness of the motor-over-wing design with blocking noise, but the test was unable to be conducted due to the COVID-19 pandemic. Wind tunnel testing was also conducted to validate airfoil selection and aerodynamics analysis, as described in Appendix I.

Operation of the payload was tested separately from the UAS throughout the semester. Unfortunately, the payload could not be integrated into the full-scale UAS before the COVID-19 pandemic enforced school closures. Work conducted on manual flight testing, which was also halted due to the COVID-19 pandemic, is also documented in this section.

7.1 Structural Testing

Structural tests were conducted with SIMULIA Static Test within the 3DEXPERIENCE platform on the bending of the wing, the pylon, and the tail boom in response to aerodynamic forces and motor thrust. Plans for physical tests were written up for each of these cases to serve as a parallel for FEA results, but some physical tests could not be conducted due to the COVID-19 pandemic.

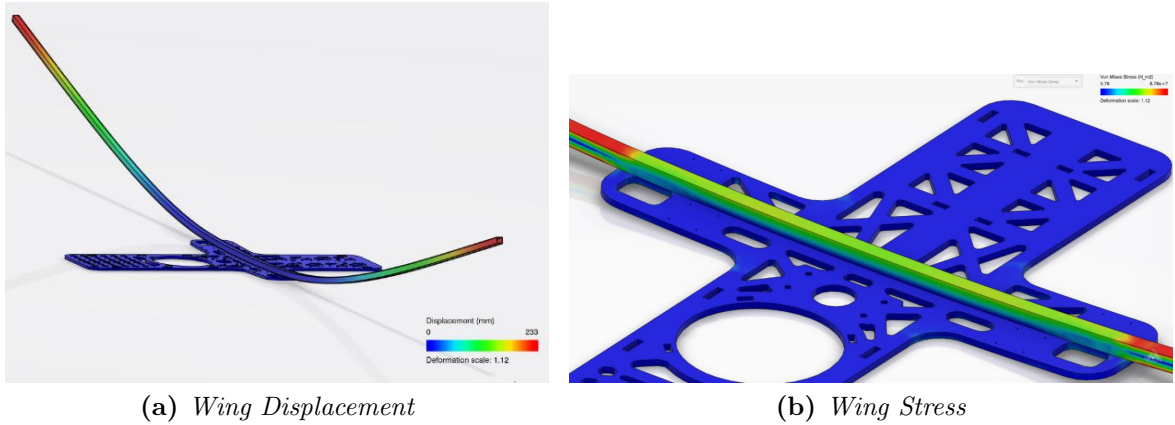
7.1.1 Wing Bending

The objective of this test was to determine if the payload board and wing supports would withstand the bending forces from the lift on the wing surfaces. Because of issues with getting the entire wing and payload board to run in the analysis, the model was simplified to only the carbon fiber structural members and the payload board by removing the foam and fiberglass layer from the model. The plate was fixed along the front and rear edges of the electronic board to allow for the electronics board to flex with the wing. Pressure was then applied to the bottom of the carbon fiber rods that would be equivalent to the lift force of the wing, which for steady-level flight conditions was 12-lbf.

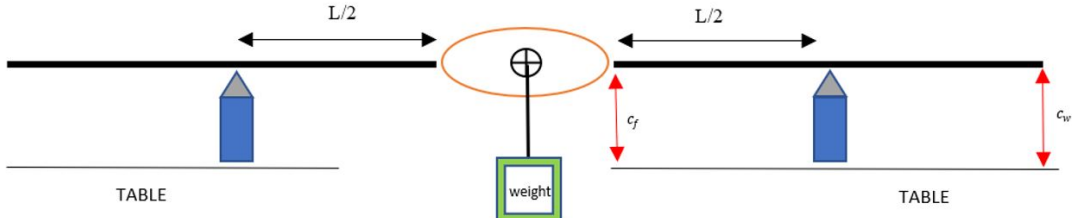
The results from the FEA showed that most of the bending stress from the wing was contained to the base of the wing to the electronics board, but the electronics board was not taking much stress from this force. The maximum stress in the carbon fiber spars was 12.76-ksi. With an ultimate compressive stress of 300-ksi, the factor of safety was 23.5. The deflection of the wing spars was at 9.15". from the 12-lbf lifting force on the wing. A screenshot of the wing displacement and wing stress from the FEA can be seen in figure 29a and figure 29b respectively.

Hand calculations were then performed to compare with the results of the FEA. From the hand calculations, the deflection of the spar should have been 7.7". After looking at the FEA, it was seen that the deflection measurement was taken from the fixed lowest point to the height at which the spar was deflected. Some of the difference in deflection came from the electronics board warping in the middle where the wings connect, causing the deflection to be higher. The calculated values can be seen in Table 7.

Physical bending tests were planned to be conducted, but due to the COVID-19 outbreak, they could not be completed. The original plan was to set up the aircraft applying force to the mid-span of each wing, mimicking the lift force on the wing. Weight would then be applied to the body until the weight reached 12-lbf. The setup for the test can be seen in Figure 30.

**Figure 29:** Wing Bending FEA**Table 7:** Wing Displacement Comparison

Applied Force (lbf)	FEA (in.)	Hand Calculation (in.)
2	1.525	1.288
4	3.050	2.576
6	4.575	3.864
8	6.100	5.152
10	7.625	6.440
12	9.15	7.728

**Figure 30:** Physical Wing Bending Setup

7.1.2 Pylon Bending

The objective of this test was to determine if the motor mount and pylon could withstand the thrust from the motor during flight. The base of the pylon was fixed for the analysis to replicate being fully adhered to the aircraft. A force of 3.6-lbf was then applied to the face of the motor mount, replicating the required thrust at takeoff.

Initially, the motor mount was planned to be 3D-printed with ABS plastic. Initial FEA showed that the stress in the pylon and in the motor mount was within the limits of the material, although there were some force concentrations on the motor mount. After presenting the results at the Manufacturing Readiness Review, a concern emerged regarding the potential risk of layers delaminating due to the stress. Another concern was how heat could affect the plastic in the motor mount. If the heat from the motor was too high, it could cause the motor mount to deform and ultimately fail. To reduce these potential failure modes, a redesign and material change of the motor mount was considered. The weight penalty was marginal by switching to aluminum. Ultimately the design shown in

Figure 31 was used.



Figure 31: Motor Pylon FEA Setup
Motor Pylon FEA Setup with 3.6-lbf force applied to face

In production, the aluminum mount was adhered to the motor pylon using Hisol bonding solution. The FEA was reran using the same constraints from the first test. The stress concentration in the motor mount was reduced significantly to 0.54-ksi. With an ultimate stress of 30-ksi, the factor of safety was 55. A screenshot of the FEA can be seen in Figure 32.

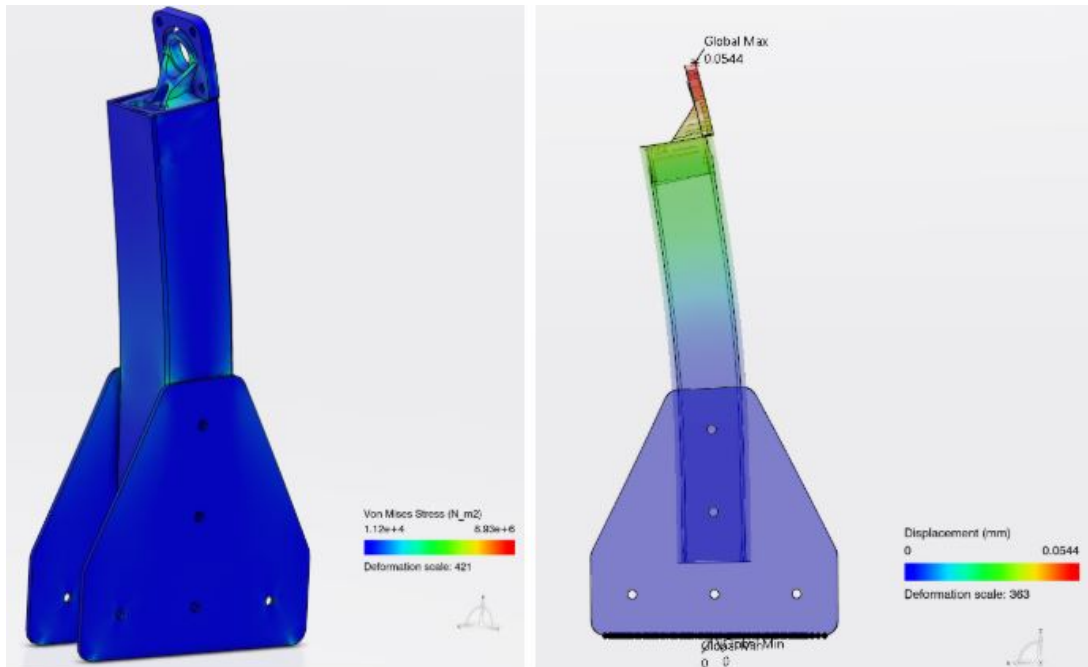


Figure 32: Motor Pylon FEA

7.1.3 Tail Boom Bending

The objective of this test was to determine whether the payload board and tail boom could withstand forces acting on the tail during flight.

To simplify analysis, all unnecessary components not contributing to the forces being examined were removed from the assembly, leaving the payload board, supports, channels, tail boom, the wing spar connector, and tail connector. All surfaces were fully adhered to one another to test the stress in the payload board and tail boom, rather than in the connections. A screenshot showing the FEA setup for this configuration is shown in Figure 33.

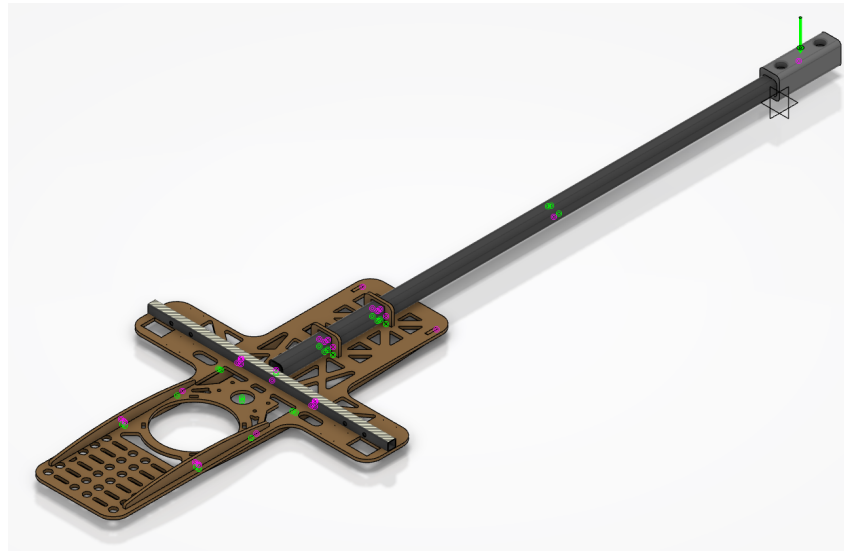


Figure 33: Tail Boom FEA Setup

The maximum expected loading was 1.6-lbf; this was derived from the motor generating a pitching moment of approximately 23.4-in-lb (6.5-in. above CG * 3.6-lbf thrust at takeoff = 23.4 in-lb), which would be neutralized by an approximately 0.6-lbf downward force from the tail ($23.4\text{-in-lb} / 39\text{-in. aft from CG} = 0.6\text{-lbf}$). An additional 1-lbf was added as a buffer to account for adverse conditions (steady, level, unaccelerated flight required 0.06-lbf downward force from the tail according to AVL). However, it was desired to test over the range of 1-lbf to 5-lbf to examine potential worst-case scenarios.

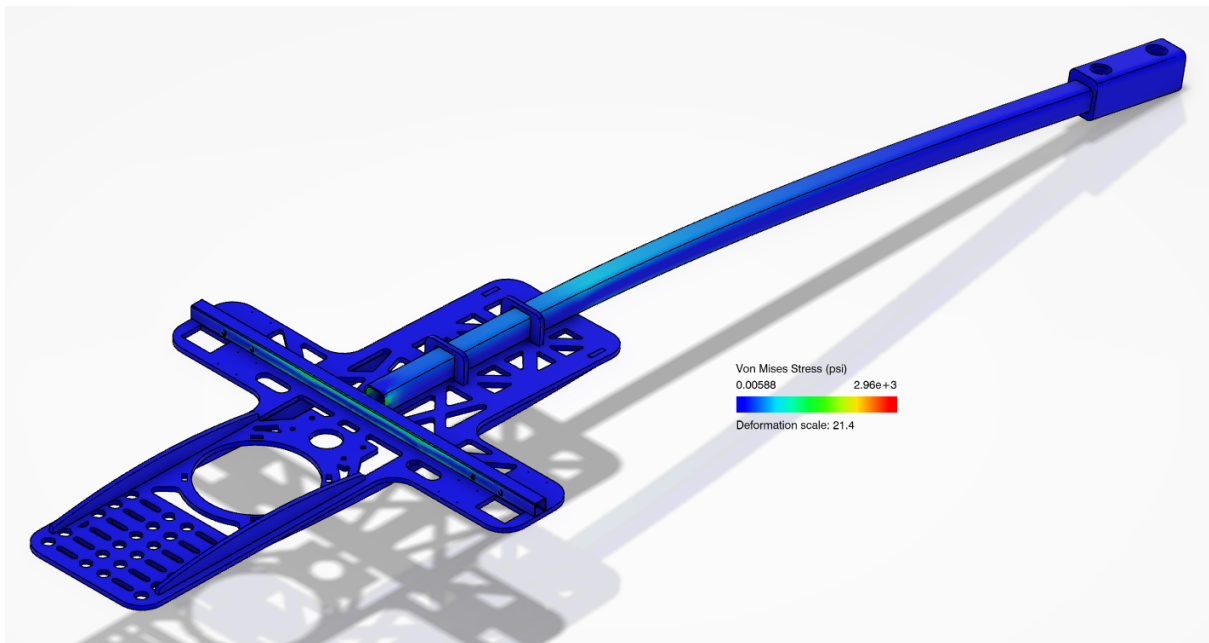
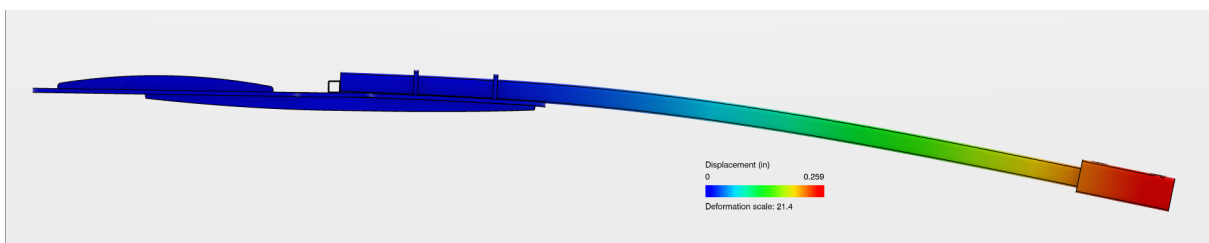
Forces were incremented by 1-lbf over a range of 1-lbf to 5-lbf, with an additional data point for a 1.6-lbf force, resulting in six total cases. The wing spar connector was fixed to simulate the constraint of the wing spars holding the electronics board in place within the overall UAS.

A physical test was conducted to supplement the results from FEA, but a data point was not gathered for 1.6-lbf due to the lack of precision available. Hand calculations were also conducted to serve as a parallel to FEA and physical results. A comparison of the collected displacement data is shown in Table 8.

Screenshots of the resulting von Mises stress distribution and deformation in response to a 1.6-lbf load are shown in Figures 34 and 35, respectively.

Table 8: Tail Boom Displacement Comparison

Applied Force (lbf)	FEA (in.)	Physical Test (in.)	Hand Calculation (in.)
1	0.162	0.472	0.215
1.6	0.259	N/A	0.345
2	0.324	1.023	0.431
3	0.485	1.496	0.646
4	0.647	1.653	0.861
5	0.809	2.165	1.077

**Figure 34: Tail Boom FEA: Von Mises Stress Distribution****Figure 35: Tail Boom FEA: Deformation**

In summary, the results from the physical test differed significantly than those collected from the FEA. A multitude of reasons could have resulted in the large difference observed. One potential source of error was the difficulty of duplicating the constraints in the FEA on the physical test. The wing spar connector could not be properly constrained physically, so the wing tabs and aft end of the board were constrained, instead. Additionally, during the physical test, the displacement resulted from the bending in the payload board itself, rather than the tail boom, which did not bend at all, while the FEA suggests the opposite should have occurred.

Since significant bending was only evident with a 5-lbf force during the physical test, the moderate bending observed in response to 1-lbf and 2-lbf forces show the results fell within the design parameters to be able to withstand an expected loading of a 1.6-lbf force.

7.2 Autonomous Flight Testing

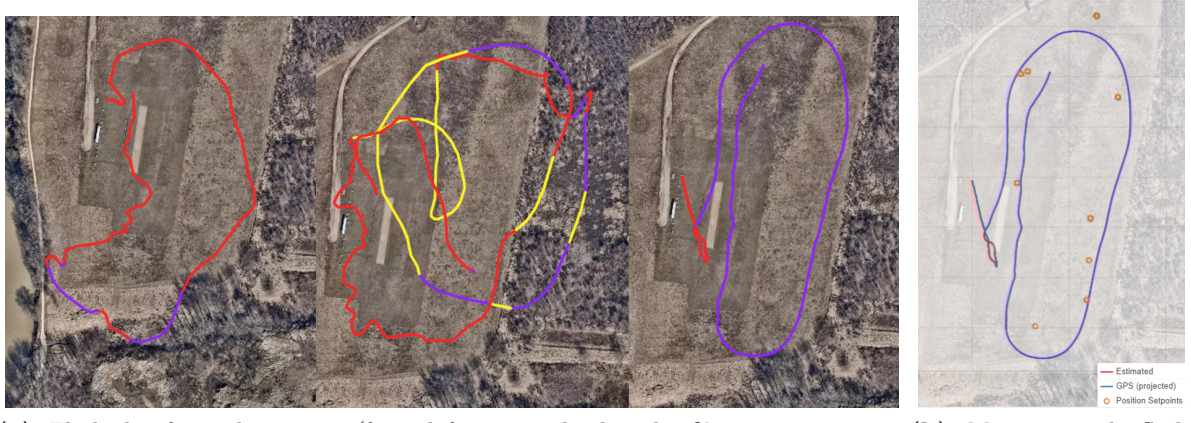
Testing of autonomous flight had three major objectives: Pixhawk and sensor setup validation, connectivity between the aircraft and the ground station, and validation of autonomous flight capability of the aircraft through Mission Planner. An off-the-shelf trainer aircraft (HobbyKing Bixler) was selected due to the similar propeller-over-wing configuration to the team's UAS. It was modified to house the Pixhawk, the sensors, such as the airspeed sensor and the Here2 GPS, and communication devices, such as the telemetry and Spektrum radio receivers. This is shown in Figure 36.



Figure 36: Modified Bixler Trainer Aircraft configured with SAILR avionics

A total of three different flight modes were tested for the Bixler through three different flight tests. The test started with manual control to prove that aircraft can fly under pilot control, than moved to altitude control to maintain stable, level flight while airborne. Once the Bixler passed these two tests, the team executed mission mode by assigning waypoints to the aircraft. All three flight tests were conducted under a certified pilot's supervision at McAllister Field in Lafayette, Indiana. The vehicle was intended to fly an elliptical path around the airfield. On the day of test flight, the aircraft experienced heavy wind gusts toward the east above treetop level, which made manual and altitude mode flight tests hard to maintain the planned flight path. However, under autonomous mode, the aircraft was able to continuously follow its planned trajectory and autonomously land at the specified location. The flight paths are shown in Figure 37.

Through the flight tests, the team was able to learn how to setup the aircraft for autonomous flight and also created a checklist to repeat the process for future users. A problem was discovered in the radio communication. Despite numerous successful ground range tests, the receiver would loose connection periodically being in range. A possible solution that was going to be explored before work halted was experimenting with the antennae orientation. Other than this, it was concluded that the avionics for SAILR were capable to conduct a fully autonomous mission without any human interaction along a pre-determined flight path.



(a) Flight log from three tests (from left: manual, altitude, & mission mode flight)

(b) Mission mode flight waypoints (orange dots) and actual recorded trajectories

Figure 37: Flight paths from trainer aircraft testing

7.3 Propulsion Testing

The objective of the propulsion testing was to confirm the results generated by MotoCalc during the design phase and to determine the effects of increased free stream velocity on the thrust output and power draw. The test included static testing and dynamic testing. Static testing aimed to confirm the thrust output and to determine the expected thrust output during takeoff. Static testing was conducted by mounting the motor and propeller onto the test stand, and operating it at varying speeds. The dynamic test aimed to confirm the effects of an increased free stream velocity on the thrust output and power draw. The motor was mounted in the Boeing wind tunnel at Purdue on the test stand as shown in Figure 38. The static test was performed in the wind tunnel on the same setup but with the wind tunnel turned off. To protect the motor, limitations were configured in the test stand program. The ESC signal range was set to be 1000- μ sec to 1900- μ sec. Pushing the motor above 1900- μ sec triggered the automatic cutoff of power.

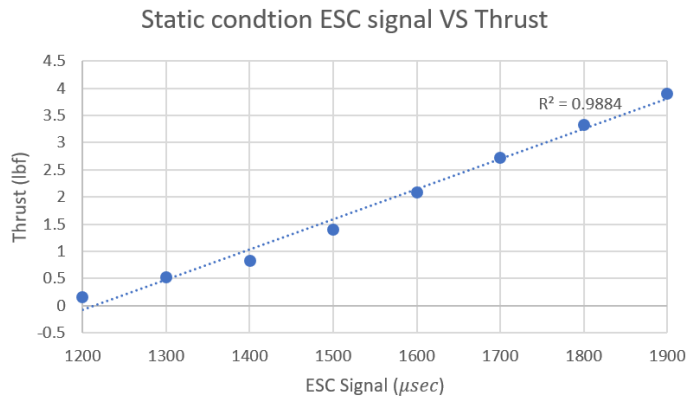


Figure 39: Static condition ESC signal VS Thrust

As shown in Figure 39, the static thrust data suggested that a linear relationship existed

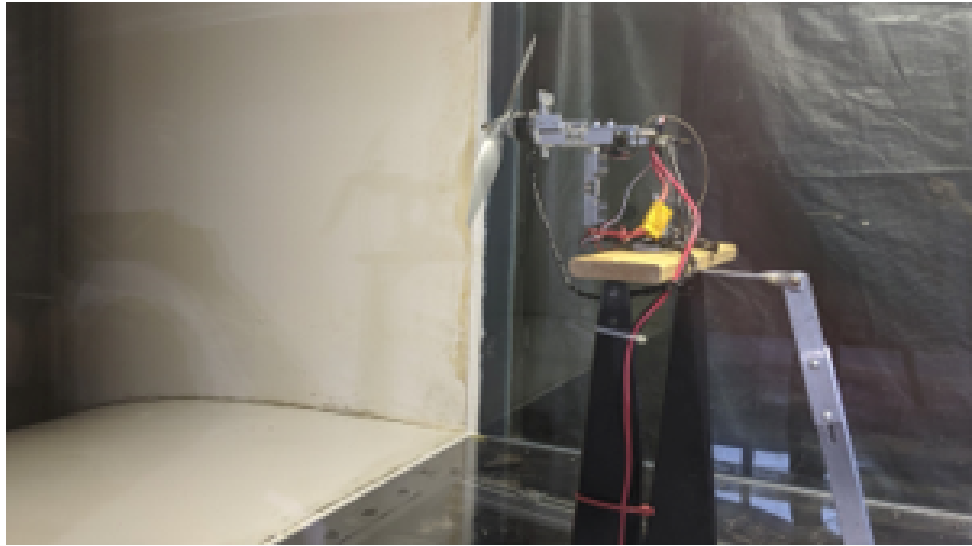


Figure 38: Propulsion wind tunnel test setup

between the increase in ESC signal and increased thrust. The data also suggested that 1200- μ sec was the lowest ESC signal necessary to overcome the magnetic forces in the motor. At 1200- μ sec, the motor generated 0.16-lbf, and at 1900- μ sec, the motor generated 3.90-lbf.

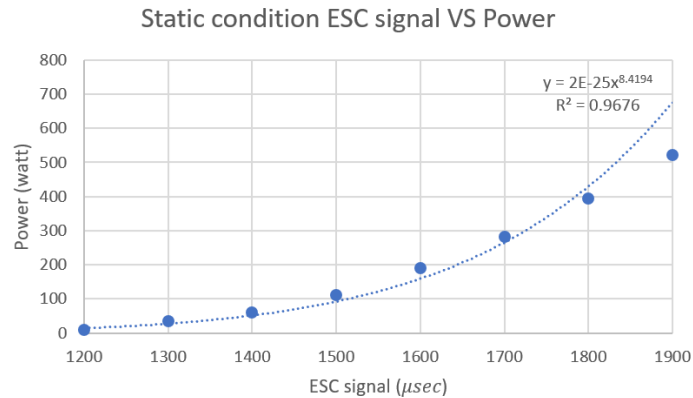


Figure 40: Static condition ESC signal VS Power

Figure 40 shows that the power draw had a powered relation between the increase in throttle and power draw. At the minimum ESC setting of 1200- μ sec, the power draw was only 9.0-W, but as the ESC signal increased to 1900- μ sec, the power draw increased to 522-W. These results closely resembled those generated during the design phase and, at some conditions, exceeded expectations with lower power and current draw.

Figure 41 shows the thrust recordings during the dynamic test. The results from different wind tunnel speeds presented on the same graph suggested that as the free stream velocity increased, the propeller produced less thrust proportionally. The data also suggested that as free stream velocity increased, the motor still performed with a linear relationship between the ESC signal and the thrust output. The most significant drop observed was when the tunnel speed increased from 50-ft/s free stream velocity to 80-ft/s free stream

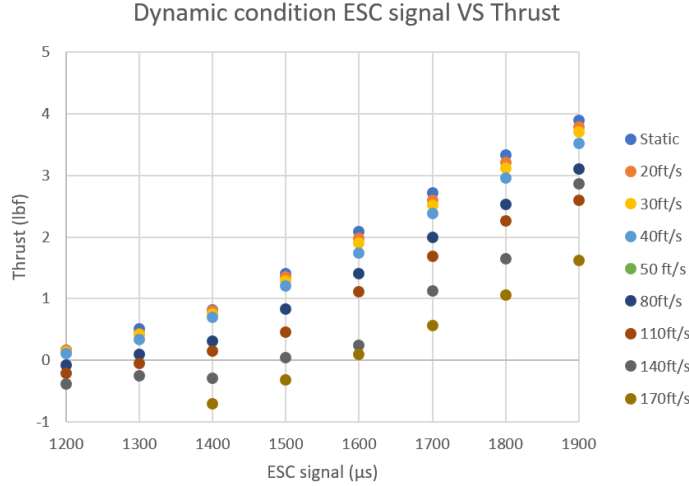


Figure 41: Dynamic condition ESC signal VS Thrust

velocity. The data also showed that from 80-ft/s onward, at 1200- μ sec, the propeller did not produce any thrust, and was windmilling, instead.

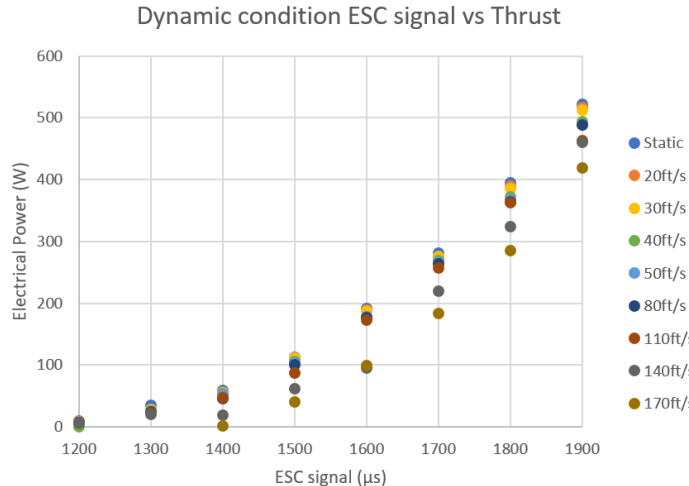


Figure 42: Dynamic condition ESC signal VS Power

Figure 42 showed that with increasing free stream velocity, the motor drew less power at the same ESC setting. This result agreed with the theory that the propeller and motor do less work when in a higher free stream velocity. The data suggested that when the free stream velocity reached 140-ft/s, the power draw dropped substantially.

In conclusion, the propulsion test confirmed that the motor and propeller combination would perform as expected from the detailed design. The data obtained from the test closely resembles the data generated from MotoCalc. The test also suggests that the motor and propeller should be able to provide the required propulsion for takeoff and cruise without drawing a substantially large amount of power from the battery.

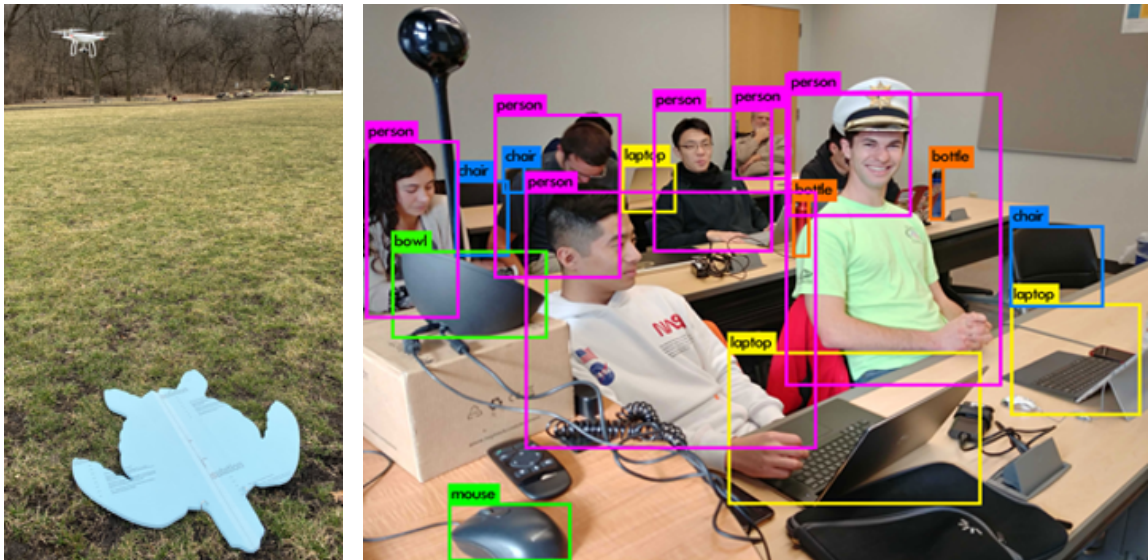
7.4 Payload Testing

Due to the COVID-19 pandemic, payload development was unable to be completed. As a result, the team was unable to validate the payload and vision system in totality. Instead, the validation efforts were shifted to a piecemeal perspective.

The Sony IMX camera interface with the Raspberry Pi was verified to be functional after merely plugging it in a member's Raspberry Pi.

A functioning LTE system and database were unable to be completed. The former required hardware locked in a lab, and the later was stalled by reduced help available when working remotely.

Progress was made in advancing the vision detection. The accuracy of the neural network is highly dependent on having quality images to perform the inference on, so validating the camera performance was of vital importance to achieve the desired performance of the neural network. Over 700 images were captured using a drone to train the object detection model. The test model, shown in Figure 43a, was intended to mimic an adult loggerhead turtle. Payload testing would have allowed us to create a proof-of-concept demo for the fly-off to show the capability of training the model on a custom dataset; however, the stock recognition capabilities were successfully configured as a stepping stone to a custom inference model. An example output to the stock capabilities is shown in Figure 43b. In the future, a higher-fidelity model would be created to detect an actual sea turtle nest as well as expand the model basis to include nest and track detection to improve the field robustness.



(a) Gathering images for custom dataset

(b) Sample output of YoloV3 Object Detection model

Figure 43: Payload testing

7.5 Manual Flight Testing

Manual flight testing was not completed due to campus shutdowns resulting from the COVID-19 pandemic. The plan was to complete the test in two parts: ground control,

and takeoff to landing with flaps. The tests were to be completed at Embry-Riddle with an experienced UAS pilot.

The goal of ground testing was to understand the behavior of the UAS when it is still on the ground or runway. The test would have been completed on a large section of pavement allowing the aircraft to maneuver or drive about. The deliverables for the ground testing were to determine the maximum speed the aircraft should be taxiing at before losing friction to the ground and to determine the rate at which the aircraft naturally slowed down to a stop. Determining the taxi speed was to be done by driving the aircraft in a circle and slowly increasing thrust until the aircraft deviated from the path. Maximum taxi speed would have been the speed at which the deviation occurred. The natural deceleration would have been found by bringing the aircraft to taxi speed on the pavement and cutting power. The distance would be measured from where the power was cut to where the aircraft stopped. Deceleration would have then been extrapolated from the distance and the overall time it took to stop.

The goal of the "takeoff through landing" test was to determine maneuverability of the aircraft during all stages of flight, the takeoff and landing distances, as well as maximum time in flight. Takeoff and landing distances would have been measured during each stage of flight and compared to the hand calculations for takeoff and landing. This would also serve as a benchmark for the runway requirements when flying the aircraft. Maneuverability would have been checked by inputting pitch, roll, and yaw commands into the aircraft, and the UAS would be monitored for aggressive motion. If the aircraft was maneuvering too aggressively or not maneuvering enough, the gains and deflection angles would be adjusted accordingly for this control issue.

Running these tests would have provided useful information on aircraft performance that could have been used to fine-tune the aircraft and to inform users on how to operate the UAS.

7.6 Flight Checklists

Flight checklists were generated to ensure safe and consistent operation of the UAS. While they were unable to be put into practice due to the COVID-19 pandemic, the checklists were still of beneficial use as a guide during autonomous flight testing. Checklists were generated for day before flight, pre-flight, in-flight, post-flight, and emergency scenarios. All checklists are shown in Appendix J, and would be also be included with the user's manual upon customer delivery.

7.7 Glider Prototype

In an effort to understand construction methods and to prove the design outside of digital models, a prototype glider was constructed at 75% scale during the fall (Figure 44). This scale was set due to the size constraint of the CNC hot wire cutter used to manufacture the wing sections.

7.7.1 Manufacturing

The wings of the prototype glider were constructed out of scrap foam available in the Purdue lab. The wings were cut in half-spans using a CNC hot wire foam cutter and covered in packaging tape to provide a smooth surface for better aerodynamic performance and protect the airfoil from light damage. Cutouts for a carbon-fiber spar (also a lab



Figure 44: Prototype glider

scrap) were added ex post facto. The spar was designed to run along the length of both wings; however, the actual spar used was about 3" short of the ends due to material availability. Cutouts were also made on the wings for flaps and ailerons, which were also scaled down from the calculations made in Section 3.4.

The wings were mounted to a carbon-fiber square tube (the tail boom) using a 3D-printed bracket (Figure 45). The wing spar was to be inserted through the hole located through the fin on the top half of the bracket. The wing spar was first inserted through the bracket, after which the wings were fit around the spar. The wings were semi-permanently secured to the bracket using packaging tape.

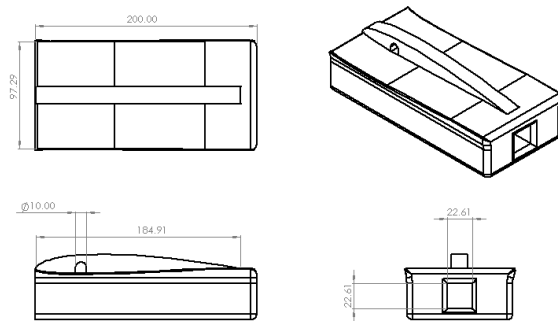


Figure 45: Three-view drawing of 3D-printed bracket

The bracket was attached to the tail boom via the square hole through its lower half. The tail boom was inserted via friction fit and was secured in place using epoxy. A vertical tail was mounted on the tail boom using a carbon-fiber spar through the tail at quarter-chord position. This spar extended through the bottom and top of the vertical stabilizer to mount it to the tail boom and horizontal stabilizer, respectively. The horizontal stabilizer was attached to the vertical stabilizer using epoxy. The spar extending from the bottom of the vertical stabilizer was inserted into a hole drilled into the tail boom, and was semi-permanently secured to the tail boom with packaging tape.

The glider's initial center of gravity was located at the end of the wing's trailing edge. This was an unfavorable position, since it should be located near 25% to 38% of the mean

aerodynamic chord. To move the center of gravity forward, ballast was cantilevered off the front of the bracket on a wooden bar. Adding a 0.75-lb weight located 10.5" in front of the leading edge of the wing adequately moved the center of gravity to a more preferred location. A foam housing was constructed around the ballast and epoxied to the 3D-printed bracket to provide structural support and to mimic a fuselage. The ballast was attached to the glider using Velcro to provide flexibility in center of gravity location.

7.7.2 Test Results

Flight tests were performed on Nov. 26, 2019. The glider was thrown three times from a height of 9.84' at a 5° angle of attack, resulting in an immediate stall, followed by a roll left and a steep nose-first dive to the ground. The glider was thrown two more times at a 1° angle of attack to avoid stalling, and while stall was not observed in either instance, the glider yawed immediately to the left upon launch, followed by a roll left and a nose-first dive to the ground for both subsequent flights. In all three test flights, the glider traveled approximately 20'. Images of the flight are shown in Figure 46.

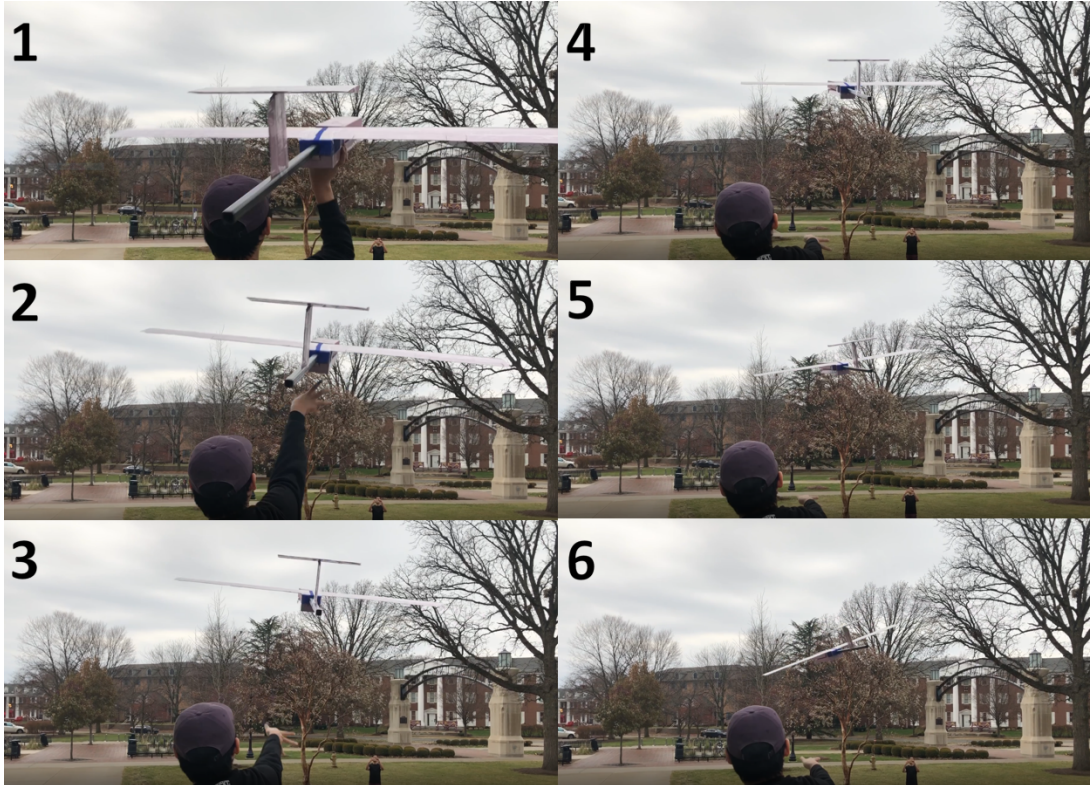


Figure 46: Glider flight time lapse

By evaluating video footage of each flight test, it was confirmed that the glider dove faster than anticipated. According to the *Glider Flying Handbook* by the FAA, glide ratio can be obtained from equation 3.

$$\text{Glide ratio} = \frac{\text{Lift}}{\text{Drag}} : 1 \quad (3)$$

This showed that the glide ratio is proportional to $\frac{L}{D}$ ratio, and also explains why drag

minimization was critical for the glider (“Glider Flying Handbook”, 2013). At a 1° angle of attack with an estimated hand-launch speed of 16.4-ft/s, the L/D from wind tunnel testing (see Appendix I) was approximately 4, meaning the glider was expected to fly about 13.1' forward for every 3.3' of descent. However, in actual flight, the glider experienced a steeper rate of descent (6.6' of forward travel for every 3.3' of descent).

The observed discrepancy was likely due to the weight of the glider being heavier than anticipated (2.53-lb total weight). With a large weight, the glider was likely not being thrown with enough initial velocity for stable flight. Additionally, a slight breeze of wind from the left of the planned flight path may have contributed to the yaw and roll observed during testing.

7.7.3 Glider Use and Lessons Learned

The team concluded that poor planning during glider manufacturing in the fall resulted in a hastily-constructed glider that contributed to poor glider performance and quality. While the team intended on modifying the glider for powered flight and wind tunnel testing, sweeping changes made to the aircraft sizing and configuration during winter break rendered the glider significantly out-of-date with the final configuration. Consequently, the work needed to modify the glider into a model representative of the full-scale UAS would have detracted significantly from the work necessary for final manufacturing. These changes, coupled with the poor glider quality, prompted the team to cease glider work in the spring, and the glider was effectively abandoned; an off-the-shelf aircraft was sourced for powered flight tests in its place. Despite this, several valuable lessons were learned from the process of manufacturing the glider.

The glider manufacturing was rushed due to poor planning. The overall bulk of the 3D-printed bracket resulted from the part being hastily designed. Care would need to be taken on the actual UAS to design parts. Consequently, manufacturing protocol was overhauled for the spring. Job instruction and process specifications were drafted for manufactured components of the UAS to ensure a streamlined and coordinated manufacturing experience.

It was concluded that the CNC hot wire foam cutter was an extremely effective tool for cutting out the shape of the wings, but the spar cutouts would be incorporated within the initial cut profile for the final UAS, instead of being manually added in later cuts. It was also resolved that a fiberglass layup should be used as structural reinforcement for the wings and tail, rather than the packaging tape used for the glider. All of these suggestions were followed when manufacturing the wings and tail for the final UAS.

In summary, while the glider was not used during the spring for testing, the lessons learned during its fabrication process provided valuable experience for the team during full-scale UAS manufacturing.

8 Conclusion

The mission to locate sea turtle nests is unique and empowering because it is relatable to some team members. Just as unique is the motor over wing configuration. Much analytical and experimental work has been completed on validating this configuration. The UAS currently sits at ERAU as a grounded airplane. The structure is fully assembled and electronics are fully integrated sans the payload. A controller and 14 CFR Part 107



Figure 47: Team SAILR, from left to right, Allen Perron, Jefferson Kim, Dylan Lurk, Evan Lee, David Eddy, Josh Neumann, Josh Norris, Kayla Hollis, Jake Falck, and Stanley Liu.

certified pilot is all that is needed to begin the ground test program, which will be followed by the flight test program. Concurrently, the sea turtle recognition needs to be finalized, and the LTE & database development needs to be completed. Once the payload is fully developed, it can be integrated into the grounded airframe prompted with full system tests to complete the validation of the requirements. The team recognizes that despite all the subsystem testing and detailed analysis, some rework may be necessary to ensure all requirements are met before delivery (theoretically) to the customer.

Among the collection of models, drawings, and manufacturing documentation, the team feels the project could be passed off to a subsequent design team to complete the development. All documents not herein covered, namely manufacturing job instructions and test plan instructions, are available upon request to the project manager, Dylan, at dlurk97@hotmail.com. Seeing as though the customer expects a completed product ready to use, it would not be appropriate to deliver the incomplete product to them given they have limited engineering background. The user guide they would be provided with covers operation and basic troubleshooting only.

Aside from the technical and managerial lessons already cited, some themes have emerged as lessons learned. Working effectively across time zones, disciplines, and cultural backgrounds proved challenging. The team had to come to trust everyone; each person brought a unique perspective and skill level to the project, stemming from unique technical and cultural backgrounds. The solution to effectively working with open-ended direction was a balancing act between giving direction and leaving the task open ended to promote creativity. Schedule delays were encountered and the effect of those delays on other people responsible for subsequent tasks was learned. Lastly, a plan on paper is great, but it requires follow-up to ensure targets are being met and then to update the plan when deadlines are not met. In conclusion, this has been a valuable experience that team members will build on in future endeavours.

References

- Glider flying handbook. (2013). In (chap. 3). Federal Aviation Administration.
- Information about sea turtles: Loggerhead sea turtle.* (n.d.). <https://conserveturtles.org/information-sea-turtles-loggerhead-sea-turtle/>. Sea Turtle Conservancy. (Accessed: 2020-1-11)
- Ossmann, M. (2018, 08 23). *Thermal imaging, drones, and sea turtles: a case study using flir's new duo pro r camera.* <https://www.wildlabs.net/resources/case-studies/thermal-imaging-drones-and-sea-turtles-case-study-using-flir%E2%80%99s-new-duo-pro-r>. (Accessed: 2019-10-7)
- Raymer, D. P. (2004). *Aircraft design: A conceptual approach* (2nd ed.). American Institute of Aeronautics and Astronautics, Inc.

Appendices

A Organization Structures

Table A.1: Team organization prior to MCR/SRR

Scrum Team	Members	Sprint Objectives
Mission Definition	Kayla, Allen	Define the mission objective and problem statement
Concept of Operation	Jefferson	Develop the concept of operation
Stakeholders	Kayla, Allen	Identify stakeholders and interview them as available to identify their wants in this product
Requirements/ KPIs	David, Stanley	Formalize stakeholder wants & team wants into requirements and KPIs
Payload Definition	Jefferson	Investigate and recommend a payload configuration
Cost Estimate	Jake	Develop a cost estimate based on anticipated equipment to be used
Competitive Assessment	Josh Neumann, Josh Norris	Investigate products currently on the market and areas of research in sea turtle locating
Project Management	Dylan, Evan	Prepare the schedule and framework for the team to function

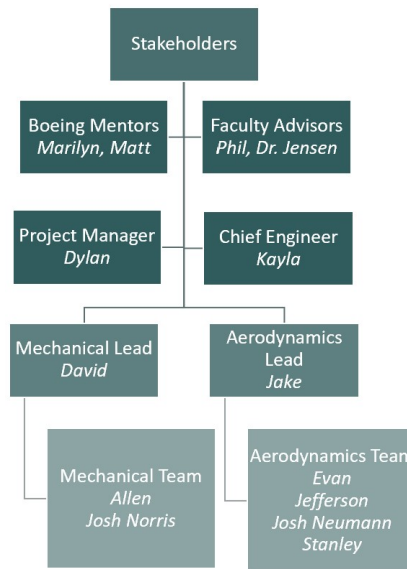


Figure A.1: Organization of Team SAILR following the MCR/SRR to MRR

B Detailed Schedule

The figures contained within this section shows the work breakdown as a Gantt Chart for the project. For each task, the light gray bar on top indicates the planned start and finish time; the dark bar underneath it indicates the actual start and finish time. The green/red status icons indicate if a task is complete or incomplete and late, respectively. An alternate color, yellow, shows if the task is incomplete but at risk of being late.

In Figure ??, the “Project Management” and “Mission Development” items were superseded tasks. Due to delays in having a functional collaboration space in 3DEXperience, tasks for that period were tracked in an Excel tool. Tasks were determined based on MCR/SRR needs. These tasks, along with people assigned to them, are presented in Table A.1. The items in Figure ?? are placeholders for the work that was completed in that time period.

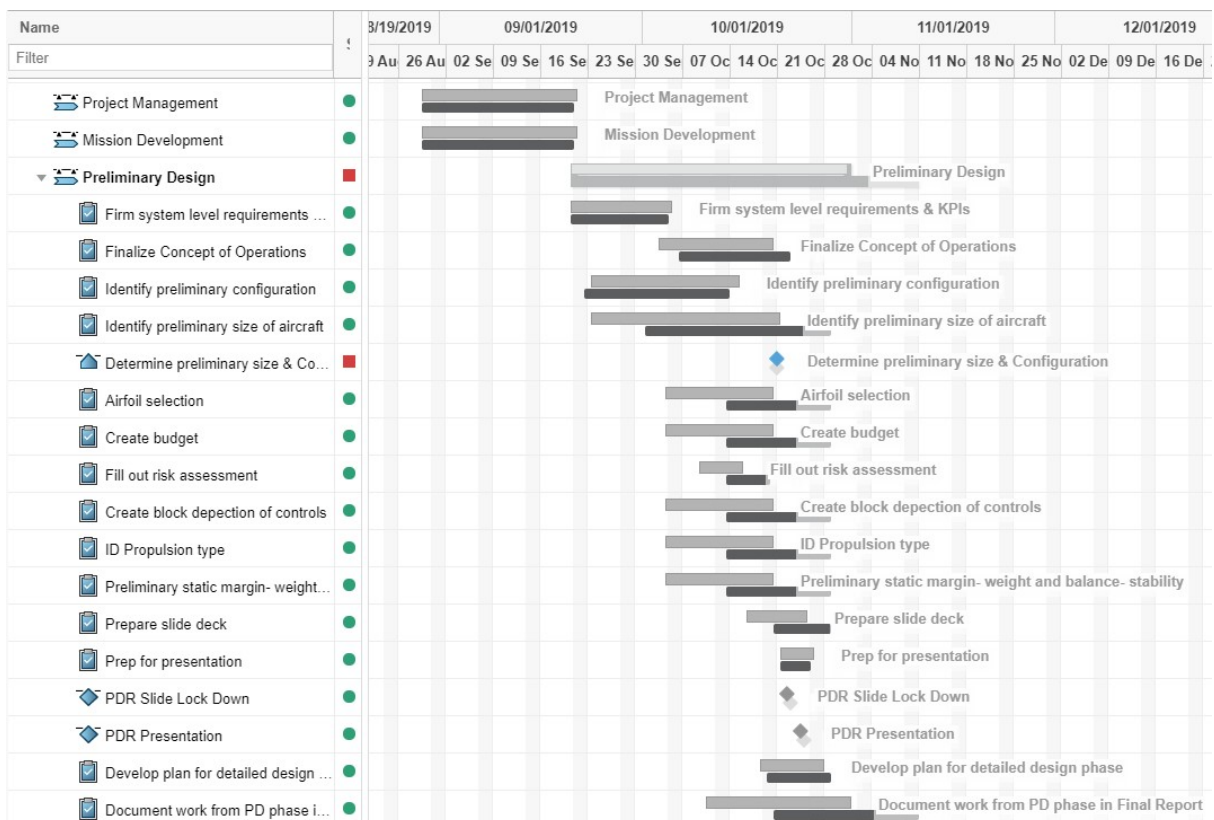


Figure B.1: Preliminary Design Schedule.



Figure B.2: Detailed Design Schedule. Note that the tool was not used through late December and January due to technical difficulties being resolved in conjunction with the 3DEXPERIENCE support team. The main task that occurred during this time was improving the quality of the CAD which was rushed earlier in the semester due to being delayed.

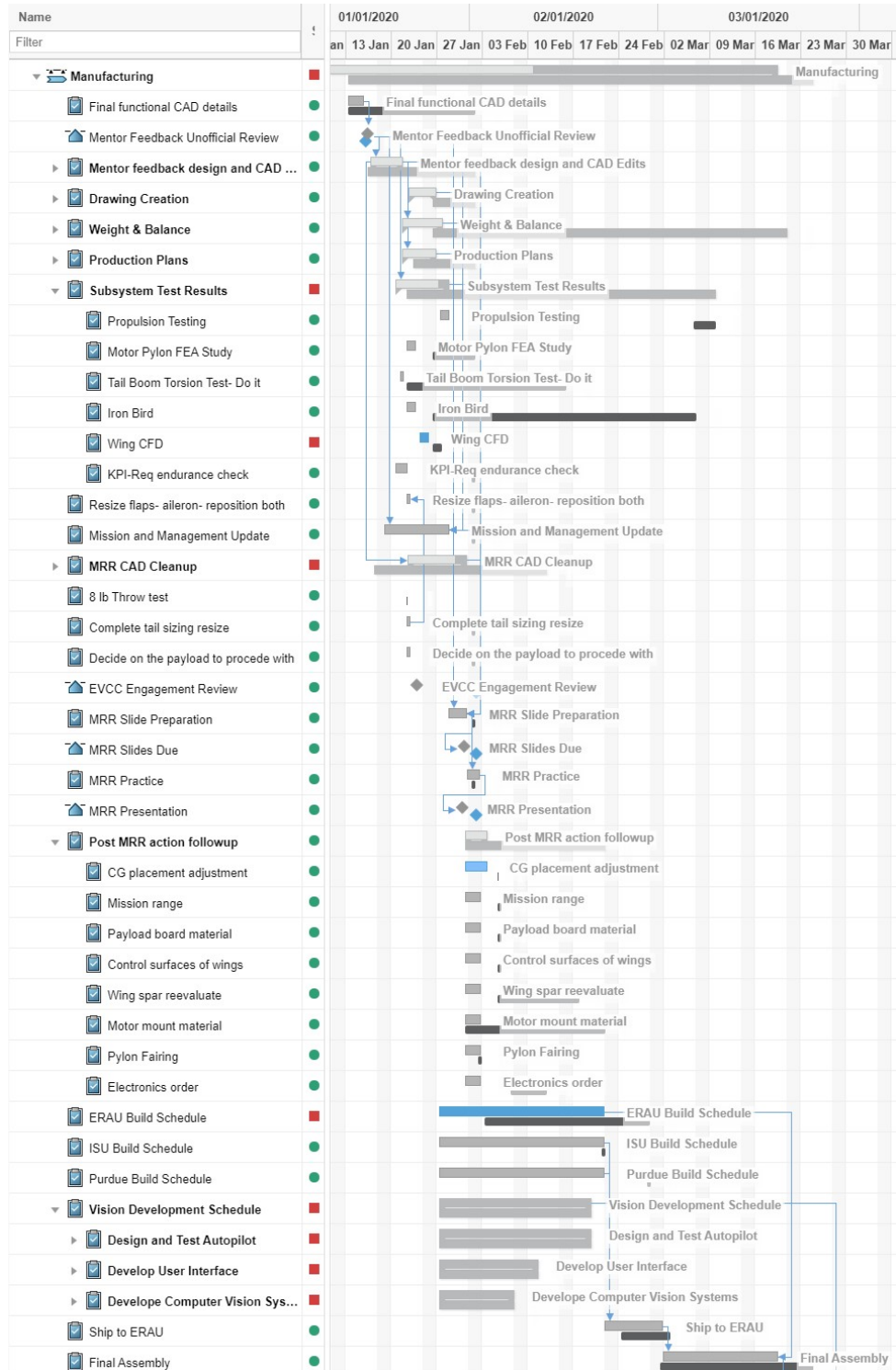


Figure B.3: Manufacturing Schedule.

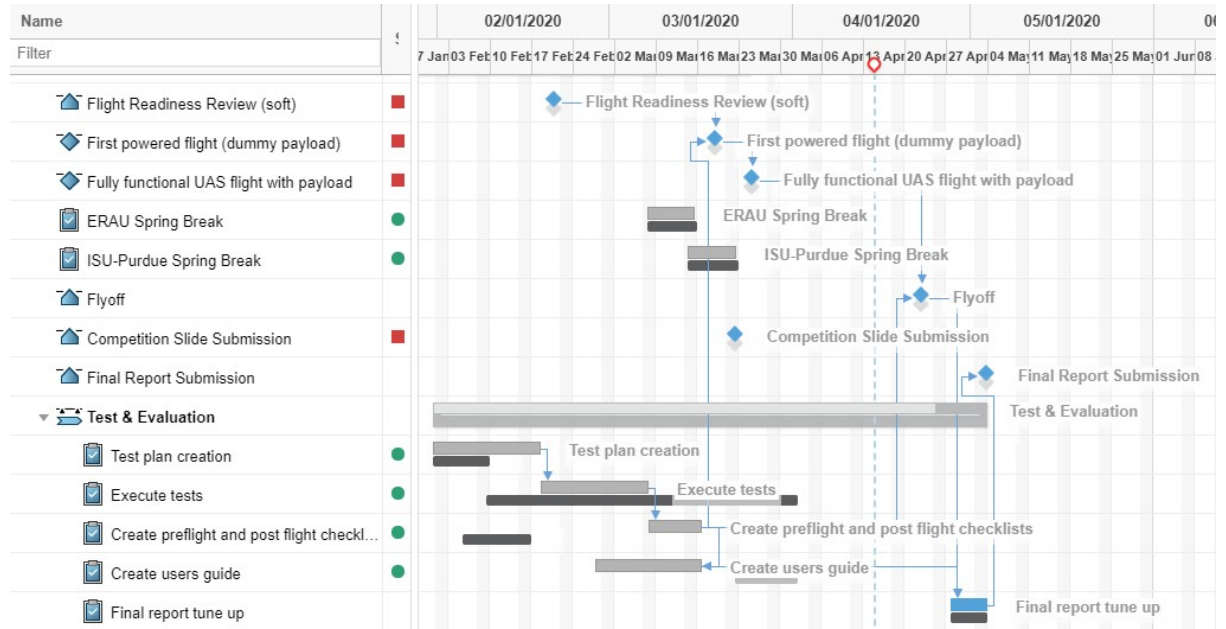


Figure B.4: Test & Evaluation Schedule.

C Budget & Expense Breakdown

Category	Revised	Budget	Actuals	Available
Shipping	\$	250	\$ 128	\$ 121.67
ISU to ERAU (fuse)	\$	100	\$ 76.65	\$ 23.35
ISU to ERAU (Propulsion	\$	30	\$ 11.61	\$ 18.39
Purdue to ERAU (wings, tail)	\$	40	\$ 29.28	\$ 10.72
Purdue to ERAU second shipmer	\$	40	\$ -	\$ 40.00
ERAU to flyoff (assembly)	\$	-	\$ -	\$ -
Purdue to ERAU (electronics)	\$	40	\$ 10.79	\$ 29.21
Payload	\$	465	\$ 329	\$ 136.28
Gimbal	\$	105	\$ 103.14	\$ 1.86
Camera	\$	45	\$ 29.99	\$ 15.01
Raspberry Pi	\$	40	\$ 73.94	\$ (33.94)
Data Plan (3mo + wiggle for fees	\$	200	\$ -	\$ 200.00
LTE Radio Hat	\$	75	\$ 121.65	\$ (46.65)
Propulsion	\$	490	\$ 415	\$ 74.62
Motor	\$	110	\$ 83.54	\$ 26.46
ESCs	\$	105	\$ 58.95	\$ 46.05
Battery	\$	175	\$ 253.98	\$ (78.98)
Propeller	\$	100	\$ 18.91	\$ 81.09
Controls	\$	862	\$ 691	\$ 170.96
Misc Wires/connectors	\$	200	\$ 19.05	\$ 180.95
Flap servos (2 total)	\$	70	\$ 67.18	\$ 2.82
Aileron servos (2 total)	\$	70	\$ 78.40	\$ (8.40)
Elevator servo (1)	\$	18	\$ 38.34	\$ (20.34)
Rudder servo (1)	\$	26	\$ 25.99	\$ 0.01
Pitot Tube	\$	50	\$ 51.21	\$ (1.21)
Here2GPS	\$	30	\$ -	\$ 30.00
PixHawk	\$	300	\$ 339.00	\$ (39.00)
BEC (2)	\$	48	\$ 46.88	\$ 1.12
Spektrum Receiver	\$	25	\$ 24.99	\$ 0.01
RFD900 Radio	\$	-	\$ -	\$ -
Pixhawk Power Module	\$	25	\$ -	\$ 25.00
Ground control radio	\$	-	\$ -	\$ -
Build Materials	\$	1,145	\$ 1,144	\$ 1.50
Construction materials	\$	-	\$ -	\$ -
Foamular XPS 150	\$	20	\$ 32.99	\$ (12.99)
Wing, tail composite materials a	\$	-	\$ -	\$ -
Fuselage composite materials ar	\$	200	\$ 176.20	\$ 23.80
Spar	\$	240	\$ 346.82	\$ (106.82)
Spar insert	\$	60	\$ 56.25	\$ 3.75
Tail boom	\$	205	\$ 191.29	\$ 13.71
Electronics board	\$	50	\$ 28.82	\$ 21.18
Ball Detents	\$	20	\$ 9.99	\$ 10.01
3D print spools	\$	50	\$ 39.98	\$ 10.02
Landing gear	\$	-	\$ 8.99	\$ (8.99)
Misc Hardware	\$	150	\$ 154.95	\$ (4.95)
Misc Adhesive-Fasteners	\$	150	\$ 97.22	\$ 52.78
Glider Build Activities	\$	-	\$ -	\$ -
SAILR Gear	\$	370	\$ 367	\$ 2.90
Stickers	\$	30	\$ -	\$ 30.00
Shirts	\$	340	\$ 367.10	\$ (27.10)
Undistributed Cash	\$	418		\$ 418.00
Total	\$	4,000	\$ 3,074	\$ 926

Figure C.1: The budgeted amount, actual cost, and difference for the budget categories and items that comprise those categories

D Wing & Propulsion Sizing Sheets

Constraint_sizing_electricHL					
Airplane			Vapproach		
g	9.8 m/sec^2		Altitude	100 m	
aspect ratio	7		CLMax	1.4 ~	
Cdo	0.05		Vapp	9 m/s	29.52 fps
span efficiency (e)	0.83		Density at.	1.21 kg/m^3	
propeller efficiency	0.7		W/S	68.88 N/m	
motor efficiency	0.8				
k - Drag due to lift factor	0.054787				
(L/D) max (emax)	9.553181				
Hand Launch			Plot_Vapproach		
CLmax	1.5		68.88234	0	
Vthrow	6.75 m/s	22.1 ft/s	68.88234	100	
		15.0552 mph			
Maximum Speed			Rate of Climb		
Altitude	150 m		Rate of Clir	100 m/min	328 ft/min
velocity	20 m/sec	66 ft/sec	Rate of Clir	1.666667 m/sec	
q	241.8062 N/m^2		Altitude	396.24 m	
Density of air	1.209031 kg/m^3		Density at.	1.180653 kg/m^3	
Landing			Thrust	1	Not used for electric
Altitude (landing)	100		Cl	1.654659	at min D/V
CLMax	1 (from takeoff)		Turns		
Landing Distance	10 m		Altitude	100 m	
Reverse Force Fraction	0		Airspeed	14.8 m/s	48.544 fps
Density at Altitude	1.214856 kg/m^3		Load Facto	2.5	33 mph
Thrust	1 Not used for electric		Density	1.214856 kg/m^3	
Rho Sea Level	1.225		Thrust	1	Not used for electric
Ceiling			Dynamic P	134.162	kg/m^2
Altitude	1900 m	6232 ft			
Density	1.018237 kg/m^3				
Thrust	1 Not used for electric				
Cl	1.654659				

Figure D.1: Initial sizing constraint diagram inputs

weight_Analysis_electric_aircraft				Output			
				Battery weight fractions	Battery weight fractions	battery weight	
g	9.8 m/sec^2			Take-off	0.00018	0.00478 N	
Airplane				Best range cruise	0.09851	2.65494 N	
aspect ratio	7			Loiter	0.02840	0.76535 N	
CDo	0.05	0.56		Cruise	0.12897	3.47582 N	
span efficiency (e)	0.8			Turns	0.01370	0.36916 N	
propeller efficiency	0.7						
motor efficiency	0.8						
W/S wing loading (S)	60 N/m^2	20.05002 oz/ft^2	1.253126 lbs/ft^2	total Wb/Wto	0.26976	7.27010 N	
P/W power loading (W/N=m)	10 W/N or (m/sec)	44.4822 watts/lb	2.780138 watts/oz				
k_battery	4831.72 J/N or (m)	215703.66 J/lb		Wto	26.95 N	2.74816 kg	6.058641074 lb
We/Wto empty weight fraction	0.4			Wempty	10.78 N	1.09927 kg	2.423456429 lb
payload weight (N)	8.9 N	2.00 lb		Wbattery	7.27 N	0.74135 kg	1.634384544 lb
				Swing area	0.45 m^2	4.83482 sq. ft	
k Drag due to lift factor	0.056841	k=1/(pi*ar*e)		a. wing span	1.77 m	5.81754 ft	69.81045323 in
(L/D) max (emax)	9.378944	1/(2*sqrt(k*cd0))		chord	0.83 ft	9.97292189 in	34.90522661 half span
Density of air	1.225 kg/m^3			Power	269.50 Watts		
CLmax	1.15						
				chord	0.253312216 meter		
				wing sf	0.886592728 meter		
					0.443296364		
					0.207769206		
					0.044329636		
					0.310307455		
For Thunderpower 5S 5000 mAh	W (N)	E_batt (W-hr)	E_batt (J)	k_batt			
www.thunderpowerrc.com/air_batteries/	4.962165	74	266400	53686.24			

Figure D.2: Initial sizing weight analysis inputs and outputs

Motor (Model-Kv):	Cost(\$):	Weight(g):	Current Draw Cruise(Amp)	Recommend Props[Prop Size USED FOR SIZING]	Battery Capacity Required (mAh)		
KDE2814XF-515	\$71.95	125	1.5	[12.5x4.3(2x)],12.5x4.3(3x),15.5x5.3(2x)	6660		
KDE3510XF-715	\$92.95	175	1.54	[12.5x4.3(2x)],12.5x4.3(3x),15.5x5.3(2x)	6700		
KDE2814XF-775	\$71.95	125	1.72	[12.5x4.3(2x)],12.5x4.3(3x),15.5x5.3(2x)	6880		
KDE2315XF-885	\$60.95	75	1.275	9x3,9x4.5,10x3.3,[11x3.7],12x4.0	6435		
KDE2315XF-965	\$60.95	75	2.7	9x3,9x4.5,10x3.3,[11x3.7],12x4.0	7860		
	0.98	lbs					
Flight time(hr)		1 hr					
Current Draw (w/o Propulsion)		5.16					
Total Current Draw(Amps)		3618 mA					
Battery Selection:	Cost:	Capacity	Actual Flight Time(hr.)	Actual Flight Time(min)	Capacity/\$	Weight (lbs)	Capacity/ lbs
Lumenier 8000mAh 4s 25c Lipo Bat	\$99.99	8000	2.21	132.67	80.008	1.62	4938.272
Lumenier 6600mAh 4s 35c Lipo Bat	\$85.99	6600	1.82	109	\$76.75	1.45	4551.724
LiPo 6500 4S 14.8v	\$199.99	6500	1.80	108	\$32.50	--	--
Gens Ace 4s LiPo Battery Pack 70C	\$134.99	7200	1.99	119	\$53.34	--	--
Gens Ace 4S 100C LiPo Battery Pack	\$139.99	7500	2.07	124	\$53.58	--	--

Figure D.3: Motor & battery sizing sheet

E Stability Calculations

The CG location can be obtained by using the aerodynamic center X_{AC} found in AVL and the static margin equation as shown below.

$$\text{Static Margin} = \frac{(X_{AC} - X_{CG})}{W_c} = 0.15$$

$$X_{AC} = 17.38$$

$$W_c = 12\text{in}$$

$$X_{CG} = 15.58\text{in}$$

The resulting CG location is close to the quarter chord of the wing. This suggests that the aircraft should be stable.

F Manufacturing Supplements

Part Number	Part Name	Rev	Quantity	Material	Procurement Type	Extras Needed	Notes	Source	Status	Cost	School
1301_TailBoom_Full	Tail Boom	D1	1	Carbon Fiber	Off-the-shelf	0	Included in tailboom cost	d-tubing/sql	Ordered	\$155.99	ERAU
1511_Pylon	Pylon	A1	1	Carbon Fiber	Machined	1	-	d-tubing/sql	Ordered	\$0.00	ERAU
1512_Motor Mount	Motor Mount	A1	1	Aluminum	Machined (5-axis milled)	0	-	U Machine S	Ordered	\$0.00	ERAU
N/A_1/4 Turn	1/4 Turn Fasteners	A1	11	Metal	Off-the-shelf	0	Extras depending on QTS # of sets	in-materica	Ordered	\$42.60	ERAU
1917_Tail Wheel	Tail Wheel and Frame	A1	1	Plastic/metal	Off-the-shelf	0	-	element/df/f	Complete	\$8.99	ISU
3706_Dome_Full	Camera Dome	B1	1	Acrylic	Off-the-shelf	1	-	d/p/B07DNV	Ordered	\$14.98	ISU
N/A_Bagging Film	Stretchfilm 200 bagging film	N/A	50 yd	Plastic	Off-the-shelf	0	We need to buy this to offset the material as we used in the ISU composites lab	product/stue	Complete	\$192.45	ISU
1214_Internal_Spar_Connector	Internal Spar Connector	C1	1	Carbon Fiber	Off-the-shelf	3	Extras need 3, and order form has a quantity of 4 noted, only one spar was received	carbon-fibre-SG	In Work	\$55.10	ERAU
1211_Support_Board	Support Board	B1	1	Birch Plywood	Laser Cut	1	-	charts-1-4-in-2	In Work	\$28.82	ERAU
1228_Tail_Connector	Tail Connector	A1	1	ABS	3D Printed	0	May need to buy filament to offset cost	ERAU 3D Print	In Work	\$0.00	ERAU
1513_Motor_Mount_Fairing	Motor Mount Fairing	A1	1	ABS	3D-Printed	0	May need to buy filament to offset cost	ERAU 3D Print	In Work	\$0.00	ERAU
1905_LandingGear	Main Landing Gear Frame	A1	1	Aluminum	Off-the-shelf	0	-	from ISU Card	Complete	\$0.00	ISU
1230_Fuse_Asembly	Fuselage Snell	A1	1	Fiberglass/phenolic	Vacuum layup	0	2 Versions completed	ISU Lab	Complete	\$0.00	ISU
1909_WingDent_Full	Wing Dent	A1	4	Various	Off-the-shelf	0	-	841/reFox 3	Complete	\$9.99	ERAU
1513_DragonPlate_FDFGK_S-1-TEE_Default	Square Tube Carbon Fiber Gusset	A1	2	Carbon Fiber	Off-the-shelf	0	-	square-tube	Complete	\$14.90	ERAU
N/A_Fastener_for_Pylon	Pylon Fastener	-	-	Epoxy	Off-the-shelf	0	-	octite-L-chys	Complete	\$14.50	ERAU
1226_Standoff	Mounting Board Standoff	A1	4	Birch Plywood	Laser Cut	1	Included in Support board cost	wood	Complete	\$0.00	ERAU
1225_Payload_Top	Payload Top	A1	1	Birch Plywood	Laser Cut	1	Included in Support board cost	wood	Complete	\$0.00	ERAU
1507_APC_1106_FProp_Default	APC 1106 FPropeller	A1	1	Composite	Off-the-shelf	1/2	-	from ISU Card	Complete	\$3.68	ISU
1922_MainWheels_S	Landing gear wheels + tires	A1	3	Foam/plastic	Off-the-shelf	0	-	from ISU Card	Complete	\$0.00	ISU
1006_FoamCore_Full	Wing Foam Core	A1	4	Foam	Machined	0	Spares accounted for in Quantity	coming-test	Complete	\$35.30	PURDUE
1007_Spar_Full	Wing Spar	A1	4	Carbon Fiber	Machined	0	Spares accounted for in Quantity	product/sql	Complete	\$59.00	PURDUE
1008_AileronComposite_Full	Wing Composite Shell	A1	4	Fiberglass	Off-the-shelf	0	Spares accounted for in Quantity	Purdue Lab	Complete	\$0.00	PURDUE
1009_AileronCore_Full	Aileron Foam Core	A1	4	Foam	Machined	0	Spares accounted for in Quantity, included in FoamCore cost	coming-test	Complete	\$0.00	PURDUE
1010_FlapComposite_Full	Flap Composite Shell	A1	4	Fiberglass	Off-the-shelf	0	Spares accounted for in Quantity, included in FoamCore cost	Purdue Lab	Complete	\$0.00	PURDUE
1011_FlapCore_Full	Flap Foam Core	A1	4	Foam	Machined	0	Spares accounted for in Quantity, included in FoamCore cost	coming-test	Complete	\$0.00	PURDUE
1901_ARHorn_Full	Control Horn (Aileron, Rudder, Elevator)	A1	4	Plastic	Off-the-shelf	0	1911_AERHorn	ver1D-1e46	Complete	\$0.00	PURDUE
1902_FlapHorn_Full	Flap Horn	A1	2	Plastic	Off-the-shelf	0	1911_AERHorn	ver1D-1e46	Complete	\$0.00	PURDUE
1903_HingesSubAssembly_Full	Control Surface Hinge	A1	14	Plastic	Off-the-shelf	0	1903_HingesSubAssembly	points-6-pa	Complete	\$0.00	PURDUE
1108_VStab	Vertical Stabilizer	A1	2	Foam	Machined	0	Spares accounted for in Quantity, included in FoamCore cost	coming-test	Complete	\$0.00	PURDUE
1109_HStab	Horizontal Stabilizer	A1	2	Foam	Machined	0	Spares accounted for in Quantity, included in FoamCore cost	coming-test	Complete	\$0.00	PURDUE
1110_Rudder	Rudder	A1	2	Foam	Machined	0	Spares accounted for in Quantity, included in FoamCore cost	coming-test	Complete	\$0.00	PURDUE
1111_Elevator	Elevator	A1	2	Foam	Machined	0	Spares accounted for in Quantity, included in FoamCore cost	coming-test	Complete	\$0.00	PURDUE
1114_HSpar	Horizontal Spar	A1	2	Wood	Off-the-shelf	0	Spares accounted for in Quantity, included in FoamCore cost	from f	Complete	\$0.00	PURDUE
1113_VSpar	Vertical Spar	A1	2	Carbon Fiber	Off-the-shelf	0	Spares accounted for in Quantity, included in FoamCore cost	indised-seat	Complete	\$30.00	PURDUE

Figure F.1: Engineering bill of materials

PN#	Item	Purchase	Cost Per Unit	Unit of Issue	QTY	Cost	Reseller	Length (mm)	Width (mm)	Height (mm)	Weight (g)	Gross Weight (g)	Voltage	Max Current (A)	Max Power (W)	Duty Cycle (%)	Power Requirement (Wh)
Pixhawk 2.1		Completed	\$ 238.00	KIT	1	\$ 238.00	IRLock	94.46	44.29	31.42	250.0	250.0	5.0	2.75	13.8	100%	13.8
RFD900X 900MHz telemetry radio		Completed	\$ 192.40	KIT	1	\$ 192.40	IRLock	30.00	57.00	12.80	14.5	14.5	5.0	0.80	4.0	100%	4.0
Here2 GPS Receiver (M8N)		Completed	\$ 95.00	KIT	1	\$ 95.00	IRLock	76.00	76.00	16.60	49.0	49.0	3.3	0.03	0.1	100%	0.1
Holybro Air Speed Sensor		Completed	\$ 49.99	EA	1	\$ 49.99	GetFPV	139.70	101.60	55.88	18.1	18.1	3.3	0.00	0.0	100%	0.0
Spektrum DSMX quad rate receiver with diversity		Completed	\$ 24.99	EA	1	\$ 24.99	GetFPV	26.00	21.00	8.00	3.6	3.6	3.3	0.03	0.1	100%	0.1
KD2814XF-515		Order Form Subj	\$ 71.95	EA	1	\$ 71.95	KDE	35.50	35.50	41.45	95.0	95.0	22.2	24.00	535.0	50%	267.5
Raspberry Pi 4 model B 4GB Ram		Order Form In Pn	\$ 55.00	EA	1	\$ 55.00	Canakit	56.00	85.00	24.00	46.0	46.0	5.0	3.00	15.0	80%	12.0
Raspberry Pi 3G/4G<E Base HAT		Order Form In Pn	\$ 39.00	EA	1	\$ 39.00	Sixfab	57.00	65.00	20.00	25.1	25.1	5.0	0.20	1.0	100%	1.0
Quettel EC25-A Mini PCIe 4G/LTE Module		Order Form In Pn	\$ 54.90	EA	1	\$ 54.90	Sixfab	51.00	30.00	4.90	9.8	9.8	3.3	0.03	0.1	100%	0.1
LTE Main & Diversity & GNSS Triple Port u.FL Antenna - IMX219 Board with M12 mount		Order Form In Pn	\$ 12.75	EA	1	\$ 12.75	Sixfab	224.40	120.40	2.00	20.0	20.0	0.0	0.00	0.0	100%	0.0
Hitech HS-250MG mini servos		Order Form In Pn	\$ 29.99	EA	1	\$ 29.99	Sainsmart	25.00	24.00	18.00	18.2	18.2	3.3	0.41	1.3	100%	1.3
Storm32 v1.32 gimbal controller		Order Form In Pn	\$ 25.99	EA	6	\$ 155.94	Tower Hobbies	44.07	36.28	16.77	31.0	186.0	5.0	1.20	6.0	30%	10.8
Pan Tilt Servo Gimbal for FPV Drone Board Cameras - Includes 2x 9g Servo		Order Form In Pn	\$ 71.72	KIT	1	\$ 71.72	eBay	80.00	80.00	80.00	175.0	175.0	12.0	1.50	18.0	10%	1.8
		Order Form In Pn	\$ 17.95	KIT	1	\$ 17.95	Amazon								Subtot al		312.489
PN#	Item	Purchase	Cost Per Unit	Unit of QTY	Cost	Reseller	Length (mm)	Width (mm)	Height (mm)	Weight (g)	Gross Weight (g)	Voltage	Max Current	Max Power (W)	Duty Cycle (%)	Power Requirement (Wh)	
KDEXF-UAS35			\$ 58.95	EA	1	\$ 58.95	KDE	298.00	25.00	11.00	28.0	28.0	22.2	30.00	666.0	90%	297.2
TURNIGY 8-15A UBEC for Lipoly		On Hold	\$ 22.59	EA	1	\$ 22.59	Tower Hobbies	42.00	39.00	9.00	34.0	34.0	5.0	8.00	40.0	90%	32.7
DC-DC Buck convertor for gimbal		Not Required?	\$ -	KIT	1	\$ -	-	45.00	20.00	14.00	12.1	12.1	2.50	30.0	30.0	60%	3.0
Pixhawk 2.1 power distribution board								53.00	18.00	14.00	14.0	14.0	22.2	30.00	666.0	90%	15.3
Lumier 8000mAh 6S LiPo battery			\$139.99	EA	1	\$ 139.99	GetFPV	190.00	55.00	45.00	1075.0	1075.0	22.2	200.00	4440.0	178	0.510

Figure F.2: Electronics bill of materials



1 Record of Changes

Date	Revision	Pages	Description
2/3	6.2	3	Ensure that fume hoods are used if required look on SDS to determine if they are needed

2 Purpose

This procedure provides guidance on the process of making the fuselage shell.

3 Definitions

4 Responsibility & Authority

4.1 Process Owner

The process owner is responsible for producing products in accordance with this specification.

The team 4 ~~AerosPACE~~ students at Iowa State University are responsible for, and should take ownership for, the fuselage manufacturing. David Eddy shall be the lead member on this job.

5 Resources

5.1 Drawing & Models

Refer to 1806 or the most current airplane assembly on 3DX

5.2 Tooling

- Scissors
- Measuring tape
- Marking tool (sharpie, pen, etc)
- Brushes
- Stir cups
- Stir rods

5.3 Materials

- Fiberglass cloth
- Honeycomb sheet (1/2 inch thick)
- Epoxy resin
- Epoxy hardener

5.4 Consumables

- Foam ~~molds~~
- Breather fabric
- Release film
- Sealant putty
- Vacuum hose

Figure F.3: Page 1 of a sample job instruction sheet for the fuselage manufacturing



6 Safety

6.1 Personal Protection Equipment

- Safety glasses
- Latex gloves
- Mask (optional)

6.2 Material Safety

Review all material safety data sheets and follow manufacturer recommendations.

- Epoxy is very dangerous if handled improperly. Make sure epoxy never contacts your skin, and that you do not directly inhale any ~~vapors~~. Additionally, resin and hardener must be mixed in exact ratios. Use either the manufacturer's pump for volume ratio or an accurate scale for weight ratios
- Fiberglass cloth is very fine and can cut you similarly to a paper cut. Always wear gloves when handling fiberglass cloth and avoid grabbing cloth by the edges where the fiber ends are exposed. In addition, the fiberglass cloth can stretch and shrink in different directions, so handle the material as little as possible.

6.3 Equipment safety

N/A

7 Process

Initial in the left box when complete.

7.1 Preparation

1.	Review safety information of section 6
2.	Collect mold from JpBo – ISU lab tech
3.	Gather & prepare all tooling of section 5.2
4.	Gather all materials of section 5.3 and 5.4

7.2 Work

1.	Measure and mark fiberglass to the approximate size of the mold . Oversize the cut by a couple inches on each edge. (10 min)
2.	Cut the fiberglass cloth along the marks. (20 min)
3.	Cut release film and breather about the same size as the fiberglass cuts. (10 min)
4.	Score the honeycomb to fit the mold shape. (60 min)
5.	Mix the epoxy resin and hardener in the stir cups. Stir slowly to avoid creating air bubbles in the mixture. The epoxy should heat up when it is ready. (10 min)
6.	Cover the mold with release film (2 min)
7.	Lay a layer of fiberglass cloth on the mold and paint on a layer of epoxy mixture. Be careful to not lose brush bristles in the layup. (10 min)
8.	Repeat step 7 for as many fiberglass layers are needed

Figure F.4: Page 2 of a sample job instruction sheet for the fuselage manufacturing



9.	If using a honeycomb layer, place that over the previous fiberglass layer. (10 min)
10.	Repeat step 7 on the other side of the honeycomb.
11.	Place the other layer of release film and the breather layer on top of the last fiberglass layer. (5 min)
12.	Seal the layup to the table, tape the vacuum tube inside the layup, and seal the bag. As the bag pulls air, ensure there is a tight seal and the layup is not leaking anywhere (10 min)
13.	Let the layup sit under vacuum pressure for 24 hours (~24 hr)

7.3 Finishing

1.	Record measurements of these critical features: Length Thickness Width
2.	Remove the cured layup from the mold.
3.	Cut excess material off. Sand for a clean finish.
4.	Update Process Owner, Manufacturing Programs Lead, Chief Engineer, and stand-up chat of completion.
5.	Prepare for shipping.

Figure F.5: Page 3 of a sample job instruction sheet for the fuselage manufacturing

G Risks & FMEA Analysis

This Appendix shows the risks and failure modes and effects analysis items the team has identified.

Sea Turtle Locator UAV : Risks									
View: Details; Filter:All									
Level	Name	Title	State	RPN	Impact	Probability	Impact	Probability	Effective Date
2	R-0000001	Sea Turtle Detection (Vision)	Create	25	5	5	5-High	5-Almost Certain	1/1/2020
2	R-0000009	Structural Integrity of Motor Pylon	Create	15	5	3	5-High	3-Possible	10/17/2019
2	R-0000010	Flight instability due to over-wing Pylon	Create	12	4	3	4-Major	3-Possible	10/25/2019
2	R-0000011	Unequal spread of manufacturing tasks	Create	9	3	3	3-Moderate	3-Possible	10/17/2019
2	R-0000012	Pylon over-wing does not abate noise	Create	15	5	3	5-High	3-Possible	1/24/2020
2	R-0000013	Electronics heat generation	Create	12	4	3	4-Major	3-Possible	10/25/2019
2	R-0000015	Cross wind handling	Create	16	4	4	4-Major	4-Likely	10/25/2019
2	R-0000016	Time of day/weather operational constraints	Create	6	2	3	2-Minor	3-Possible	10/18/2019
2	R-0000017	Not being able to meet design weight	Create	9	3	3	3-Moderate	3-Possible	1/24/2020
2	R-0000018	Failure mode	Create	9	3	3	3-Moderate	3-Possible	10/18/2019
2	R-0000019	Salty Air interactions with hardware	Active	6	3	2	3-Moderate	2-Unlikely	10/25/2019
2	R-0000023	Sand interference with components	Active	6	3	2	3-Moderate	2-Unlikely	10/25/2019
2	R-0000024	Back loading work in Detailed Design Phase	Create	15	3	5	3-Moderate	5-Almost Certain	10/25/2019
2	R-0000026	Wire Management	Create	6	2	3	2-Minor	3-Possible	10/25/2019
2	R-0000027	Plane communication with ground station	Create	12	4	3	4-Major	3-Possible	1/1/2020
2	R-0000028	Team communication	Create	9	3	3	3-Moderate	3-Possible	10/19/2019
2	R-0000030	Ability to test detection system	Create	12	4	3	4-Major	3-Possible	1/1/2020
2	R-0000031	Protection of Payload in a crash	Create	8	4	2	4-Major	2-Unlikely	10/25/2019

Figure G.1: Risks page 1 columns 1 through 10

2	R-0000032	Craftsmanship of Manufactured parts and systems	Create	12	3	4	3-Moderate	4-Likely	10/22/2019
---	-----------	---	--------	----	---	---	------------	----------	------------

Figure G.2: Risks page 2 columns 1 through 10

Description	Abatement Plan	Measure of Success	Slip Days
Ability to develop the vision software required to detect the sea turtles	Devote development resources to create requirements, design, and test the system.	Successfully ID a nest.	0
Concern that motor mount pylon will not be adequately designed	Create schedule item and tasks assigned to people to develop the design and analysis	Detailed design and analysis of pylon and associated interfacing systems that explain integrity of design	0
Concern that a large bending moment will cause instability in the flight characteristics of the aircraft	A detailed analysis of the over-wing pylon will be added to the schedule with tasks assigned to people. The analysis should justify tail and other component sizing to drive stability into the design.	Analysis (analytical and system testing as needed) to show a stable flight profile	0
Concern that manufacturing tasks will be heavily loaded on one/two schools.	1. Survey team for skills and university resources available. 2. Assess scheduling constraints for university shared resources 3. Develop a sourcing and manufacturing plan to predict work loads and component flows	Time delays for components to be produced due to resource unavailability	0
Configuration decision has been based in part on noise abatement. The winning design was more strongly weighted in this (need to verify this); however, this is only a fact based hunch. There is concern that the pylon over wing design does not abate noise as much (or even at all) as intended. Because there is more design and analysis required for the riskier pylon over-wing design, we want to be sure the extra cost has some benefit.	Add tasks and schedule items to develop analytical and test (As needed) configurations.	Have data to compare noise from the pylon over-wing design with a conventional design	0
Concern that the ESCs and onboard image processing will generate large amounts of heat.	Approximate the heat generation and design for cooling as necessary		0
Concern that cross winds might disrupt flight	Devote design resources to investigate (And test as needed) for larger tail, controls		0
Concern that going with a color camera and neural network using long shadows limits the time of day operation (early or late) and the effect that clouds would have on that	Get okay from stakeholders on the operational constraints	Approval from stakeholders	0
Concern that our UAV will balloon in weight upon manufacturing	Detailed review of weight rollup to include estimates for misc hardware, adhesives, etc.		0
Concern of what the UAV does if components fail (e.g. how to avoid crashing into people on the beach)	Devote design resources to develop an evacuation plan (per requiremnet xx)	Evacuation plan in place	0
Concern that salty air might corrode components or interfere with electronics	Devote design resources to select materials that do not react with salty air and design enclosures for electronic components	No corrosion failures	0
Concern that sand might interfere with components including (but not limited to) motor cooling, cooling of components in fuselage, and damaging prop.	Devote design resources to mitigate ways for sand to enter components/aircraft	A documented checklist for each component that shows it has sand entrance mitigation has been considered.	0
Concern that we will mull over analyses for too much time.	Schedule gates to force the incremental locking of design components.		0
Concern that our wires will be crazy	Develop a wiring diagram to illustrate connections and routing.	Wires that look great and are well managed	0
Concern of how the plane will respond in the event that communication connections are lost	Develop a failure mode of how the plane respond when communication is lost	Successfully demonstrate the plane responds safely to a communication loss	0
Concern that information will be lost/delayed due to poor communication.	Emphasize the importance of communication, do activities to open up communication lines	People feel like they are in the know (team surveys)	0
The detection system is one of the most complex aspect of the project and will likely go through many design iterations. Must be able to test the system in a real or simulated environment.	Research methods to simulate environment through virtual world Reach out to sea turtle research groups to inquire about image data to train & test detection system	Ability to create simulated environment or obtain similar image data to what we expect in the final system	0
Since we are using expensive electronics with non-negligible lead times, the payload should be protected as best as possible not to set back the project timelines	Special consideration when designing payload enclosure and fixtures to reduce effects of crash impact.	Payload can sustain flight testing & operational crashes	0

Figure G.3: Risks page 1 columns 11 through 14

The quality of manufacturing has a direct effect on the total system performance. To ensure parts and components meet design spec the quality of manufactured parts must be kept. There is concern that the team will not produce quality components.	Half-scale manufacturing test parts NDE testing of select parts Detailed manufacturing plans with quality planning included	All parts are manufactured to spec and with quality standards in accordance will	0
---	---	--	---

Figure G.4: Risks page 2 columns 11 through 14

Estimated Start Date	Estimated End Date	Actual Start Date	Actual End Date	Assignee
1/1/2020	4/1/2020			
10/25/2019	11/17/2019			
10/25/2019	11/17/2019			
10/25/2019	11/17/2019			
10/25/2019	11/17/2019			
10/25/2019	11/17/2019			
10/25/2019	11/17/2019			
10/25/2019	11/17/2019			
10/25/2019	11/17/2019			
10/25/2019	2/14/2020			
1/1/2020	1/31/2020			
10/25/2019	11/17/2019			
10/25/2019	11/17/2019	10/18/2019		
10/25/2019	11/17/2019	10/18/2019		
10/19/2019	10/22/2019			
10/25/2019	11/17/2019			
1/1/2020	4/1/2020			
10/19/2019	11/17/2019			
1/1/2020	4/1/2020			
10/25/2019	11/17/2019			

Figure G.5: Risks page 1 columns 15 through 19

1/1/2020	4/1/2020			
----------	----------	--	--	--

Figure G.6: Risks page 2 columns 15 through 19

Title	RPN	Impact	Probability	Abatement Plan
Sea Turtle Detection (Vision)	25	5-High	5-Almost Certain	Devote development resources to create requirements, design, and test the system.
Cross wind handling	16	4-Major	4-Likely	Devote design resources to investigate (And test as needed) for larger tail, controls
Back loading work in Detailed Design Phase	15	3-Moderate	5-Almost Certain	Schedule gates to force the incremental locking of design components.
Pylon over-wing does not abate noise	15	5-High	3-Possible	Add tasks and schedule items to develop analytical and test (As needed) configurations.
Structural Integrity of Motor Pylon	15	5-High	3-Possible	Create schedule item and tasks assigned to people to develop the design and analysis
Electronics heat generation	12	4-Major	3-Possible	Approximate the heat generation and design for cooling as necessary
Flight instability due to over-wing Pylon	12	4-Major	3-Possible	A detailed analysis of the over-wing pylon will be added to the schedule with tasks assigned to people. The analysis should justify tail and other component sizing to drive stability into the design.
Plane communication with ground station	12	4-Major	3-Possible	Develop a failure mode of how the plane respond when communication is lost
Failure mode	9	3-Moderate	3-Possible	Devote design resources to develop an evacuation plan (per requirement xx)
Not being able to meet design weight	9	3-Moderate	3-Possible	Detailed review of weight rollup to include estimates for misc hardware, adhesives, etc.
Team communication	9	3-Moderate	3-Possible	Emphasize the importance of communication, do activities to open up communication lines
Unequal spread of manufacturing tasks	9	3-Moderate	3-Possible	1. Survey team for skills and university resources available. 2. Assess scheduling constraints for university shared resources 3. Develop a sourcing and manufacturing plan to predict work loads and component flows
Salty Air interactions with hardware	6	3-Moderate	2-Unlikely	Devote design resources to select materials that do not react with salty air and design enclosures for electronic components
Sand interference with components	6	3-Moderate	2-Unlikely	Devote design resources to mitigate ways for sand to enter components/aircraft
Time of day/weather operational constraints	6	2-Minor	3-Possible	Get okay from stakeholders on the operational constraints
Wire Management	6	2-Minor	3-Possible	Develop a wiring diagram to illustrate connections and routing.

Figure G.7: Risks summary

Item Number	Item	Potential Failure Mode	Effects of failure	Severity Ranking (S)	Potential Causes	Occurrence Ranking (O)
	Servos	Connections upon assembly	loss of flaps	8	breaking connectors when attaching the wings before flight	4
		Applied torque exceeds threshold	Mechanical damage to the servo itself	8	Severe weather, extreme drive of the aircraft	3
	Camera shield	scratches from dirt	lower quality images	7	belly landing and having the sand scratch the surface the camera sees through	4
	Battery	Loss of power	Loss of all operations	10	Not enough charge, faulty connection	1
	Fuselage/payload	Rough landing	Damage to payload/fuselage, loss of payload	7	Rough form factor of fuselage, lack of landing mechanism	6
			Loss of Control, Crash	10	Not enough control authority.	4
			motor mount pylon failure	8	Full flight envelope not account for	10
				10	insufficient structural design	4
				10	mistakes in modelling of FEA analysis	4
	Payload	code crashing / instability	mission failure	10	not sufficient resources dedicated to testing and debugging or improper testing procedure	6
		loss of power		10	dead batteries, low voltage, wire chaffing, unplugged connectors	6
		overheating		10	hot weather, improper ventilation	4
		vibration fatigue	potential failure of all electrical systems	10	improper vibration testing or lack of NVH mounts	2
		Damage upon landing	Damage on camera, preventing future use of drone and its reusability	8	Improper protection on payload, landing method	10
	Wing/ Control Surfaces	Flutter	Max Stresses exceeded/wing break	9		
		Hard Landing	Max Stresses exceeded/wing break	8	Improper wing mounting/improper wing stiffener design.	5
	Wing/fuselage connection	Damage upon assembly	Aircraft will not be flightworthy	8	Unpredictable forces applied on the structure during handling	7
		Structural Integrity during flight	Structural breakup in flight	10	Connection joint not being as strong as the rest of the wing	4
	Wing Spar connection	Strong gust winds	Structural breakup in flight	10	Flying in unsafe weather	2
		abnormal landing attitude	Airfoil leading edge or trailing edge or wing tip damaged on landing	4	bad operating technique or auto landing error	5
		bad handling by operator	Airfoil is bent or leading edge is damaged or wing tip is damaged.	3	Unpredictable forces applied on the structure during handling	7
	Tail boom fuselage connection	Tail strike on landing	tail is bent	7	Insufficient structural strength	5

Figure G.8: FMEA page 1 columns 1 to 7

		Incorrect handling from operator		7	Unpredictable forces applied on the structure during handling	7
	Tail boom tail structure connection	Tail strike on landing	T tail connection structure dislodged	8	Insufficient structural strength	6
	T tail horizontal stabilizer	Tail strike on landing	T tail is destroyed	8	Insufficient structural strength	6
	T tail vertical stabilizer	Tail strike on landing	T tail is destroyed	8	Insufficient structural strength	6

Figure G.9: FMEA page 2 columns 1 to 7

Current Controls	Detection Ranking (D)	RPN	Recommended actions	Responsible	Target completion date	Action Taken	New S	New O	New D	New RPN
type of connector	9	288	put it on the preflight checklist	Mech	before demo					0
Select servo with wide range of torque value	5	120	Test out limits of aircraft's controllability and make a guideline in tutorial for the vehicle	Mech/Aero	before demo					0
material selection	6	168	choose an anti scratch material or camera placement so that the material does not land on the sand	Mech	before demo					0
Pixhawk, DMM,Lipo Battery Checker	2	20	Check battery level on preflight checklist; ensure battery has large enough capacity; check all connections	Aero	before demo	Recharge battery after every flight, add battery check on pre-flight checklist	10	1	1	10
Fuselage design, landing speed	3	126	Design an alternate landing mechanism, redesign fuselage exterior, landing location	All	before demo	Add landing skids, redesign fuselage belly, or ensure UAV lands at low speed	3	5	3	45
AVL stability analysis, wind tunnel testing	3	120	As much wind tunnel testing as possible, pylon over wing hand launch test, analyze time response using AVL/Simulink	Aero	early January	Planning to run wind tunnel test to validate AVL.				0
Plan to determine loading depending on mission segment	1	80	Need initial design of pylon ASAP, prototype manufacturing of pylon and testing with actual motor.	Aero/Mech	early January	N/A				0
proper checks and balances in critical design analysis	2	80		Aero/Mech	early January	N/A				0
testing of structure past predicted flight envelope.	2	80		Aero/Mech	early January	N/A				0
none	5	300	enlist the help of computer vision specialists	mech	before demo					0
voltage monitoring via flight controller	1	60	properly engineer connections and add electronics checks to pre-flight checklist	mech	before demo					0
none	8	320	flow analysis and thermal analysis of electronics bay	mech	before demo					0
planned NVH isolators	1	20	request help	mech/aero	before demo	designed NVH isolators				0
Camera shield for payload protection	1	80	Nose up during belly landing or attach a skid or landing gear	Mech	early January					0
material selection/ wing to fuselage connection.	3	120	Decrease impulse from landing (come in at slower speeds)/carefully evaluate wing and material integrity	Mech/ Aero	Late January					0
none	6	336	Make connection as ergonomic as possible to avoid excessive handling	Mech	Before production					0
none	3	120	Run Multiple FEA load cases on the connection part	Mech	Before production					0
None	5	100	Alert message to remind operator	Aero / Controls	before demo					0
None	5	100	Autopilot protection against abnormal or abrupt inputs to controls and use a stronger build method	Aero / Controls	before production (for structural enhancement) before demo (for autopilot protection)					0
Instruction manual	9	189	Run FEA and build stronger connections using stronger material	Mech	Before production					0
None	5	175	Autopilot protection against abnormal or abrupt inputs to controls and use a stronger build method	Aero/Mech	before production (for structural enhancement) before demo (for autopilot protection)					0

Figure G.10: FMEA page 1 columns 8 to 18

Instruction manual	9	441	Run FEA and build stronger connections using stronger material	Mech	Before production					0
None	5	240	Autopilot protection against abnormal or abrupt inputs to controls and use a stronger build method	Aero/Mech	before production (for structural enhancement) before demo (for autopilot protection)					0
None	5	240	Autopilot protection against abnormal or abrupt inputs to controls and use a stronger build method	Aero/Mech	before production (for structural enhancement) before demo (for autopilot protection)					0
None	5	240	Autopilot protection against abnormal or abrupt inputs to controls and use a stronger build method	Aero/Mech	before production (for structural enhancement) before demo (for autopilot protection)					0

Figure G.11: *FMEA page 2 columns 8 to 18*

H Requirements Verification

This appendix lists the system and subsystem requirements of the UAS, each marked with verification of whether the requirement was met or not met with proper rationale.

Title	Details	Verified	Reason
SDR-001: Fixed Wing	Aircraft to have fixed wing design	Yes	Fixed Wing
SDR-002: Electric Propulsion	Aircraft will have electric propulsion system	Yes	Electric Motor
SDR-003: Weight	12 Pound Maximum	Yes	Weight = 10.5 lb
SDR-004: Transportation Size	Easily transportable (fit within a box 20" x 24" x 100")	Yes	Measured to fit
SDR-005: Cost	Cost less than \$4,000	Yes	Total Cost = \$2,579.00
SDR-006: Autopilot	Fly with autopilot to established mission profiles	Yes	Shown to work with Bixler
SDR-009: Takeoff	Wheeled takeoff from surface in less than 200-ft	Yes	Calculated Takeoff Distance = 33.6 ft
SDR-011: Detecting Sea Turtle Nests	Carry a payload capable of aiding in detection of sea turtle nests	No	Not able to identify turtle specifically
SDR-012: Government Regulations	Aircraft complies with FAA, State, and Government Regulations	No	Waiver needed for BVLOS, operation from moving vehicle
SDR-014: Maintenance	Capable of handling multiple flights/operations without need for replacement or significant repair.	No	No Study Completed
SDR-015: Ease of Use	Easy to use and easy to setup	Yes	Intuitive access and design for easy use
SDR-016: GPS Accuracy	GPS accuracy of 5 meters or less	No	Not Verified
SDR-017: Location of Subject	GPS accurately pinpoints the location of camera subject matching mission criteria	No	Not Verified
SDR-018: Marine Disturbance	Make any attempt to avoid marine life in the area	Yes	Mission flight altitude
SDR-019: Flight Cycles	Withstand 200 flights	No	Not Verified
SDR-021: Range-distance	15-mile minimum range	Yes	Calculated Range = 36 Miles
SDR-023: Setup Time	Structure shall have a setup time (out of box to launch) of less than 30 minutes	Yes	Setup Time = 10 minutes
SDR-024: Setup Tools	No more than 2 external tools to set up for flight	Yes	Tools Needed = 1
SDR-025: Autonomous	Autonomous control for the entire mission profile	Yes	Bixler
SDR-026: Handbook	A detailed pilot operating (POH) & maintenance handbook shall be included with every UAS	Yes	Documents Created
SDR-027: Manual Control	Manual control override when in autonomous flight	No	Manual Flight not Checked
SDR-029: Visible Lights	Aircraft should have no visual operating lights as viewed from the ground	Yes	No lights on underside
SDR-030: Noise	Produce no more than 50 dB of noise at a distance of 200ft altitude	No	Unable to Verify due to COVID-19
SDR-031: Reliability	99% reliable with respect to component failure	No	Not Verified
SDR-033: Emergency Landing	Aircraft should have return-to-home emergency landing	No	Not Verified
SDR-036: Stowing Time	Stowing time (controls disarmed & disassembled) not greater than 30 minutes	Yes	Stow Time = 10 minutes
SSDR-001: Wing Removal	Wings shall be removable	Yes	Removable and attach with detents
SSDR-002: Bottom Facing Sensor Access	Fuselage allows bottom facing sensor	Yes	Sensor faces downward in aircraft
PR-001: GPS Accuracy	GPS accuracy of 5 meters or less	No	Not Verified
PR-002: Multimedia Capture	Aircraft can record video and/or capture images	Yes	Camera for image capture
OR-001: People Clearance	Aircraft shall not be flown within 5 meters of another person besides the operator	Yes	Safety plan put in place for operation
OR-002: Wildlife Clearance	Aircraft shall not be flown within 5 meters of wildlife	Yes	Safety plan put in place for operation

Figure H.1: Verification Status of System and Subsystem Requirements

I Wind Tunnel Testing

To confirm the aerodynamics analysis, the Boeing Wind Tunnel at the Purdue University Airport was used. A 68% scaled wing was built using a CNC foam cutter, with dimensions of $1.5m \times 0.2m \times 0.03m$. A pseudo-boom made out of cardboard was attached to the wing to provide a mount point for the angle of attack control arm; the cardboard also mimics a tail boom that will be mounted in the real aircraft. Per regulation, the motor driving the air could not exceed 25 Hz, which was equivalent to $17m/s$. Therefore, a wing was tested under wind speed ranging between $5.21m/s$ to $15.68m/s$ and angle of attack between -10° to 15° with increments of 1° . Collected data follows.

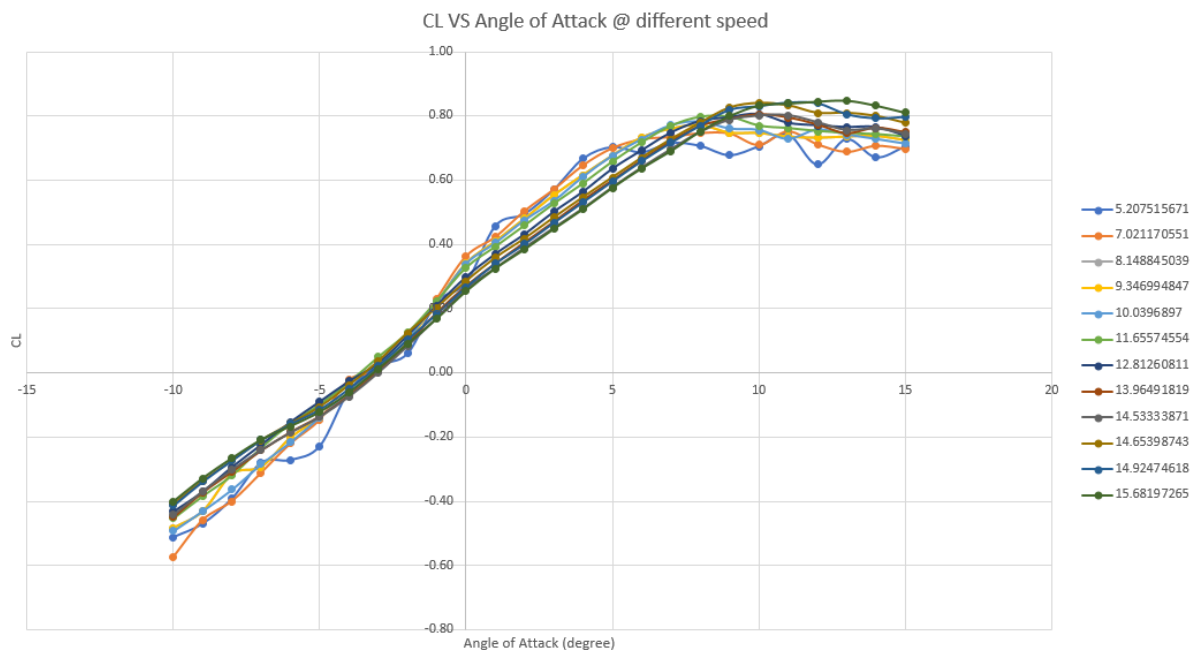
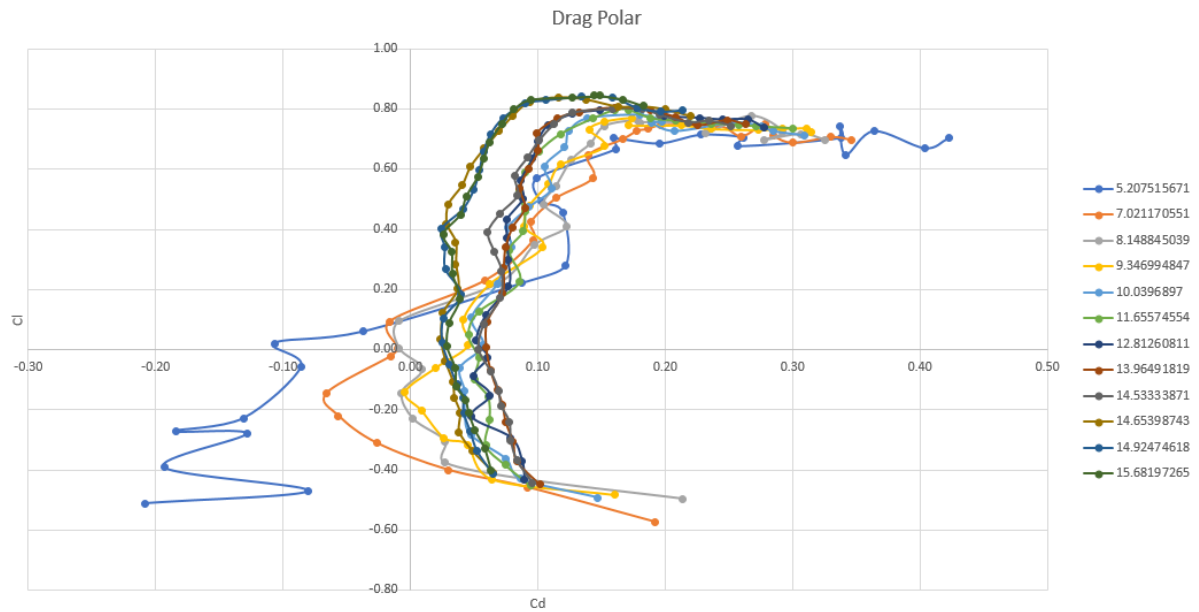
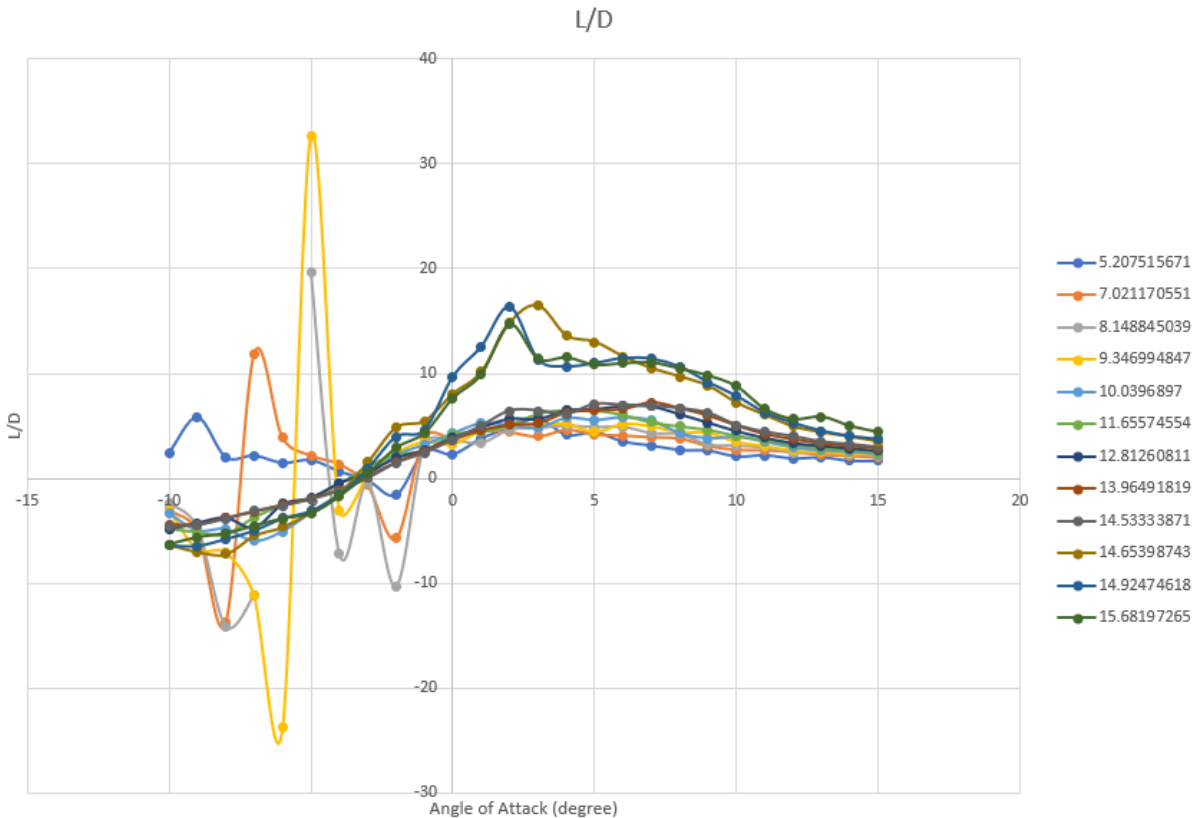


Figure I.1: C_L vs α

**Figure I.2:** Drag polar**Figure I.3:** Lift-to-drag

A C_L vs α graph is presented in Figure I.1. A region where the angle of attack is linearly proportional to the lift coefficient between $\pm 10^\circ$ was observed. The wing approaches its stall as the angle of attack approaches and exceeds 10° which matches expectations from

the XFLIR analysis of the 2D wing. The magnitude of the coefficient of lift is slightly smaller than that of the 2D wing examined, but this is expected because of the 3D wing. The wing's chord was also 2.54-cm shorter than planned because the wing was too thin for the CNC machine to cut. Considering this, lift coefficient data obtained were considered valid: 0.70 at take off speed and 0.58 at cruise speed with 5° angle of attack. Figure I.2 is a drag polar graph which shows that minimum drag occurs with a C_L of 0.4 and a C_{D_0} at 0.03. Proceeding to the L/D to α graph in Figure I.3, we observe that the maximum L/D reached between 5° and 7° angle of attack, while ignoring the outliers.

There was a concern about not having enough lift force during takeoff, especially since it will be conducted at a slow speed. To address this, flaps were added to the wing and deflected at approximately 10°. With collected data, a C_L vs α graph and a drag polar graph were created, as presented in Figure I.4 and Figure I.5.

CL VS Angle of Attack @ different speed with flaps

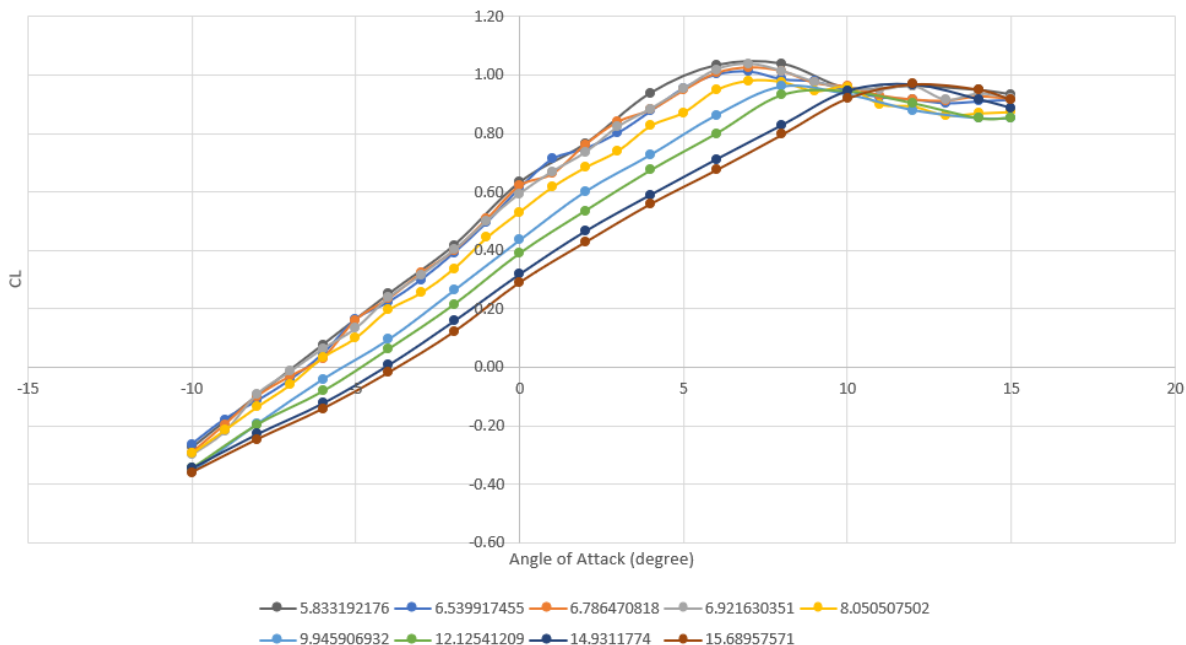


Figure I.4: C_L vs α with flap

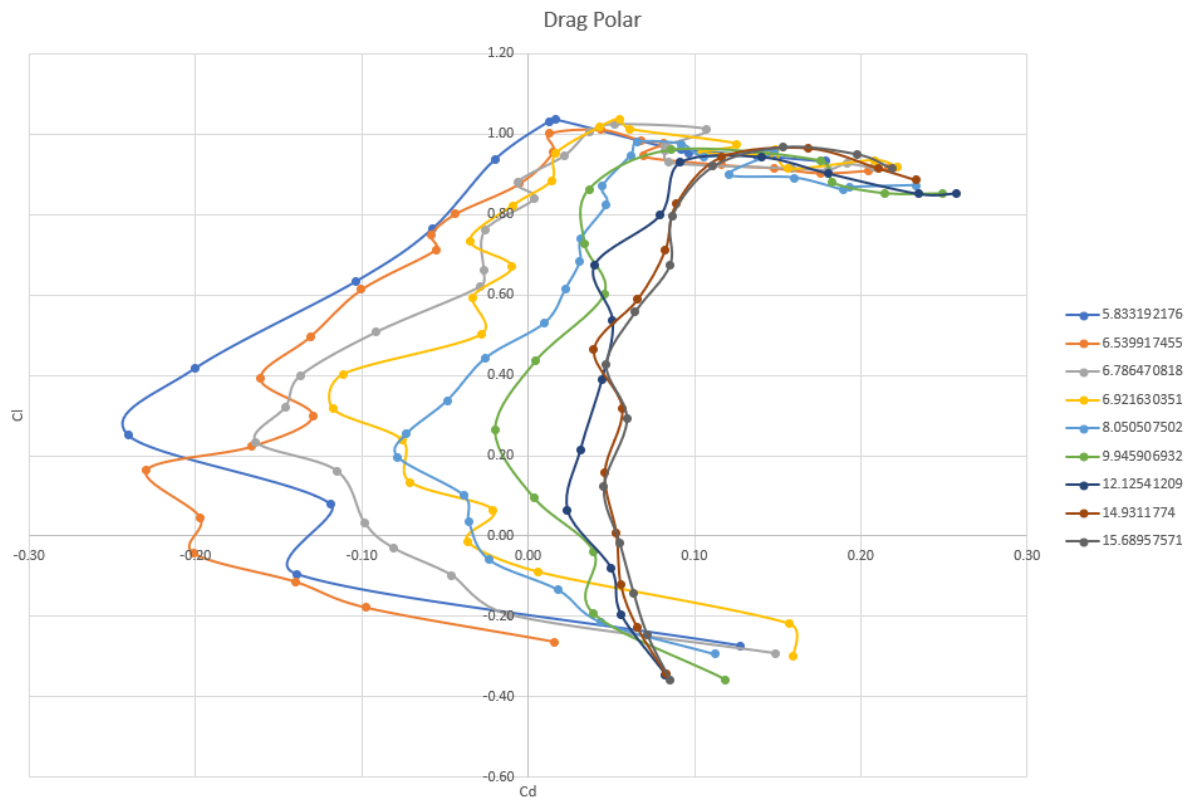


Figure I.5: Drag polar with flap

With the flaps deflected to 10° , the coefficient of lift was increased by 20% to 25% along the linear region of the graph, shown in Figure I.4, and the C_{Lmax} was reached at 6.5° of angle of attack. The drag polar graph has become more radical with the flap deployment due to increased drag.

During the wind tunnel testing, significant bending along the wing span was observed, especially at high speeds near the cruise speed. It was expected that the wing tip would be curved upward as the flight speed increased, but it concerned some of the members. Of course, the test wing was made out of foam and it was only reinforced by a small carbon fiber rod inserted in the middle, yet the deflection on both tips exceeded the expectation.

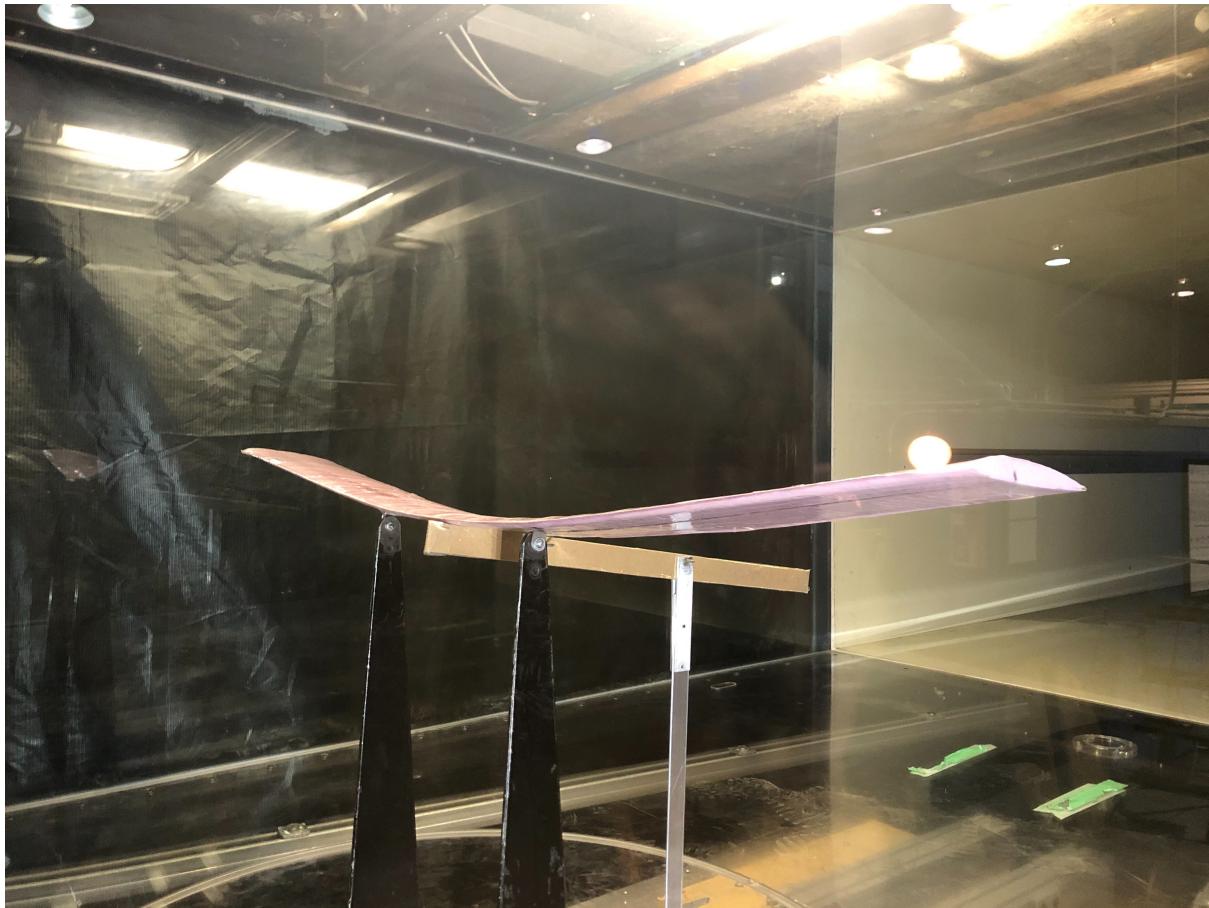


Figure I.6: *Wind tunnel testing*

J Flight Checklists

Flight checklists for day before flight, pre-flight, in-flight, post-flight, and emergency situations were created for use when operating the UAS. This Appendix section reproduces these checklists.

Day Before Checklist		
Criteria	Status	Notes
Component Check		All components organized/accounted for
UAV		
Fuselage		
Wing		
Tail		
Propeller		
Motor		
Battery		Ensure battery is charged
Controller		Check battery power and connectivity
Pilot		Ensure licensed pilot is available
Ground Station		
Fully charged		
Software requirements		
Weather Check		No precipitation, up to 8 mph winds

Figure J.1: Day Before Flight Checklist

Pre-Flight Checklist		
Criteria	Status	Notes
Assembly		
Remove fuselage bottom cover		
Insert wings into fuselage slots		Do not fully engage
Connect flap and aileron servo wires		
Insert wings fully into slot		Verify latching mechanisms engaged
Secure battery and plug in		
Power ON electrical components		
Replace fuselage bottom cover		
Structural		
Connection Points		<u>Ensure secure connection points</u>
Electronics/payload to electronics board		
Electronics board to fuselage		
Tail to boom		
Boom to electronics board		
Wing spars to electronics board		
Landing gear to electronics board		
Pylon to boom		
Motor to pylon		
Propeller to the motor		
Control horns to wing/tail		
Servos to wing/tail		
Control surfaces to wing/tail		
All fuselage components secured		
Weight		
Aircraft weight < 10 lb		
Aircraft CG location = 13.25 in. from nose		
Electrical		
Battery level		LiPo Checker or Pixhawk
Wiring		Fix incorrect/loose connections
Power		Components powered on correctly
Pixhawk		Check operational
System is DISARMED		
Communications		Check operational
Telemetry		
LTE link		
RC transmitter		
Sensors		
GPS		Locked & correct home location
Airspeed		
IMUs		Calibrated & all green
Payload		Check operational
Gimbal		
Camera		
Raspberry Pi		
Manual Mode ON		
Control Surfaces		
Manual Mode		Engage roll/pitch/yaw using controller
Flaps		Flaps deploy DOWN at same rate
Roll left		Left aileron UP, right aileron DOWN
Roll right		Left aileron DOWN, right aileron UP
Pitch up		Elevator UP
Pitch down		Elevator DOWN
Yaw left		Rudder LEFT
Yaw right		Rudder RIGHT
Stabilize Mode		Engage roll/pitch/yaw by moving UAV
Correcting roll left		Left aileron DOWN, right aileron UP
Correcting roll right		Left aileron UP, right aileron DOWN
Correcting pitch up		Elevator DOWN
Correcting pitch down		Elevator UP
System is ARMED		

(a)

(b)

Figure J.2: Pre-Flight Checklist

<u>In-Flight Checklist</u>		
Criteria	Status	Notes
Takeoff		
Check GPS		
UAV centered on runway		
Runway clear of bystanders/debris		
Announce takeoff occurring		
Apply full throttle		
Rotate at 20 MPH		
Cruise		
Switch to Autopilot		
Monitor UAV attitude		Check for unexpected behavior
Pitch		
Roll		
Yaw		
Sensors		Check datalink is uninterrupted
GPS		
Airspeed		
LTE		
Propulsion		
Power draw		
Battery capacity		
Constant airspeed		
Constant altitude		
Autopilot		
UAV reaches target location(s)		
Landing		
Switch to Manual		
Runway clear of bystanders/debris		
Announce landing is occurring		
Flaps DOWN		
CUT throttle at 50 FT		
DISARM System		

Figure J.3: *In-Flight Checklist*

<u>Post-Flight Checklist</u>		
<u>Criteria</u>	<u>Status</u>	<u>Notes</u>
DISARM System		
Safe system		
Damage		
Structural deformation		
Connection points		
Cracks in fuselage		
Landing gear		
Battery		
Pictures of all damage		
Download flight logs		
<u>Disassembly</u>		
Remove bottom fuselage cover		
Remove and recharge battery		
Depress detent latches		
Slide wings out 6 inches		
Unplug servo wires		
Fully slide out wings		
Inspect fuselage interior for loose components		
Reattach fuselage cover		
Secure components for transport		

Figure J.4: *Post-Flight Checklist*

<u>Emergency Checklist</u>		
<u>Criteria</u>	<u>Status</u>	<u>Notes</u>
Telemetry Interruption		
Switch to RTL Mode		
<u>Loss of Autopilot Control</u>		
Stabilize Mode		
Emergency land at origin		
<u>All Other Issues</u>		
Manual Mode		
If BVLOS, Stabilize Mode		
Assess situation		
Response to aileron input		
Response to elevator input		
Response to throttle input		
Response to rudder input		
Continue or abort?		
Respond w/ appropriate inputs		

Figure J.5: *Emergency Checklist*

K Drawing Package

Nine drawings are provided on the ensuing pages for the overall UAS assembly in complete, exploded, and three-view form, for the wing, tail assembly, tailboom, fuselage, motor pylon, and payload assembly.

